UNIVERZITA OBRANY BRNO
FAKULTA VOJENSKÉHO ZDRAVOTNICTVÍ
HRADEC KRÁLOVÉ

PREPARATION AND EVALUATION OF POTENTIAL DRUGS INHIBITING MITOCHONDRIAL ENZYMES

Disertační práce

Mgr. Ondřej Benek

Školitel: doc. PharmDr. Kamil Musílek, Ph.D.

Školitel specialista: prof. Ing. Kamil Kuča, Ph.D.

Doktorský studijní program *T o x i k o l o g i e*

Hradec Králové
2016

ACKNOWLEDGEMENTS

I would like to thank to all people who supported me throughout my postgraduate studies and enabled me to write-up this thesis. Special thanks belong to my supervisors assoc. prof. Kamil Musílek for all his advices and experience he gave me and prof. Kamil Kuča for keeping the wheels turning. I would also like to thank to the collective at Department of Toxicology and Military Pharmacy and Centre of Biomedical Research for their kind collaboration at both the scientific and the social level, prof. Frank Gunn-Moore and his group at St Andrews for biological assessment of prepared compounds, dr. Rona R. Ramsay for introducing me to the world of biochemistry and prof. José Luis Marco-Contelles and his group in Madrid for the great time I spent in their laboratory during my COST-STSM intership.

Finally, I acknowledge the financial support of the Ministry of Education, Youth and Sports CZ (No. SV/FVZ201201), the Ministry of Health CZ (no. NV15-28967A) and COST CM1103.

DECLARATION

I declare that this thesis is my original work. All used literature sources are listed in the list of references and properly cited within the text.

Hradec Králové Ondřej Benek

Index

Abbreviations

ABAD	A*β* binding alcohol dehydrogenase
ABAD-DP	ABAD-decoy peptide
AD	Alzheimer's disease
AChE	acetylcholinesterase
AChEI	AChE inhibitor
APOE	apolipoprotein E
APP	amyloid precursor protein
A*β*	amyloid-beta peptide
BBB	blood-brain barrier
BChE	butyrylcholinesterase
CypD	cyclophilin D
Ep-I	endophilin I
ER	endoplasmic reticulum
GAPDH	glyceraldehyde-3-phosphate dehydrogenase
IDE	insulin degrading enzyme
IMM	inner mitochondrial membrane
JNK	c-Jun N-terminal protein kinase
MAMs	mitochondria-associated membranes
MAO	monoamine oxidase
MAOI	MAO inhibitor
MTDLs	multitarget-directed ligands
OMM	outer mitochondrial membrane
PreP	presequence protease
ROS	reactive oxygen species
SDR	short chain dehydrogenase reductase
TIM	translocase of the inner mitochondrial membrane
TOM	translocase of the outer mitochondrial membrane

1 Introduction

(based on attachments I and II)

1.1 Alzheimer's disease

Alzheimer's disease (AD) is the most common cause of senile dementia and about 20 million people worldwide currently suffer from this devastating illness, with the number continuing to steadily rise due to an aging population [1]. This neurodegenerative disease was firstly described by German psychiatrist Alois Alzheimer in 1906. It is characterized by progressive decline of cognitive functions and memory caused by the extensive death of neurons, which starts in the entorhinal cortex and hippocampus and proceeds to other parts of the brain cortex and subcortical grey matter [2].

Despite first being identified over a century ago and subject to intensive research, the pathogenic mechanisms of AD are still not fully understood and consequently an effective treatment is yet to be developed and patient's death remain a certainty.

1.1.1 Causes and Risk factors

A minor part (< 1%) of AD cases is caused by three known genetic mutations, which are all connected with increased amyloid-beta peptide (Aβ) production. These mutations involve the gene for the amyloid precursor protein (APP) and the genes for the presenilin 1 and presenilin 2 proteins. People inheriting any of these genetic mutations are almost certain to develop AD, usually before the age of 65, and in such cases we talk about so called familial early-onset form of AD. The exact causes of the sporadic late-onset form of AD, which accounts for over 99% of the cases and manifest principally after the age of 65, are not yet understood [3].

The major risk factor for developing AD is advancing age, although AD is not a normal part of aging. Familial history is another important risk, as people who have a parent or a sibling suffering AD are more likely to develop the disease. This could be due to the genetic factors and/or the shared lifestyle and environment [4, 5].

AD is genetically connected to the presence of ε4 form of the gene apolipoprotein E (*APOE* ε4). *APOE* gene provides the blueprint for a protein that transports cholesterol in the blood and can be found in three isoforms (ε2, ε3 and ε4), however, only allele ε4 increases the risk of AD. On the contrary, the presence of allele ε2 decreases the risk of developing AD [5, 6].

Other risk factors include mild cognitive impairment, depression, head trauma and brain injury, low education level, cardiovascular diseases and their risk factors (e.g. high cholesterol, obesity, smoking, physical inactivity) and diabetes mellitus type 2 [8, 7, 9–13, 3].

1.1.2 Pathological hallmarks

The main pathological hallmarks of AD represents extracellular A*β* deposits also termed senile plaques, intracellular deposits of phosphorylated *τ*-protein, termed neurofibrillary tangles, and loss of neurons, especially the cholinergic ones [2, 14]. Further AD is connected to loss of synapses, mitochondrial dysfunction and inflammation [15–17].

1.1.3 Treatment

Current AD therapy is based on so called cholinergic hypothesis, which asserts that the decreased level of acetylcholine in the brain leads to cognitive and memory deficits, and that sustaining or recovering cholinergic function should therefore result in amelioration of the symptoms [18–20]. Accordingly, inhibitors of enzyme acetylcholinesterase (AChE), which are able to increase acetylcholine levels in cholinergic synapses, are used for AD treatment. To date, the number of approved drugs is limited to three AChE inhibitors, namely rivastigmine, donepezil, and galantamine, and the neuroprotective *N*-methyl-D-aspartate (NMDA) receptor antagonist memantine (Fig. 1). However, none of these drugs can prevent or cure the disease, but afford only symptomatic treatment [20, 21].

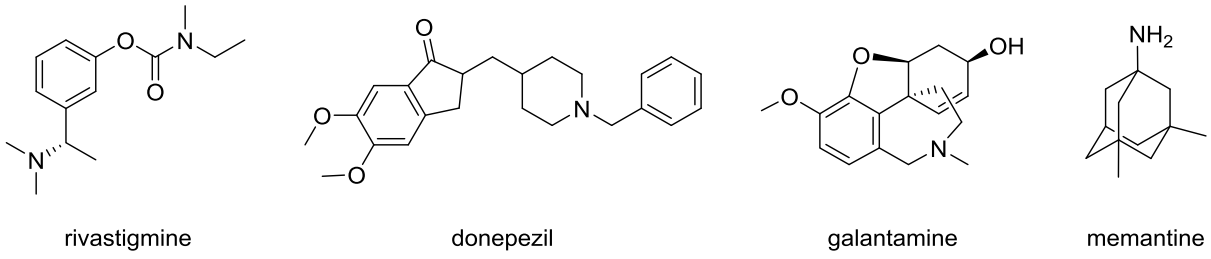

Figure 1: Clinically used drugs against AD.

1.1.4 Amyloid cascade hypothesis

Although the aetiology of AD is still unknown, a build-up of A*β* is considered to play an important role in disease progression. A*β* peptide is generated from APP (amyloid precursor protein) via its sequential cleavage by *β*-secretase and *γ*-secretase (Fig. 2). This action takes place at several intracellular sites, including within Golgi apparatus, endoplasmic reticulum (ER), endosomal-lysosomal systems, and multivesicular bodies. Mutations in either *APP* or in the *presenilin* genes have been linked to familial, early-onset forms of AD. However, these early onset cases represent only a small minority of AD patients, whereas the vast majority of AD cases have developed sporadically [22, 23]. The original amyloid cascade hypothesis defined by Hardy *et al.* in 1992, proposed that insoluble extracellular plaques were responsible for the majority of A*β* toxicity. This hypothesis has

since been refined, as recent data indicates that soluble intracellular oligomers are now responsible for the majority of A*β* induced toxic effects [24–28].

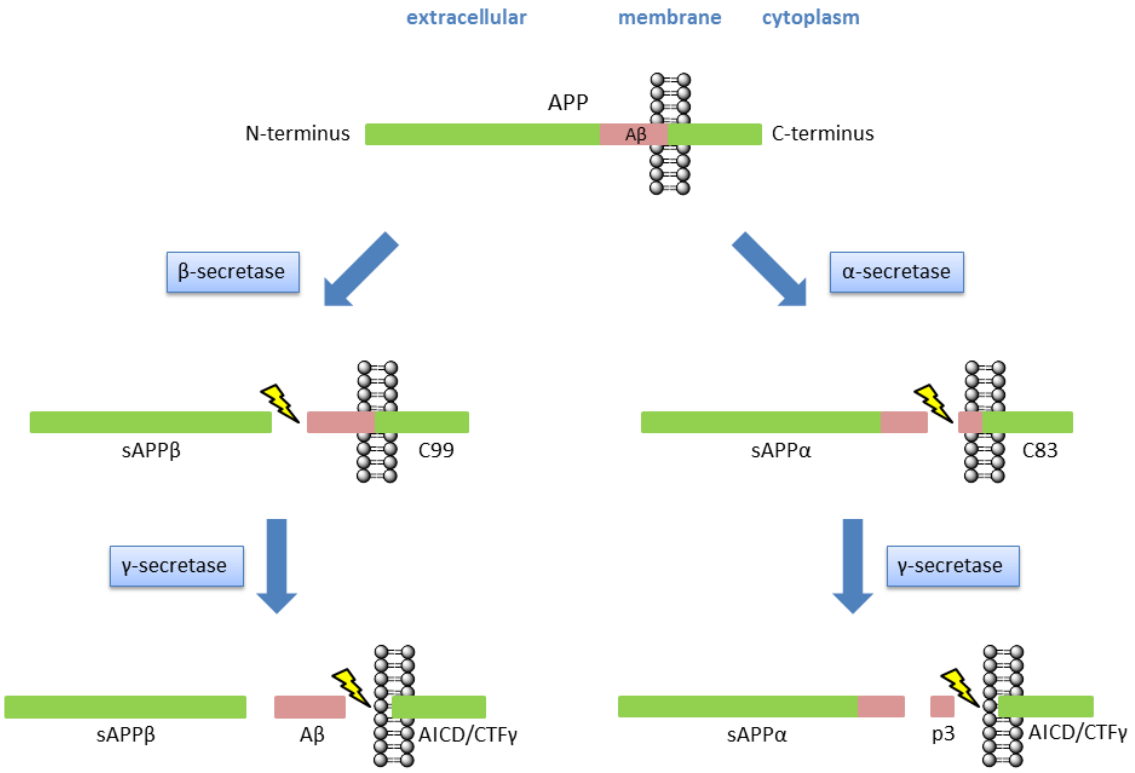

Figure 2: The structure and processing of APP showing amyloidogenic (on the left) and non-amyloidogenic (on the right) pathways. A*β* (pink box) constitutes part of the transmembrane domain and an adjacent short fragment of the extracellular domain. Reproduced from Haass and Selkoe 2007, Nature Reviews. Molecular Cell Biology, 8, 101–112 [29]. © Nature Publishing Group.

1.1.5 Mitochondrial dysfunction in AD

A link between mitochondrial dysfunction and AD has long been suggested to exist. Mitochondria are central to many processes including: cellular energetic metabolism, regulation of intracellular Ca^{2+} levels, the regulation of cell death and they are also the main source of reactive oxygen species (ROS). All these functions are found to be disturbed in AD, as well as in the presence of increased intracellular concentrations of A*β* in different *in vitro* and *in vivo* studies. These findings are summarized in recent review articles, therefore suggesting that A*β* is responsible for the induction of mitochondrial dysfunction typically observed in AD (Fig. 3) [30–32].

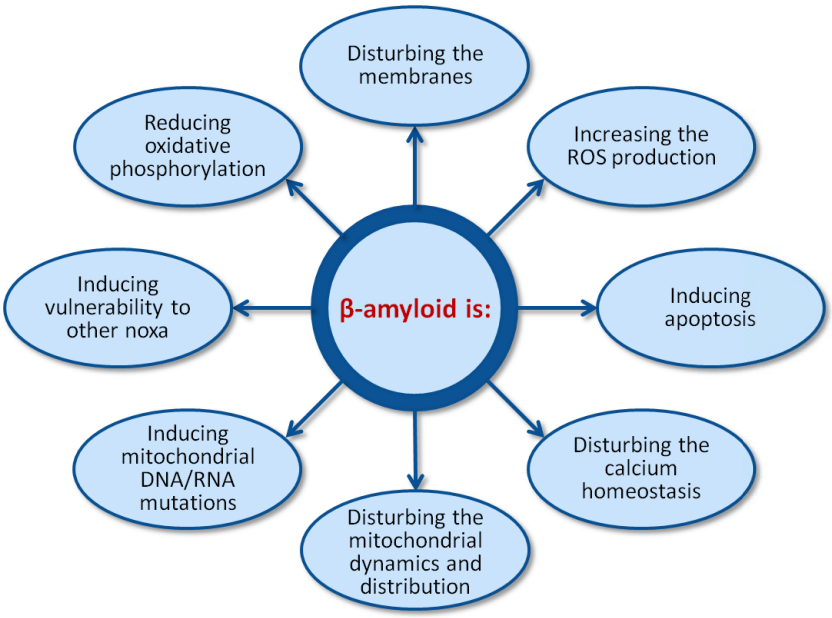

Figure 3: Possible mitotoxic mechanisms induced by A*β* in AD. Reproduced from Tillement *et al*. 2011, Mitochondrion, 11, 13–21 [10]. © Elsevier.

Although A*β* is known to be present in mitochondria, its precise location within this compartment is a contentious issue. In most studies A*β* was found associated with the inner mitochondrial membrane (IMM) and not in the mitochondrial matrix, which is in contrast with findings that A*β* interacts with several proteins residing in the mitochondrial matrix. This discrepancy can be explained by the rapid A*β* degradation occurring in the matrix by mitochondrial proteases (e.g. PreP or IDE) [33–35].

Also the origin of mitochondrial A*β* is still a matter of debate. There is experimental evidence for both local production (described later in the mitochondrial *γ*-secretase section of this review) and direct import either from ER or from cytosol. The strongest evidence supports the hypothesis that A*β* can be transported into the mitochondria from the cytosol via mitochondrial TOM/TIM (translocase of the outer membrane/ translocase of the inner membrane) protein-import machinery. In accordance with this theory, TOM40 complex was shown to transport A*β* across the outer mitochondrial membrane (OMM). However, the mechanistic details of how A*β* gains access to the different mitochondrial sub-compartments are currently unestablished, since there are several pathways for protein translocation across (TIM23 complex) and into the IMM (TIM23 or TIM22 complexes). Another theory assumes mitochondria-associated membranes (MAMs) of the ER to be responsible for the import of A*β* from this compartment. MAMs are a physical connection between the ER membrane and the mitochondrial outer membrane, where lipids and membrane proteins are thought to be exchanged directly between the organelles (Fig. 4) [33–35].

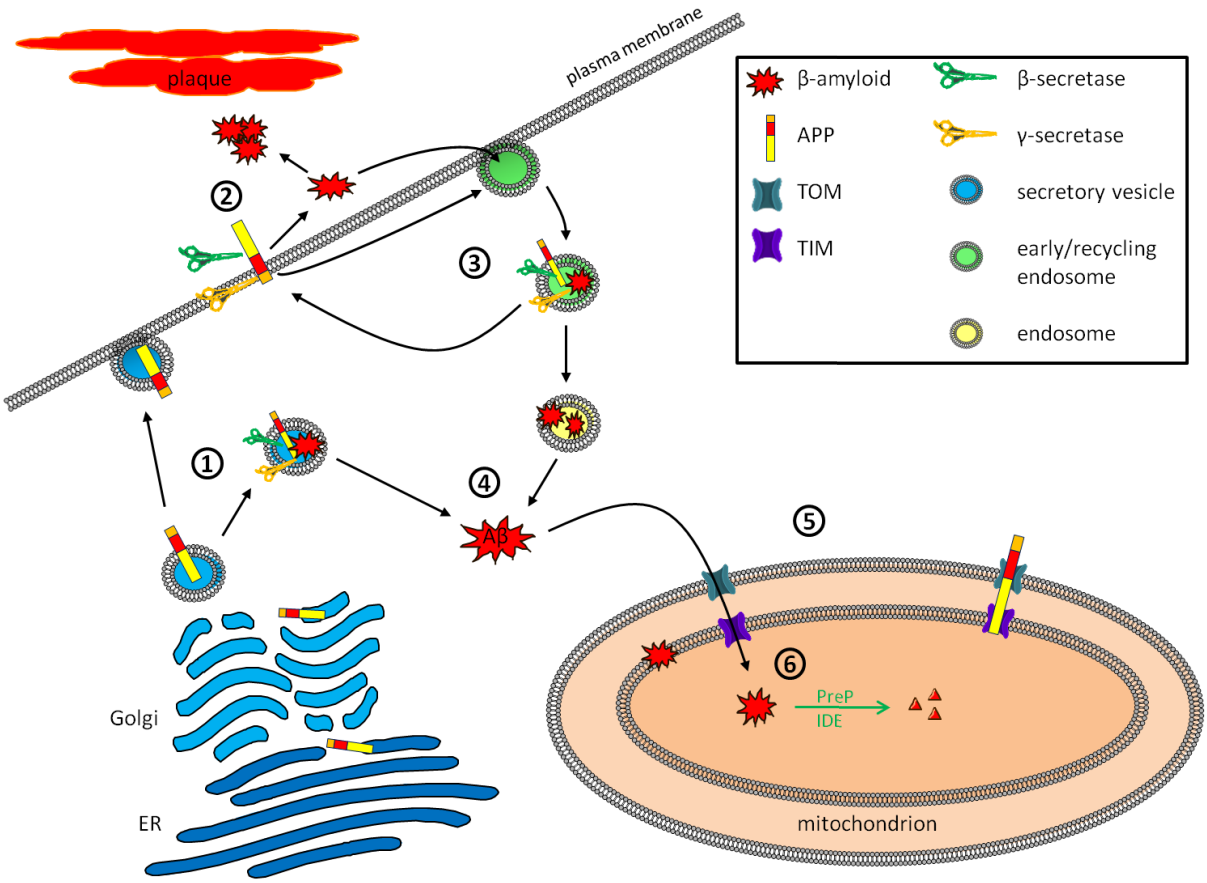

Figure 4: APP and A*β* inside the cell. During protein synthesis, the APP is targeted to the ER and transported to the plasma membrane by vesicular transport through the Golgi apparatus. Amyloidogenic processing of APP by the *β*- and *γ*-secretases at the plasma membrane produces the A*β*. This cleavage has also been found to take place prior to exocytosis in the trans-Golgi network (1). A*β* can aggregate extracellularly forming extracellular plaques, which are one of the hallmarks of AD (2). APP undergoes endocytosis and is normally recycled to the plasma membrane via recycling endosomes. A*β* peptides can also enter the cell by endocytosis, but can also be produced from APP by *β*- and *γ*-secretase cleavage in endosomes (3). A*β* can also compromise the integrity of endosomes and secretory vesicles and can be found in the cytosol, probably due to leakage out of these compartments (4). A*β* can be imported into the mitochondria via the TOM/TIM mitochondrial import machinery. Owing to its chimaeric targeting sequence, APP can also be transported to mitochondria where it gets stuck within TOM and TIM proteins, disturbing mitochondrial protein import (5). Mitochondrial peptidases PreP and IDE are capable of degrading A*β* in the mitochondrial matrix (6) Reproduced from Muirhead *et al*., 2010, Biochemical Journal, 426(3), 255–270. © The Biochemical Society [34].

1.1.6 Mitochondrial proteins directly interacting with Aβ

The particular molecular mechanism, through which Aβ exerts its toxicity in mitochondria, has not yet been determined. However, several mitochondrial proteins were ascertained to, or are thought to, directly interact with Aβ (Table 1). Such interactions could lead to the disruption of their physiological functions and consequential mitochondrial dysfunction finally resulting in the development or progression of AD [36].

Table 1: A*β*-binding proteins, their mitochondrial localization, evidence for the direct interaction with A*β*, significance of their role in AD pathophysiology and their potential and suitability as a drug target for AD treatment. The number of stars represents the degree of significance with *** being the highest score, ** an intermediate score and * the lowest score [36].

Protein	Localization in mitochondria	Evidence for direct interaction with A*β*	Significance in AD pathophysiology	Potential as a drug target
ABAD	matrix	***	***	***
CypD	matrix, IMM	***	***	***
ANT	IMM	**	**	**
VDAC	OMM	**	**	**
ETC - Complex I	IMM	**	**	*
ETC - Complex IV	IMM	**	**	*
ETC - Complex V	IMM	*	**	*
KGDHC	IMM	**	*	*
PDHC	matrix	**	*	**
CK	IMS	*	*	*
γ-secretase	OMM	***	***	***
NOS	IMM	**	**	**
PAD	not specified	**	**	**
SOD1	IMS, matrix, OMM	***	**	*
Catalase	matrix	***	**	**
Drp-1	OMM	**	**	**
GAPDH	OMM	***	***	***
HtrA2	IMS	***	**	**
PreP	matrix	***	**	**
IDE	not specified	***	***	***
Hsps	not specified	***	**	**
HAX-1	not specified	*	*	*

As presented in Table 1, at least five such A*β*-binding partners (druggability score ***) seem to be very rational drug targets for AD treatment, namely ABAD, CypD, *γ*-secretase, GAPDH and IDE. These proteins have all been successfully targeted *in vivo* using neurodegenerative animal models and a change in either their expression or their pharmacological modulation resulted in a decrease of neurodegeneration symptoms.

1.2 Amyloid beta-binding alcohol dehydrogenase

Enzyme A*β* binding alcohol dehydrogenase (ABAD) was first described in 1997 by Yan *et al.* [37] and a year later it was identified as the human analogue of newly discovered bovine hydroxyacyl-CoA dehydrogenase type II [38]. Originally it was termed ERAB (endoplasmic reticulum-associated amyloid-binding protein) as it was initially (and incorrectly) identified within the ER [38], however, its actual localization is within the mitochondrial matrix [39]. ABAD has also several alternative names derived from different substrates, which it can utilise, namely, 17*β*-HSD10 (17*β*-hydroxysteroid dehydrogenase type 10) [39], SCHAD (human brain short chain L-3-hydroxyacyl-CoA dehydrogenase) [40], HADH II (human hydroxyacyl-CoA dehydrogenase type II) [41], MHBD (2-methyl-3-hydroxybutyryl-CoA dehydrogenase) [42].

ABAD is an NAD-dependant oxidoreductase belonging to SDR family and catalysing oxidation of alcohols and reduction of ketones and aldehydes (Scheme 1) [43]. It has quite low substrate specificity as it was experimentally shown to catalyse broad range of structurally diverse substrates. Question remains, which of these *in vitro* identified substrates ABAD actually utilizes under *in vivo* conditions [34].

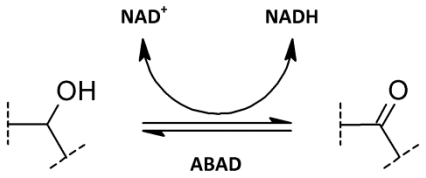

Scheme 1: General scheme of ABAD catalysed reaction.

According to its mitochondrial localization, it seems that the main physiological function of ABAD is the *β*-oxidation of fatty acids with short branched sidechain, a process involved in energy production and metabolic homoeostasis [44]. Another proposed role of ABAD could be in metabolism of hydroxysterioids or steroid modulators of the $GABA_A$ receptor. The role in in metabolism of sex steroids, especially oestradiol, could explain, why women are more likely to suffer from AD [43, 45]. ABAD also takes part in the isoleucine degradation pathway. Nonsense mutations of ABAD resulting in catalytically inactive enzyme were connected to loss of mental and motor skills, psychomotor retardation and epilepsy, typical symptoms of MHBD deficiency [42]. Further, ABAD seems to serve as a structural core for mitochondrial RNAse P, an enzyme essential for production of tRNA and consequently synthesis of proteins in mitochondria [46, 47]. The latest proposed function of ABAD is oxidation of damaged cardiolipin and doing so the blockage of the apoptotic pathway [48].

1.2.1 Structure and mechanism of function

ABAD forms a homotetramer with each 27 kDa unit comprising a Rossman fold dinucleotide-binding motif and the Ser^{155}, Tyr^{168}, Lys^{172} catalytic triad typical for SDR family (Fig. 4) [44].

Co-factor NAD^+/NADH binds to the enzyme in proximity of catalytic triad and forms non-covalent interaction with its respective amino acids. The substrate binding site includes a region with positively charged lysine and histidine residues, which are supposed to interact with negatively charged parts of substrates comprising in its structure the CoA group. Therefore, substrates lacking the CoA domain are metabolised less effectively. Hydrophobic residues lining the space between the catalytic triad and positively charged region is organized favourably for binding the aliphatic side chains of fatty acids, which further supports the theory that acyl-CoA is the primary substrate of ABAD [44, 49].

Proposed mechanism of catalysis can be presented on reduction of a ketone to an alcohol. First, Tyr^{168} interacts with carbonyl group thereby increasing electrophilicity of the carbon atom. Ammonium group of Lys^{172} interacts with Tyr^{168} to lower its pK_a. Co-factor NADH acts as the donor of hydride for the reduction. Simultaneously with the hydride transfer to the activated carbonyl deprotonation of Tyr^{168} takes place and the resulting proton is transferred on the newly created hydroxyl anion. Negative charge on Tyr^{168} is stabilized by creating of a hydrogen bond to the Ser^{155} [44].

Compared to other members of SDR family, ABAD encompasses two extra domains (amino acid residues 102-107 and 141-146). Region comprising residues 102-107, which is situated close to the active site, is also responsible for Aβ binding to the enzyme [44, 49, 50].

1.2.2 Interaction with Aβ

The interaction between ABAD and Aβ was first described in 1997 on an yeast two-hybrid screen [37] and this observation was later confirmed using several different techniques, namely ELISA [51], crystallography [50], surface plasmon resonance [50, 52], co-immunoprecipitation [37, 50] and immunocytochemistry followed by confocal microscopy [50].

The region comprising amino acid residues 100–110, also termed loop D, was recognised as the binding site for Aβ and point mutations within this region lead to blockage of the interaction (Fig. 5) [50]. As already mentioned, ABAD is the only SDR member encompassing this region, which also explains why it is the only SDR member to interact with Aβ [44].

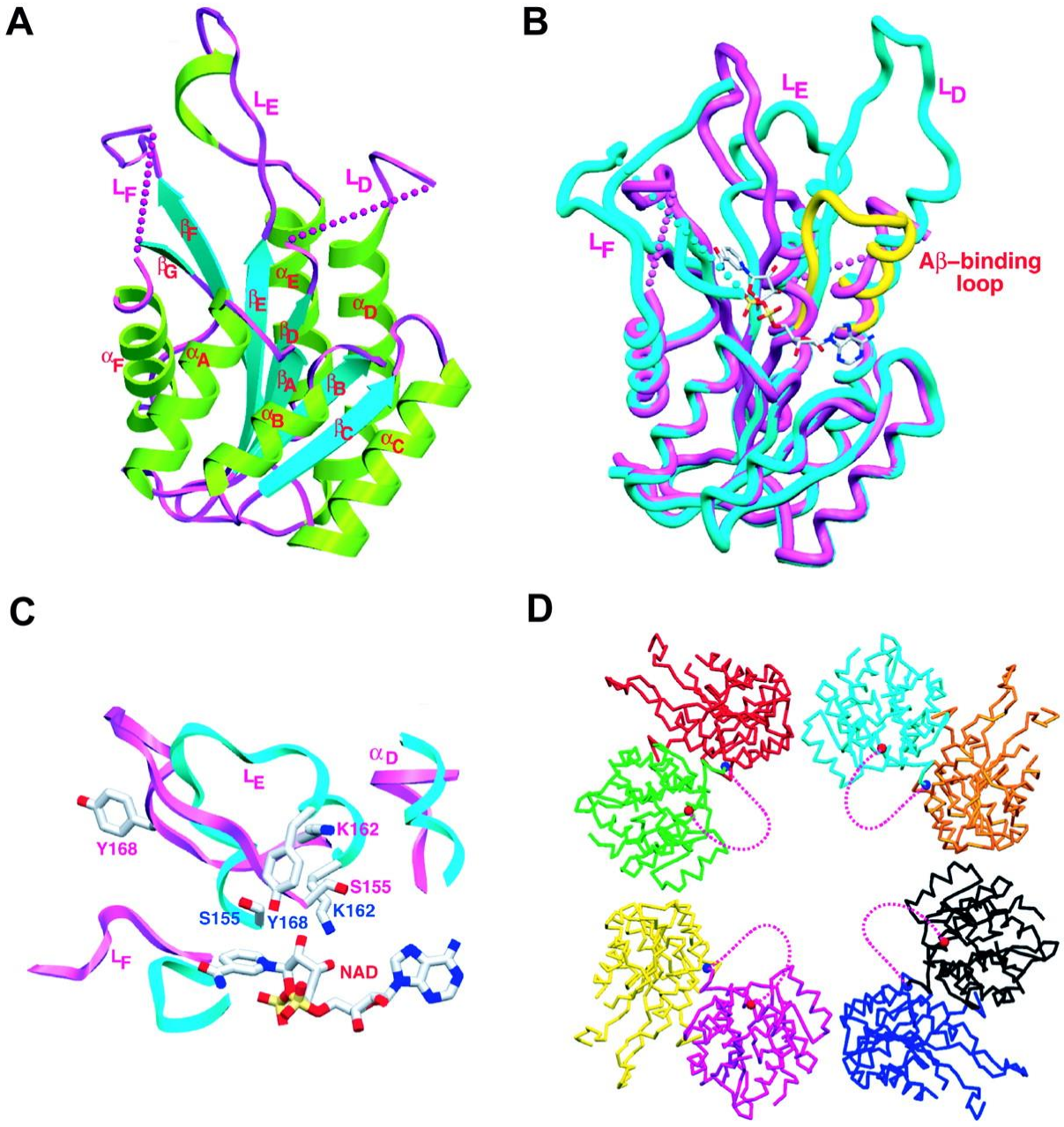

Figure 5: Crystal structure of A*ß*-bound human ABAD. **A**) A ribbon diagram with labeled secondary structures and the loop D (L_D), L_E, and L_F loops. Helices are shown in green, *ß* strands are shown in blue, and loops are shown in pink. Disordered regions are shown by dotted lines. **B**) Superposition of A*ß*-bound human ABAD (pink) and rat ABAD in complex with NAD (blue). The L_D of 3*α*-hydroxysteroid dehydrogenase is shown in yellow to demonstrate that L_D of ABAD contains a unique insertion absent in all other SDR family members. NAD^+ is shown as a stick model with grey for carbon atoms, red for oxygen atoms, blue for nitrogen atoms, and yellow for phosphate atoms. The proposed A*ß*-binding loop is indicated. **C**) Superposition of the active sites of A*ß*-bound human ABAD (pink) and rat ABAD (blue), showing distortion of the NAD^+ binding site and the catalytic triad S^{155}, K^{162}, and Y^{168}. Colors

are the same as in B). **D**) A section of the crystal packing interactions, showing the large solvent channels. Each ABAD molecule is shown in a different colour. The ordered ends of the L_D, residues 94 and 114, are marked as red and blue balls, respectively, and the hypothetical loops are shown in pink as dotted lines. Reproduced from Lustbader *et al.* 2004, Science, 304, 448–452 [20]. © The American Association for the Advancement of Science.

The interaction of A*β* with the enzyme causes conformational changes of the NAD^+ binding site thereby blocking the binding of the co-factor, which consequently leads to inhibition of enzyme's catalytic activity. Contrary, enzyme with bound co-factor cannot interact with A*β*. The binding of A*β* or NAD^+ to the ABAD therefore seems exclusive, although they bind to the enzyme at different regions [50, 52].

A*β* inhibits ABAD enzymatic activity with K_i = 1.2 – 1.6 μM for substrate acetoacetyl-CoA, however, the binding of A*β* to the enzyme can be observed at much lower, nanomolar concentrations [37, 52]. Possible explanation for this discrepancy is that the enzyme inhibition cannot be achieved by A*β* monomers only, but the aggregated oligomeric A*β* species (formed at higher Ab concentrations) are required to do the job [34].

Experiments on cells showed that A*β* has higher toxicity in cells expressing the wild type enzyme compared to cells expressing enzymatically inactive mutant or expressing no enzyme at all. Hence it is assumed, that the enhanced A*β* toxicity is not caused by inhibition of ABAD but rather by change of its properties (e.g. localization) or a gain of new toxic function to the catalytically active enzyme. This is also supported by the finding that A*β* toxicity appears at concentrations sufficient for ABAD binding but insufficient for its inhibition [53]. Similar experiments were also performed at an *in vivo* level using transgenic mice and showed similar results concluding that inactivation of the enzyme or silencing of its expression ameliorates A*β* toxicity [50].

Moreover, ABAD's expression levels are increased in the brains of AD patients, which further supports the connection between ABAD and AD [54, 55].

1.2.3 Mechanism of ABAD-A*β* complex toxicity

The mechanism of ABAD mediated A*β* toxicity is yet not known, however, several theories exist. One theory assumes that after A*β* binding ABAD takes up the production of toxic aldehydes 4-hydroxynonenal and malonyldialdehyde, which it under A*β* free conditions catabolizes. This could be result of change in enzyme's function or change in its localization, which could enable ABAD to utilise substrates unavailable in its original compartment and vice versa [56, 53, 57].

Other possibility could be that interaction with Aβ leads to excessive degradation of hormone oestradiol by ABAD, due to change in its localization or its overexpression [54]. It has been found that oestradiol ameliorates Aβ toxicity and its preventive application decreases the risk of developing AD [58].

Role of ABAD in neurosteroid metabolism, namely in oxidation of positive allosteric modulators of $GABA_A$ receptors allopregnanolone and allotetrahydrodeoxycorticosterone, and its deregulation by Aβ could present another link to development of AD as these neurosteroids are important to the maintenance of the neuronal excitability [45].

Interaction between ABAD and Aβ also leads to upregulation of protein endophilin I (Ep-I), which is known to active JNK (c-Jun N-terminal protein kinase) and consequently the mitochondrial apoptotic pathway. The increased activation JNK pathway has been connected to AD pathophysiology for some time and Ep-I could therefore present a link between JNK activation and Aβ toxicity [59, 60].

1.2.4 ABAD as a therapeutical target

Based on the knowledge of ABAD-Aβ interaction and its consequences two possible strategies for AD treatment arise; prevention of ABAD-Aβ interaction or inhibition of ABAD enzymatic activity.

Lustbader *et al.* established that the ABAD-Aβ interaction is a suitable therapeutical target by using the ABAD-decoy peptide (ABAD-DP) [50]. ABAD-DP mimics the binding region of ABAD for Aβ (loop D) and has similar binding affinity for Aβ as the native enzyme. *In vitro* studies found ABAD-DP sequestered Aβ making it unable to interact with ABAD. When tested in cell culture experiments, ABAD-DP ameliorated the mitochondrial impairment caused by Aβ and its cytotoxicity. Transgenic AD mice treated with ABAD-DP displayed improved cognitive function [50, 61, 62].

In search for small molecule inhibitors of ABAD-Aβ interaction Xie *et al.* performed an *in vitro* screening, which lead to identification of frentizole (an FDA approved immunosuppressant; Fig. 5). Consequently, a series of frentizole analogues was prepared and *in vitro* tested for their ability to counteract the ABAD-Aβ interaction with compounds **5h** and **5l** being the best hits (Fig. 6) [51]. Unfortunately, there is no data showing, whether these compounds are able to ameliorate Aβ toxicity.

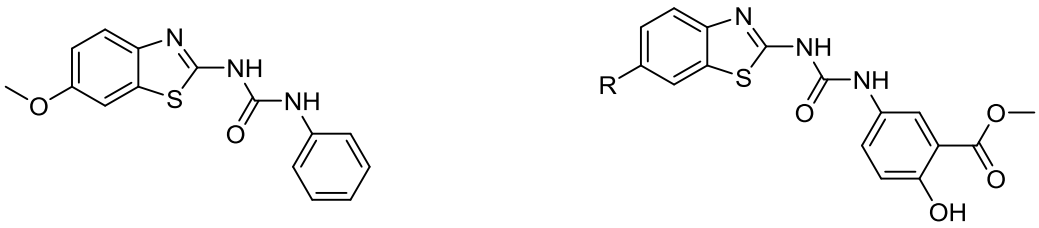

frentizole
IC_{50} = 200 μM

5h R = F; IC_{50} = 6.56 μM
5l R = Cl; IC_{50} = 6.46 μM

Figure 6: Structures and IC_{50} values of ABAD-Aβ interaction inhibitors.

Since ABAD enzymatic activity is necessary for enhancing Aβ toxicity, ABAD inhibitors could also be used as therapeutics for AD. However, some side effects may be encountered by the use of such treatments as this may potentially cause the inhibition of the enzyme's physiological functions. Currently only limited number of specific small molecule ABAD inhibitors are known (Fig. 7). AG18051 is an irreversible inhibitor creating a covalent adduct with the cofactor NAD^+ inside the active site. It has been shown to decrease Aβ toxicity at the cellular level [49, 63]. The compound named RM-532-46 is a reversible ABAD inhibitor with a steroid structure [64]. Recently, phosphonate-benzothiazole inhibitor (**4b**) with moderate activity have been identified and tested *in vitro* for its ability to ameliorate Aβ cytotoxicity with promising results [65].

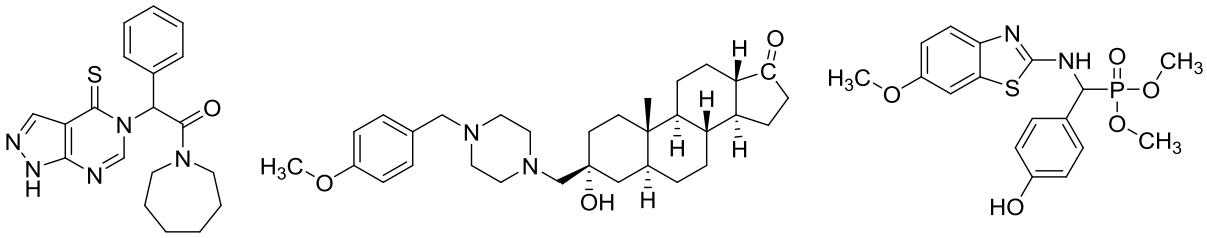

AG18051
IC_{50} = 0.092 μM

RM-532-46
IC_{50} = 0.55 μM

phosphonate-benzothiazole **4b**
IC_{50} = 52.7 μM

Figure 7: Structures and IC_{50} values of known ABAD inhibitors.

Additionally to AD treatment ABAD inhibition could also be employed in treatment of certain types of prostatic cancer, where overexpression of ABAD takes place allowing the cancer cells to generate 5α-dihydrotestosterone in the absence of testosterone [45, 66].

Eventually, irrespective of their therapeutic applications, inhibitors of the ABAD enzyme are likely to be of use in a research setting, as tools to aid our understanding of the cellular role of the ABAD enzyme and the consequences of a complete or partial loss of enzyme activity.

1.3 Multitarget-directed ligands

The ‘‘one-target one-compound’’ paradigm was highly successful in the past for many common diseases, as their molecular mechanisms were revealed and thus biologists were able to define the key target for a particular disease. Once the target was identified, medicinal chemists strategically designed a molecule to interact selectively with such a target, with a potential drug as the outcome. However, it is apparent that this target-based approach does not always guarantee success. Drugs directed to a single target might not always modify complex multifactorial diseases such as AD, even if they act in the way they are expected to proceed [67]. It is now widely accepted that a more effective therapy could result from the use of multipotent compounds able to intervene simultaneously in the different pathological events underlying the aetiology of AD [68, 69].

These so called multitarget-directed ligands (MTDLs) include dually acting inhibitors of AChE and MAO. Inhibitors of AChE are used for AD treatment for more than 20 years based on the cholinergic theory of AD described earlier in the text.

Monoamine oxidase (MAO; EC 1.4.3.4), an enzyme localised on the cytosolic side of OMM [70], is another important target that was considered for the treatment of AD because some symptoms of AD are due to alterations in the dopaminergic, serotoninergic and other monoaminergic neurotransmitter systems [71, 72]. Moreover, MAO catalysed oxidative deamination gives arise to production of hydrogen peroxide and, consequently, reactive oxygen species that have also been implicated in the progress of AD [73]. MAO inhibitors (MAOI) should increase monoaminergic neurotransmission and reduce reactive oxygen species formation, both effects potentially valuable for the treatment of AD [69, 72]. Thus, in this context, multipotent molecules able to simultaneously bind both ChEs and MAOs have been investigated [74–77].

2 Aim of the work

1) *To summarize current knowledge of AD with regard to Aβ-induced mitochondrial impairment and the role of mitochondrial enzyme ABAD in these processes.*

Despite being subject of intensive research, the pathogenic mechanisms of AD are still not fully understood and consequently an effective treatment is yet to be developed. Increased levels of A*β* and mitochondrial dysfunction are both typical pathological hallmarks of AD and potential connection between the two processes has been the topic of several studies. Within these studies mitochondrial enzyme ABAD was frequently mentioned as potential target for addressing mitochondrial dysfunction in AD. However, a clear summary of current knowledge in the field has not been published yet.

2) *To design and synthesize novel compounds, modulators of mitochondrial enzymes, as potential AD therapeutics.*

For the potential drug targets identified in the aforementioned literature review the novel small molecule modulators with potential to antagonize pathological processes in AD would be designed. As a starting point for the design known modulators / binding partners of the respective proteins would be used and their structure would be modified in order to get the desired activity or to improve their activity. The structural design would consider the physical-chemical properties of the compounds, which are crucial for the ability to cross biological membranes in order to reach target proteins. The consequent series would be designed based on the results of biological assessment of the previous series and their SAR studies. If possible, compounds of the initial series would be also designed so they can be easily synthesized in good yields from cheap and well available precursors. This would form basis for the preparation of follow-up series which should become more structurally comprehensive, and which would require more synthetic steps with expected lower yields.

3) *To establish structure-activity/toxicity relationship for the prepared compounds.*

The structure-activity/toxicity relationship studies would be performed in order to identify chemical moieties and structural motifs responsible for evoking a target biological effect. This allows rational modification of the parent compounds in order to improve their activity resp. decrease their toxicity. Information on the key structural motifs also enables designing of compounds with improved physical-chemical properties or decreased structural complexity without negative influence to the biological activity.

3 Results and Discussion

3.1 The design, synthesis and evaluation of benzothiazolyl urea analogues as inhibitors of the amyloid binding alcohol dehydrogenase

(based on attachment III)

Amyloid-beta peptide (A*β*), thought to be the main causative factor for the development of Alzheimer's disease, has been shown to interact with the mitochondrial amyloid beta-binding alcohol dehydrogenase (ABAD). *In vitro* experiments have shown this interaction to be cytotoxic and that enzyme activity is necessary for hallmarks of this cytotoxicity to be observed. Thus, the direct inhibition of the ABAD may be of therapeutic merit in treating Alzheimer's disease (AD).

3.1.1 Design

The currently known ABAD inhibitors (Fig. 8) have intrinsic properties which will likely render them poor drug candidates. Compound AG18051 (**1**) has been shown to form a covalent adduct to NAD^+ within the active site of the ABAD enzyme, altering the conformation of the Rossmann fold motif and preventing substrate binding [49]. As the Rossmann fold is a common structural feature and NAD^+ acts as a cofactor for a great many enzyme catalysed reactions, specificity of action is likely to be a problem with this inhibitor molecule. Similarly, due to the propensity for many enzymes to catalyse the interconversion of such steroidal scaffolds, compound RM-532-46 (**2**) is likely to also suffer from problems related to specificity. Whilst phosphonate derivatives of the benzothiazole core (**3**) have been shown to be capable of directly inhibiting the ABAD enzyme, they do so poorly, with the most potent published to date having an IC_{50} value of 52.7 μM [78]. As such, there is clearly a need for new more potent inhibitor molecules, which lack the intrinsic problems associated with the previously described compounds. Thus, we have focussed on generating more potent inhibitors based around the benzothiazole scaffold.

However, instead of phosphonate derivatives we decided to start with frentizole (**6**), resp. to replace the phosphonate linker with urea (Fig. 8 and 9). Frentizole analogues (**4**, **5**) were originally found to be low micromolar inhibitors of ABAD-A*β* interaction [51] and so we assumed that once these compounds have good binding affinity towards the ABAD enzyme, they could serve as a starting point in development of inhibitors with improved potency compared to the benzothiazole-phosphonates.

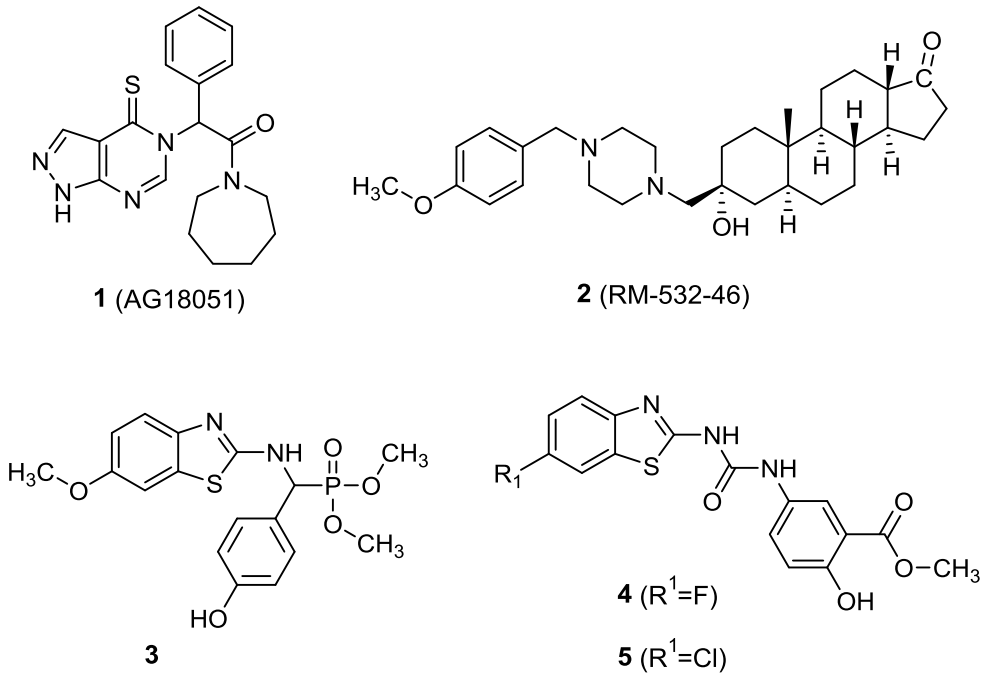

Figure 8: Direct inhibitors of the ABAD enzyme (**1**-**3**) or ABAD-A*β* interaction (**4**-**5**).

Our aim was to produce novel molecules which are able to inhibit the ABAD enzyme via a reversible mechanism, are able to penetrate the blood-brain barrier (BBB) (based upon calculated physical-chemical properties), and are more potent than the previously described benzothiazole-phosphonate inhibitors (**3**). To guide subsequent design strategies, the drug like properties for compounds known to either inhibit the ABAD enzyme directly or to perturb the ABAD-A*β* interaction were firstly calculated. The most potent compounds from the literature (**1**–**5**) were used for this purpose (Table 2). Several of the commonly used rules for assessing drug like behaviour were found to be violated, predicting poor pharmacokinetics [79–81]. Most notably, poor membrane permeability (high tPSA), high plasma binding ($ClogD_{7.4}$) and high pK_a values were predicted for the selected compounds (**1**–**5**).

In the first series of novel compounds (**7**–**32**, Fig. 9), the 6-halogen substitution on the benzothiazole (R^1) was retained identical to **4** and **5** and substitutions were made to the phenyl moiety ($R^{2\text{-}5}$). Both hydrophilic (hydroxy, carboxy) and hydrophobic moieties (chloro, ethylcarboxy, methoxy, methylcarbonyl, methylcarboxamide, phenoxy) were used. In this first series the adherence to drug like descriptors was initially relaxed with the aim of generating lead compounds for further development. Despite this, compared to the parent compounds (**2**–**4**), our novel molecules were predicted to have more favourable characteristics including lower M_W, lower tPSA, lower $ClogP/ClogD_{7.4}$ and in some cases higher solubility ($ClogS_{7.4}$).

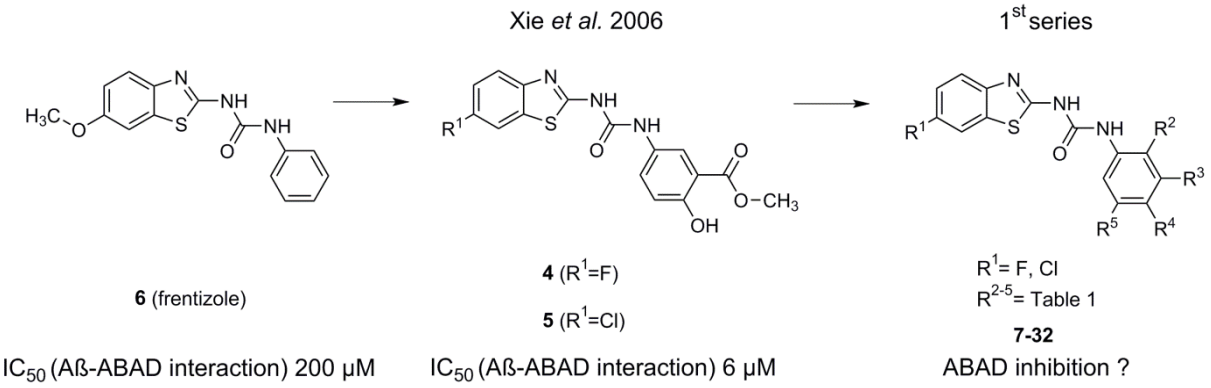

Figure 9: Design of 1st series of novel ABAD inhibitors.

A second series of novel compounds (**33**–**43**) were designed on the basis of the *in vitro* results obtained from the first (Fig. 10; Table 2). The 6-chlorobenzothiazole was retained and the phenyl moiety (R^{2-5}) was modified with the functional groups associated with inhibitory activity in the first series (chloro, hydroxy). These groups were used in various positions/ratios and further combined with other moieties (methoxy, carboxy) to generate a broader structural pool. If compared to the parent compounds (**2**–**4**), these novel structures were predicted to have similar M_W, lower tPSA, higher ClogP/Clog$D_{7.4}$ and in some cases lower solubility (Clog$S_{7.4}$).

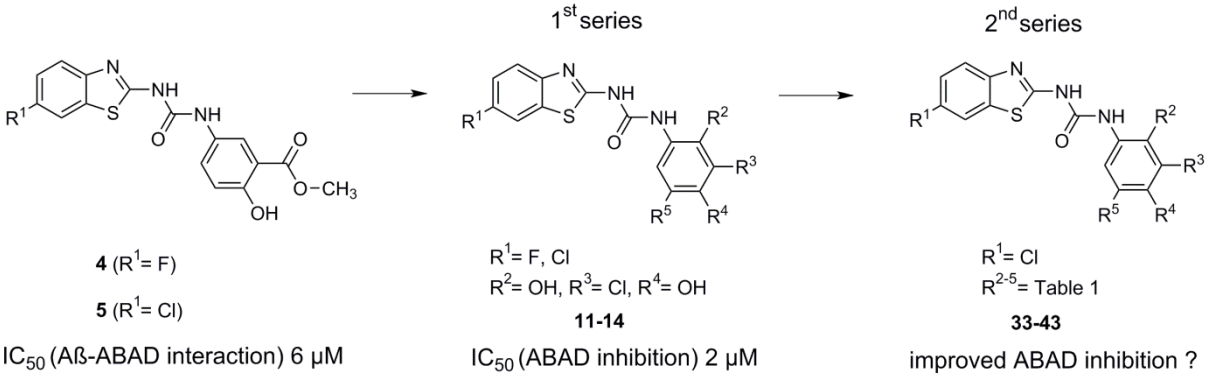

Figure 10: Design of 2nd series of novel ABAD inhibitors.

Table 2: Structure and calculated physical-chemical properties (ACDLabs PhysChem Suite v.12) of known and designed ABAD inhibitors.

Compound	R^1	R^2	R^3	R^4	R^5	M_w	H-bond acceptor/donor	Rotatable bonds	tPSA (Å^2)	ClogP	$ClogD_{7.4}$	$ClogS_{7.4}$	CpK_a
Optimal properties for CNS penetration [79–81]						**<450**	**<7 / <3**	**<8**	**<60-70**	**1-5**	**0-3**	**>(-4.5)**	**7.5–10.5**
1 (AG18051)	---	---	---	---	---	367.47	6/1	3	96.68	2.43	2.36	-4.22	8.80
2 (RM-532-46)	---	---	---	---	---	494.71	5/1	5	53.01	4.21	3.86	-3,31	14.67
3	OMe	---	---	OH	---	394.38	7/2	7	128.00	2.75	2.75	-3,54	9.42
4	F	---	COOMe	OH	---	361.35	7/3	4	128.79	3.73	3.26	-4.28	7.92
5	Cl	---	COOMe	OH	---	377.80	7/3	4	128.79	4.29	3.70	-4.68	7.74
6 (frentizole)	OMe	---	---	---	---	299.35	5/2	3	91.49	3.18	2.50	-3.72	7.02
1st series													
7	F	---	---	OH	---	303.31	5/3	2	102.49	2.80	2.43	-4.17	8.18
8	Cl	---	---	OH	---	319.77	5/3	2	102.49	3.40	2.92	-4.39	8.00
9	F	---	OH	---	---	303.31	5/3	2	102.49	2.90	2.52	-3.73	8.00
10	Cl	---	OH	---	---	319.77	5/3	2	102.49	3.60	3.11	-4.22	7.82
11	F	OH	---	---	---	303.31	5/3	2	102.49	2.91	2.23	-3.41	7.86
12	Cl	OH	---	---	---	319.77	5/3	2	102.49	3.50	2.68	-4.19	7.68
13	F	---	Cl	OH	---	337.76	5/3	2	102.49	3.77	3.12	-4.56	7.69
14	Cl	---	Cl	OH	---	354.21	5/3	2	102.49	4.33	3.54	-4.92	7.51
15	F	---	COOH	OH	---	347.32	7/4	3	139.79	3.39	-0.07	-1.11	3.07
16	Cl	---	COOH	OH	---	363.78	7/4	3	139.79	3.90	0.36	-1.6	3.07
17	F	---	---	OMe	---	317.34	5/2	3	91.49	3.21	2.84	-4.79	8.05
18	Cl	---	---	OMe	---	333.79	5/2	3	91.49	3.89	3.42	-4.95	7.87
19	F	---	OMe	OMe	---	347.36	6/2	4	100.72	3.08	2.61	-4.5	7.88
20	Cl	---	OMe	OMe	---	363.82	6/2	4	100.72	3.71	3.12	-4.58	7.71
21	F	---	COOH	OMe	---	361.34	7/3	4	128.79	3.23	-0.05	-1.69	4.01
22	Cl	---	COOH	OMe	---	377.80	7/3	4	128.79	3.63	0.26	-1.89	4.01
23	F	---	---	OPh	---	379.41	5/2	4	91.49	4.85	4.46	-5.29	8.01

Table 2 continued: Structure and calculated physical-chemical properties (ACDLabs PhysChem Suite v. 12) of known and designed ABAD inhibitors.

Compound	R^1	R^2	R^3	R^4	R^5	M_w	H-bond acceptor/donor	Rotatable bonds	tPSA (Å^2)	ClogP	ClogD$_{7.4}$	ClogS$_{7.4}$	CpK_a
Optimal properties for CNS penetration [79–81]						**<450**	**<7 / <3**	**<8**	**<60-70**	**1-5**	**0-3**	**>(-4.5)**	**7.5–10.5**
24	Cl	---	---	OPh	---	395.86	5/2	4	91.49	5.44	4.94	-5.75	7.83
25	F	---	---	COOH	---	331.32	6/3	3	119.56	3.36	0.42	-1.82	4.29
26	Cl	---	---	COOH	---	347.78	6/3	3	119.56	3.93	0.89	-2.35	4.29
27	F	---	---	COOEt	---	359.37	6/2	5	108.56	3.83	3.78	-5.29	7.77
28	Cl	---	---	COOEt	---	375.83	6/2	5	108.56	4.50	4.42	-5.9	7.59
29	F	---	---	COMe	---	329.35	5/2	3	99.33	3.17	3.11	-4.85	7.72
30	Cl	---	---	COMe	---	345.80	5/2	3	99.33	3.80	3.72	-5.73	7.54
31	F	---	---	NHCOMe	---	344.36	6/3	3	111.36	2.45	2.22	-4.34	8.01
32	Cl	---	---	NHCOMe	---	360.82	6/3	3	111.36	3.05	2.74	-4.92	7.84
2nd series													
33	Cl	---	Cl	---	---	338.21	4/2	2	82.26	4.90	4.27	-5.83	7.65
34	Cl	---	---	Cl	---	338.21	4/2	2	82.26	4.67	4.07	-5.79	7.69
35	Cl	---	Cl	Cl	---	372.65	4/2	2	82.26	5.40	4.57	-6.27	7.39
36	Cl	Cl	---	OH	---	354.20	5/3	2	102.49	4.33	3.50	-3.66	7.44
37	Cl	---	Cl	OMe	---	368.23	5/2	3	91.49	4.91	4.30	-5.72	7.67
38	Cl	---	Cl	COOH	---	382.22	6/3	3	119.56	4.67	1.15	-2.77	3.09
39	Cl	---	Cl	OH	Cl	388.65	5/3	2	102.49	5.01	3.71	-5.07	7.17
40	Cl	---	Cl	OMe	Cl	402.68	5/2	3	91.49	5.59	4.83	-6.59	7.48
41	Cl	---	COOH	OH	Cl	398.21	7/4	3	139.79	4.97	1.23	-2.09	2.42
42	Cl	---	COOH	OMe	Cl	412.24	7/3	4	128.79	4.48	0.92	-2.51	3.64
43	Cl	OH	---	OH	---	335.76	6/4	2	122.72	2.97	2.36	-3.96	7.64

3.1.2 Synthesis

The aforementioned compounds were prepared in a two-step process. Firstly, the corresponding benzothiazol-2-amine was treated with 1,1'-carbonyldiimidazole to form an imidazolyl intermediate. The produced imidazolyl intermediate was then treated with the corresponding substituted aniline (Scheme 2) [82–85]. In the case of compounds **41** and **42** the corresponding aniline derivatives were not commercially available and thus they were prepared in a two or three-step process. Firstly, 3-chloro-2-methoxybenzoic acid was nitrated [86] in position 5 to give 3-chloro-2-methoxy-5-nitrobenzoic acid, the nitro group was then reduced [87] to obtain the corresponding aniline derivative. In the case of compound **41**, demethylation of the methoxy group was performed using $AlCl_3$ [88] prior to the reduction step (Scheme 3). The two most active compounds described by Xie *et al.* (compounds **4**–**5**) [51] and frentizole (**6**) were also synthesized for the purpose of comparative biological evaluation.

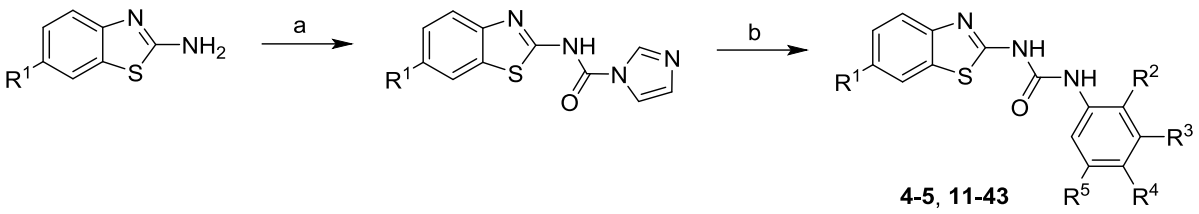

Scheme 2: Synthesis of benzothiazolylurea analogues. Reagents and conditions: (a) CDI, DMF/DCM, reflux; (b) substituted aniline, DMF/Et_3N, rt.

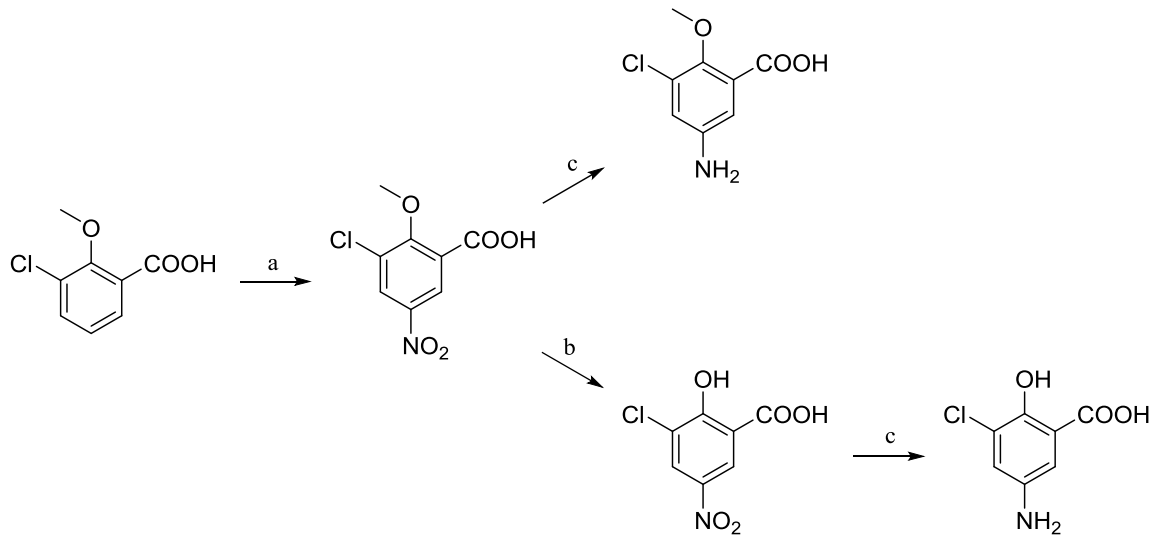

Scheme 3: Synthesis of aniline intermediates. Reagents and conditions: (a) HNO_3, H_2SO_4, 0°C–rt; (b) $AlCl_3$, DCM, reflux; (c) H_2, Pd/C, EtOAc, rt.

3.1.3 Results and Discussion

The ability of the synthesised compounds to modulate ABAD activity was assessed via a spectrophotometric based technique [89]. In brief, during the conversion of substrate to product, NADH is converted to NAD^+. NADH absorbs light at 340 nm, whilst NAD^+ does not; thus ABAD activity can be measured via a decrease in absorbance at 340 nm as NADH is oxidised. Varying concentrations of compound was added to the reaction mixture to assay any potential inhibitory effects.

An initial compound screen was performed using each compound at 100 µM. For the benzothiazolyl standards (**4**–**6**) and the first compound series (**7**–**32**), an initial screen was performed using each compound at 100 µM (Table 3). The compounds previously published as inhibitors of ABAD-A*β* interaction (**4**, **5**) [51] and the precursor frentizole molecule (**6**) were found to be ineffective as ABAD inhibitors. Novel compounds **9, 11–14** and **16** were found to be capable of markedly decreasing the activity of the ABAD with notably high inhibition by compounds **13**, **14**. A subsequent compound screen was performed at 25 µM in an attempt to isolate the most potent inhibitors. At this lower concentration compounds **12–14** showed less marked inhibition, while compounds **13**, **14** retained a similar level of inhibition as that was seen at 100 µM. In terms of structure activity relationships for the first series, various substitutions of the phenyl moiety were found to notably affect the potency of the compounds in modulating ABAD activity. At 100 µM the compounds with phenolic moiety alone (**9**, **11**, **12**) or in combination with electron withdrawing group (EWG; **13**, **14**, **16**) at various positions significantly decreased enzyme activity. For halogen substitution at position six of the benzothiazole moiety, neither fluorine (**13** vs. **14**) nor chlorine (**11** vs. **12**) gave a consistent alteration in enzyme activity. More interestingly at 25 µM, the inhibitory nature was retained with a phenolic moiety in position two (**12**) or four accompanied by an EWG (**13**, **14**) consisting of a halogen, but not a carboxyl moiety (**16**).

The inhibitory ability of **13**, **14** led to the design of second compound series (**33**–**43**) retaining the 6-chlorobenzothiazolylurea and changing the phenyl scaffold by using chlorine alone, chlorine with a methoxy/carboxy moiety, chlorine with a phenolic moiety or a phenolic moiety alone to identify further effective leads. At 100 µM, compounds **36**, **39**, **41** and **43** resulted in inhibition of the ABAD enzyme with compound **39** being the most potent from the second series. Similarly at 25 µM, compounds **36**, **39**, **41** and **43** retained some inhibitory ability with compound **39** being the most potent. From the structural point of view, the introduction of a chlorine moiety alone (**33**–**35**) or chlorine with a methoxy/carboxy moiety (**37**, **38**, **40**, **42**) led to a complete loss of inhibitory activity. On the other hand, the combination of chlorine with a phenolic moiety (**36**, **39**, **41**) or a phenolic moiety alone (**43**) showed increased potency. The best results were obtained for a four positioned phenolic moiety in combination with a chlorine in position two (**36**) or two chlorines in position three

and five (**39**). Taken together with the first series, the 6-halogen benzothiazolylurea scaffold bearing a combination of a four positioned phenolic moiety with one or two chlorines was found the most potent for the direct inhibition of the ABAD enzyme. Three compounds (**13**, **14**, **39**) were found to markedly inhibit ABAD *in vitro*.

Table 3: Relative ABAD activity in the presence of the synthesised compounds.

Compound	100 µM (% of Control ± SEM)	25 µM (% of Control ± SEM)	Compound	100 µM (% of Control ± SEM)	25 µM (% of Control ± SEM)
Control	100 ± 3.21	100 ± 1.83	**24**	102.55 ± 2.30	107.42 ± 1.93
4	95.47 ± 2.10	97.23 ± 3.84	**25**	101.97 ± 2.47	107.80 ± 1.75
5	97.24 ± 1.98	95.62 ±4.49	**26**	94.25 ± 2.27	105.50 ± 1.68
6 (frentizole)	105.39 ± 3.04	97.88 ± 3.51	**27**	104.85 ± 2.53	110.28 ± 1.71
7	91.02 ± 1.98	94.42 ± 1.13	**28**	105.39 ± 2.77	108.56 ± 2.21
8	98.56 ± 4.53	91.93 ± 1.93	**29**	108.98 ± 1.19	114.67 ± 5.35
9	83.84 ± 0.76	94.80 ± 0.97	**30**	95.04 ± 5.15	99.31 ± 3.24
10	91.20 ± 2.17	93.58 ± 1.87	**31**	100.00 ± 3.64	94.70 ± 3.27
11	57.63 ± 1.73	91.46 ± 1.51	**32**	97.85 ± 1.44	97.88 ± 3.40
12	40.57 ± 1.14	77.06 ± 0.99	**33**	99.75 ± 5.16	102.25 ± 2.73
13	31.06 ± 0.81	39.76 ± 0.48	**34**	94.78 ± 5.14	100.74 ± 2.41
14	33.93 ± 0.95	38.61 ± 0.70	**35**	90.56 ± 6.27	97.42 ± 2.31
15	92.82 ± 2.94	101.30 ± 1.61	**36**	41.22 ± 22.11	72.43 ± 5.79
16	78.64 ± 2.21	100.54 ± 1.05	**37**	105.70 ± 2.81	97.21 ± 2.47
17	107.72 ± 2.99	110.95 ± 1.84	**38**	85.41 ± 3.60	97.70 ± 1.83
18	106.10 ± 2.11	104.55 ± 1.16	**39**	31.22 ± 2.05	36.82 ± 1.12
19	99.10 ± 1.95	103.59 ± 1.91	**40**	99.28 ± 5.58	96.35 ± 1.76
20	104.31 ± 4.48	104.36 ± 1.45	**41**	51.47 ± 1.94	81.34 ± 1.91
21	102.15 ± 3.75	105.50 ± 1.48	**42**	87.80 ± 1.77	94.07 ± 1.60
22	97.31 ± 2.40	107.22 ± 2.54	**43**	58.39 ± 2.50	86.42 ± 1.45
23	103.59 ± 2.94	108.75 ± 2.20			

To further assess the potency of compounds **13**, **14** and **39**, ABAD activity was measured in the presence of increasing concentrations of each inhibitor and relative IC_{50} values were calculated. Relative IC_{50} values of 1.89 µM (95% confidence interval 1.52 – 2.35 µM), 1.67 µM (95% confidence interval 1.30 – 2.13 µM) and 1.94 µM (95% confidence interval 1.78 – 2.10 µM) were found for compounds **13**, **14** and **39** respectively (Fig. 11). Compared to previously described benzothiazole phosphonates inhibitors (the best of which had IC_{50} 52.7 µM) [78], compounds **13**, **14** and **39** were found to be more potent with IC_{50} values of approximately 2 µM, although limited solubility means

only relative IC_{50} values could be generated. Compound **39** was found to have similar potency to compounds **13**, **14** despite having increased ClogP/ClogD values and decreased solubility. Thus in terms of ligand efficiency it was deemed as a less promising lead and so it was excluded from further analysis.

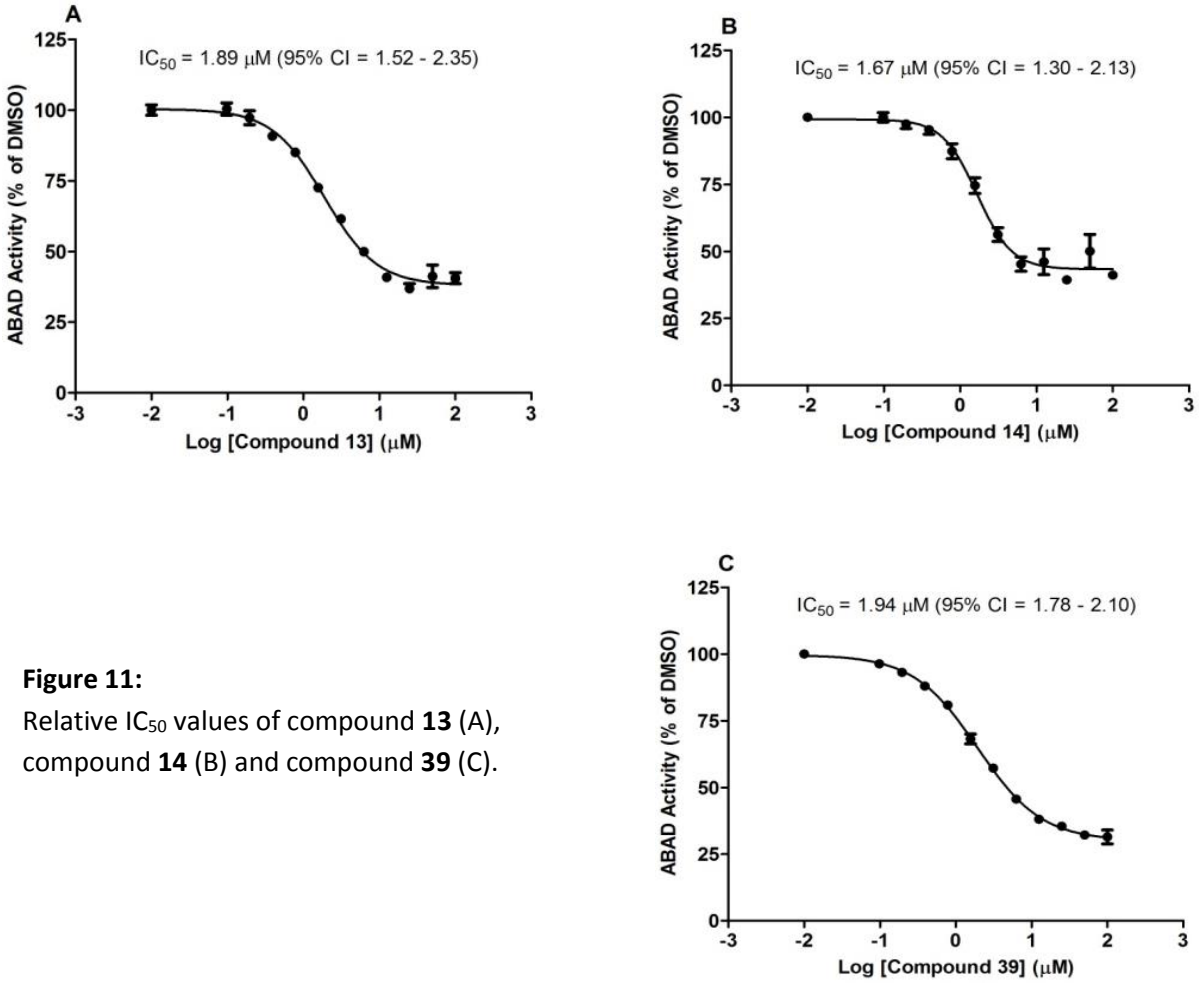

Figure 11:
Relative IC_{50} values of compound **13** (A), compound **14** (B) and compound **39** (C).

The presented ABAD inhibitors were designed to conform to the attributes associated with successful CNS penetration, improving previous benzothiazolyl compounds [79]. For this purpose, the physical chemical parameters of novel molecules were first calculated *in silico* (Table 2). To test the validity of the predicted physical chemical data, experimental values of ElogP and ElogD were determined for compounds **13**, **14** (Table 4). The calculated and experimental values for logP/D were found to correlate well, validating the predicted physical chemical properties.

Table 4: Correlation of calculated (ACDLabs PhysChem Suite v. 12) and experimental physical chemical properties for compounds **13** and **14**.

Compound	ClogP	ELogP±SD	ClogD7.4	ELogD7.4±SD
13	3.77	3.04 ± 0.35 ‰	3.12	3.02 ± 1.83 ‰
14	4.33	3.81 ± 0.29 ‰	3.54	3.79 ± 0.92 ‰

The mechanism of inhibition utilised by compounds **13**, **14** was investigated by assessing their effect on the kinetic parameters V_{max} and K_m at two concentrations (1.25 µM and 5 µM). Initial experiments utilised a fixed concentration of cofactor, NADH and increasing concentrations of substrate, acetoacetyl-CoA. At the lower concentration tested, compound **13** appears to act via a pure non-competitive mechanism, whilst at the higher concentration compound **13** appears to act via a mixed non-competitive mechanism with respect to substrate, acetoacetyl-CoA (Fig. 12A). At both concentrations tested, compound **14** appears to act via a mixed non-competitive mechanism with respect to the substrate (Fig. 12B).

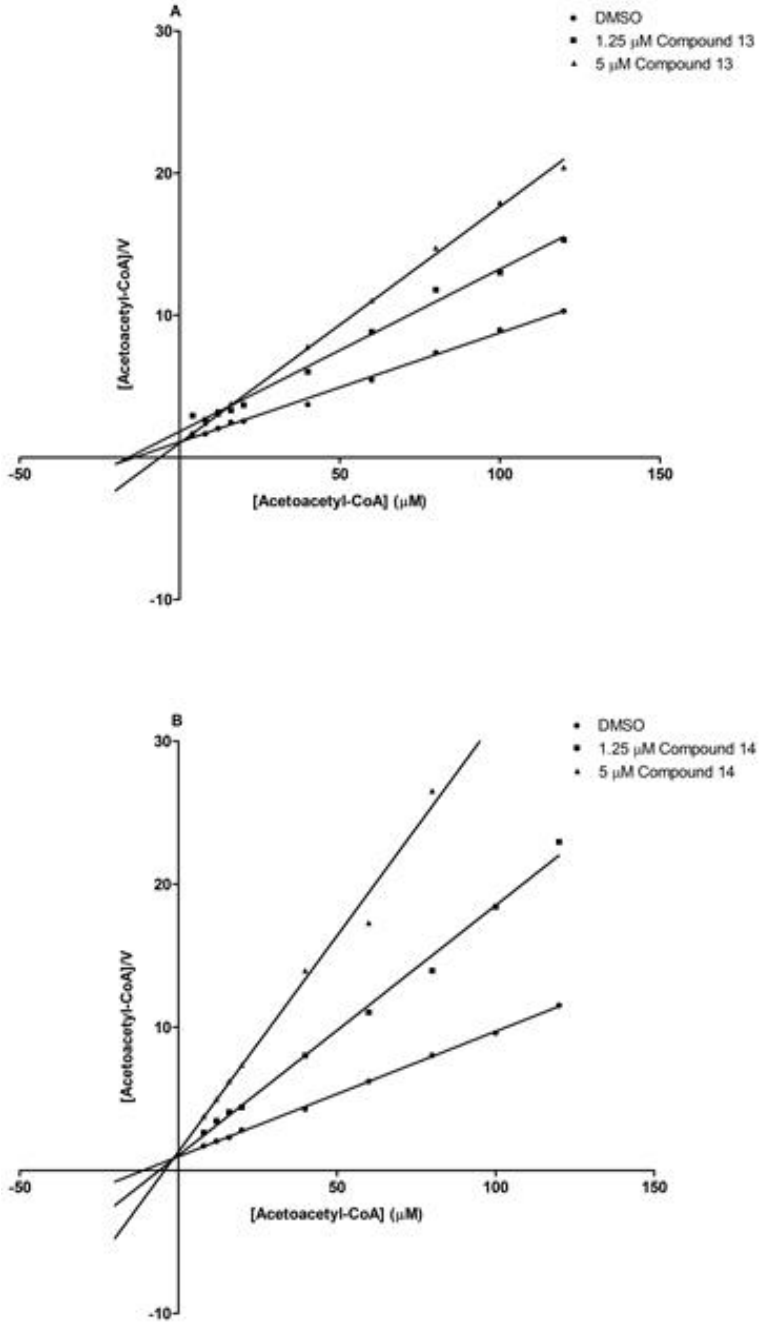

Figure 12: Hanes-Woolf plot of initial velocities of enzyme with the indicated concentrations of acetoacetyl-CoA both in the presence and absence of compounds **13** (A) or **14** (B).

Subsequent experiments utilised a fixed concentration of acetoactyl-CoA and varied cofactor, NADH. At both concentrations tested, compounds **13**, **14** appear to act via a pure non-competitive mechanism with respect to cofactor, NADH (Figure 13). Thus, there is the potential that these compounds are acting outside of the enzyme active site in an allosteric manner, although this remains to be confirmed.

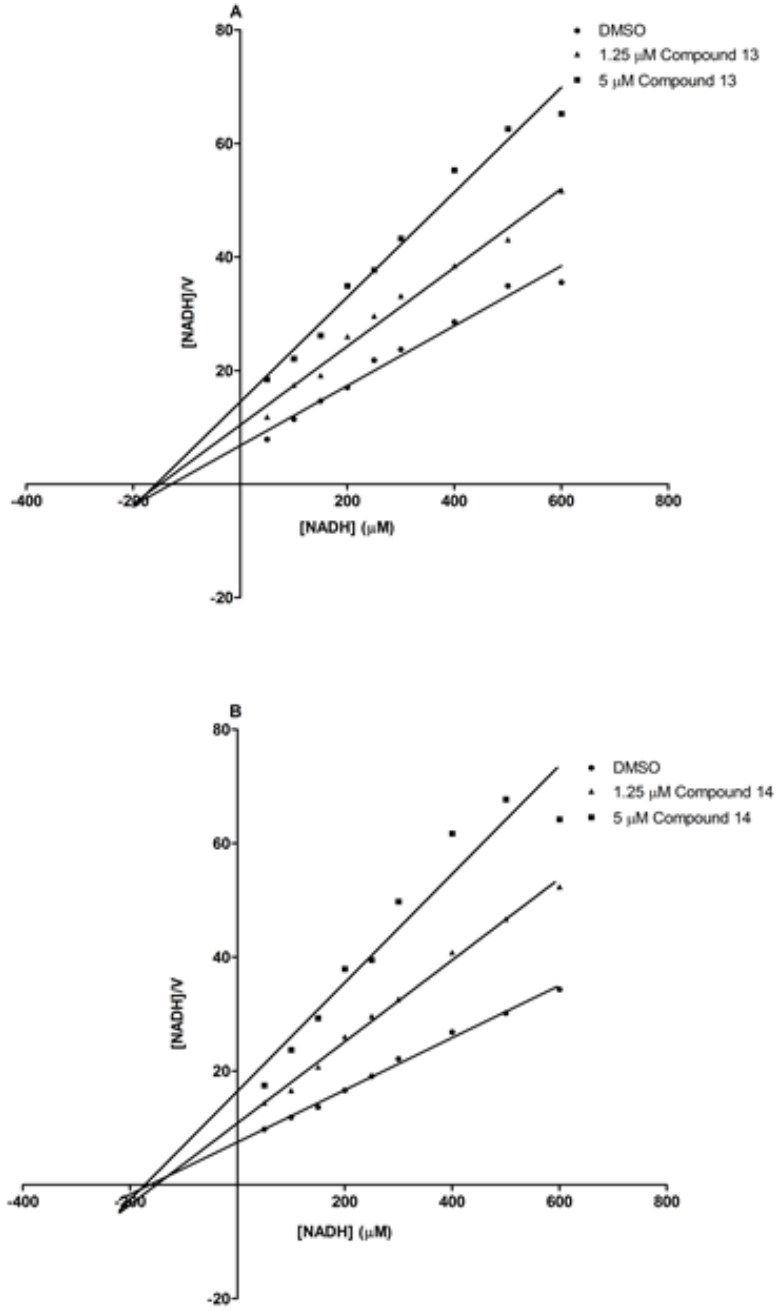

Figure 13: Hanes-Woolf plot of initial velocities of enzyme with the indicated concentrations of NADH both in the presence and absence of compounds **13** (A) or **14** (B).

To assess whether the inhibition of enzyme activity observed with compounds **13**, **14** was reversible or irreversible in nature, the ABAD enzyme was treated with a saturating dose of each molecule and subsequently diluted to yield a non-saturating dose. If reversible in nature, activity would be restored upon dilution. In both cases enzyme activity was restored following dilution (Fig. 14) indicating a reversible mechanism of inhibition for both compounds.

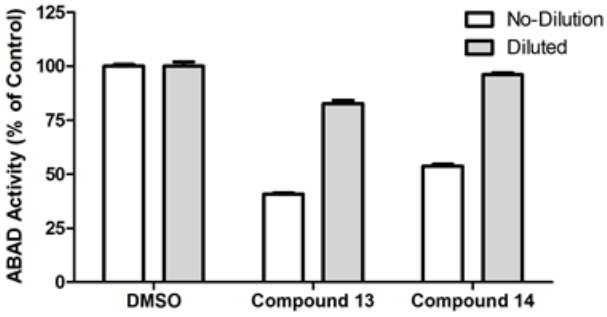

Figure 14: Evaluation of the reversible/irreversible nature of compounds **13** and **14**.

The toxicity of compounds **13**, **14** was assessed using an LDH assay, providing a measure of cell death on the basis of enhanced membrane permeability. Compounds **13**, **14** were both found to be non-toxic in two independent cell lines (HEK293 and SHSY5Y) following a 24 h incubation period (Fig. 15).

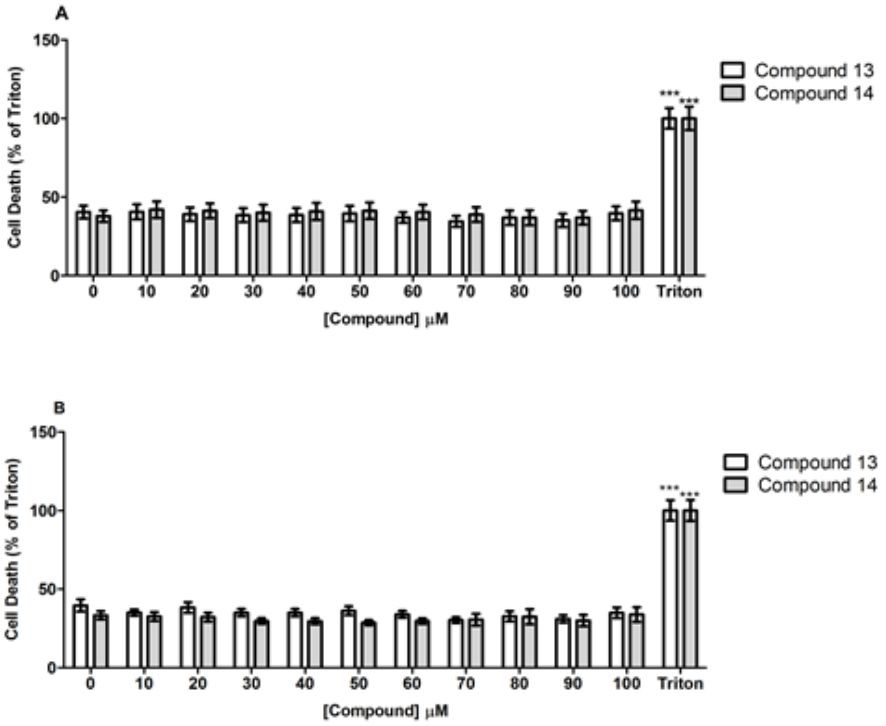

Figure 15: Cytotoxic effects of compounds **13** and **14** on SHSY5Y (**A**) and HEK293 (**B**) cells.

3.1.4 Conclusion

In summary, the novel ABAD inhibitors based on benzothiazolyl urea scaffold were designed to fulfil drug-like properties for CNS acting drugs. 37 molecules were prepared and tested *in vitro*

identifying 3 lead structures (**13**, **14**, **39**) that were found significantly better to parent benzothiazolyl standards. Two lead molecules (**13**, **14**) were further found to possess experimental physical-chemical properties valuable for pharmacokinetics and CNS penetration. They were also found to have non-competitive or mixed non-competitive mechanism of action with respect to the substrate/cofactor. The reversibly binding of both lead molecules was confirmed. Both lead molecules were also highlighted as non-toxic by *in vitro* assay after 24 h. Compounds **13** and **14** may form the basis for the development of subsequent series of more potent ABAD inhibitor molecules for the treatment of Alzheimer's disease.

3.1.5 Appendix

To the 2nd series of compounds presented above logically belong 5 more compounds, which have not yet undergone full biological assessment (Table 5). They are all derived from the most promising compound within the 1st series (**14**) and they are supposed to further broaden the SAR study of the 2nd series.

Table 5: Analogues of **14** and their preliminary inhibitory data.

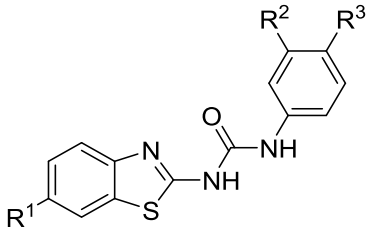

Compound	R^1	R^2	R^3	25 µM (% of Control ± SEM)
44	Cl	---	---	38.8 ± 0.39
45	Cl	OH	OH	11.8 ± 0.23
46	Cl	OMe	OH	26.5 ± 0.43
47	Cl	OH	OMe	40.7 ± 0.81
48	OH	Cl	OMe	nd

Compounds **44**–**47** were prepared using the general synthetic strategy described in Scheme 2, only in case of **45** and **46** the intermediate anilines were first prepared from corresponding nitrobenzene derivatives by palladium catalysed reduction (similar to Scheme 3, step c) [87]. Compound **48** was prepared in three steps (Scheme 4). 3-chloro-4-methoxyaniline was first treated with CDI and resulting intermediate was then reacted 2-aminobenzo[*d*]thiazol-6-ol to give the final

product. The 2-aminobenzo[*d*]thiazol-6-ol was prepared earlier from its precursor by demethylation using $AlCl_3$ [88].

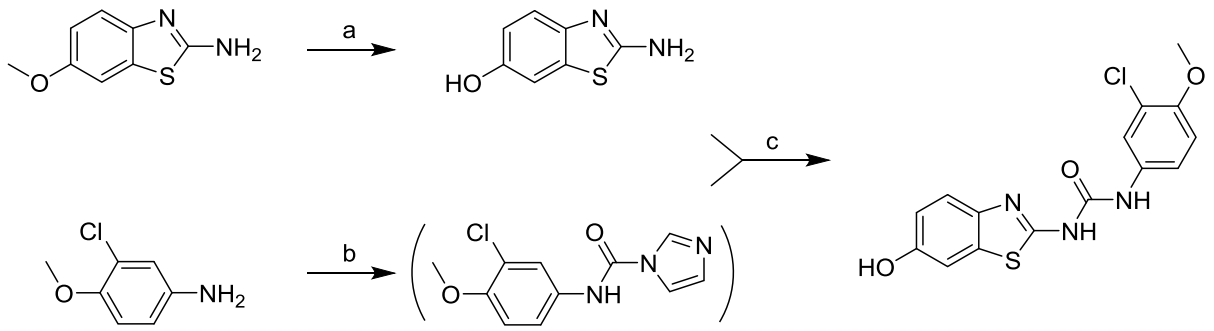

Scheme 4: Synthesis of **48**. Reagents and conditions: (a) $AlCl_3$, anh. toluene, reflux; (b) CDI, DMF, 35°C; (c) DMF, 60 °C.

Preliminary *in vitro* results support the previous finding that four-positioned phenolic moiety is crucial for inhibitory activity and its omission or methylation (**44**, **47**) has negative effect on activity. Looking at compound **45**, it seems that its hydroxyl substitution in position three further increases the inhibitory activity compared to methoxy substitution of **46** or chlorine substitution of parent **14**. Compound **48** was synthesized to check the effect of relocation of the hydroxyl group from the phenyl moiety to the benzothiazole moiety, however, its inhibitory data are not yet available.

The most promising compounds **13**, **14** and **39** were also prepared in form of their salts, sodium phenolates, which showed increased solubility in water and thus they are more suitable for prospective *in vivo* testing.

3.2 Frentizole analogues as inhibitors of ABAD: design, synthesis and *in vitro* evaluation

In this study, a series of new benzothiazolylurea analogues have been designed, prepared and evaluated *in vitro* for their potency to inhibit ABAD enzymatic activity. The most potent compounds have also been tested for their cytotoxic properties and their ability to permeate through blood-brain barrier has been predicted based on their physical-chemical properties.

3.2.1 Design

Design of novel compounds originates from the previously identified ABAD modulator frentizole and its analogues [51, 90, 78]. Our novel compounds consist of three substructural parts i.e. a benzothiazole moiety [91], a linker and a phenyl moiety (Fig. 16). The benzothiazole moiety was substituted in position 6 with a methoxy group (the same as is found in the parent compound frentizole), fluorine or an ethylcarboxyl group to see whether a change in spatial size or lipophilicity in this part of the molecule would result in a change of inhibitory ability. Three different linkers where used to see difference(s) between a hydrophilic urea (H-bond acceptor; present in parent compound frentizole) and guanidine (H-bond donor) linkers and the rather lipophilic thiourea linker. The phenyl moiety was either non-substituted (similar to the parent compound frentizole) or substituted in position 4 with hydrophilic carboxyl and hydroxyl functional groups (capable of creating hydrogen bonds) or rather lipophilic methoxy group. Frentizole was also synthesized as a reference compound.

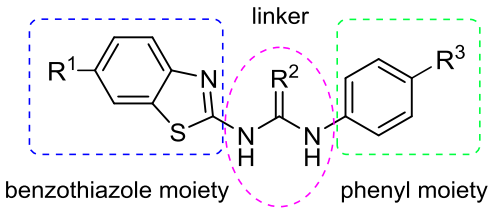

Figure 16: Design of novel frentizole analogues.

3.2.2 Synthesis

Generally, the synthesis started with activation of the corresponding benzothiazol-2-amine using 1,1'-carbonyldiimidazole resp. 1,1'-thiocarbonyldiimidazole. Only the intermediate ethyl 2-aminobenzothiazole-6-carboxylate was prepared before that in a separate step by treating 4-aminobenzoate with potassium thiocyanate and bromine in acetic acid [92]. In the next step, the reactive imidazolyl intermediate was treated with the corresponding aniline to obtain a non-symmetrically substituted urea or thiourea product (Scheme 5).

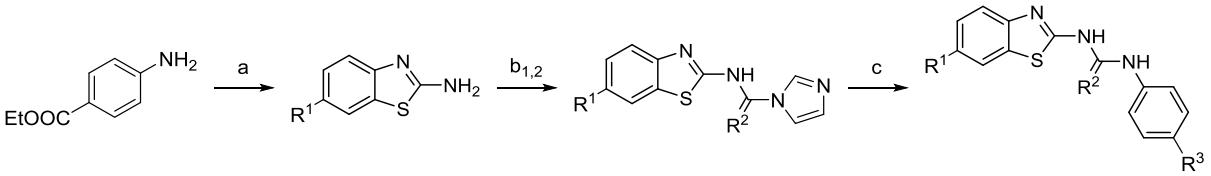

Scheme 5: Synthesis of urea and thiourea derivatives. Reagents and conditions: (a) KSCN, Br_2, AcOH, rt; (b_1) CDI, DCM/DMF, reflux; (b_2) SCDI, MeCN, reflux; (c) aromatic amine, DMF, 60°C.

Guanidine analogues were prepared by treating corresponding thiourea with mercury oxide in methanolic ammonia solution (Scheme 6). Hydrochloride with improved solubility in water (suitable for potential *in vivo* testing) was prepared by stirring guanidine **59** in mixture of diethyl ether and THF saturated by gaseous hydrochloric acid.

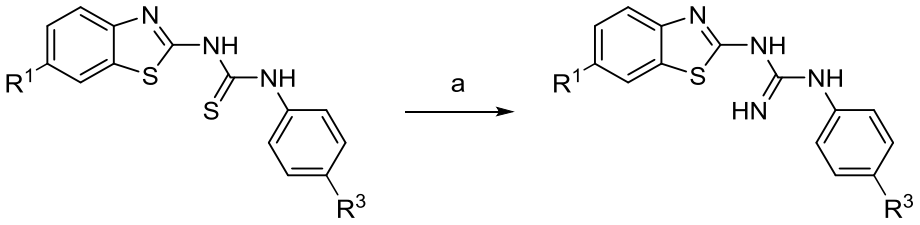

Scheme 6: Synthesis of guanidine analogues. Reagents and conditions: (a) NH_3, HgO, MeOH, rt.

3.2.3 Results and discussion

To assess the ability of the synthesised compounds to modulate ABAD activity, a spectrophotometric assay was employed as outlined in Hroch *et al.* [89]. An initial compound screen was performed using each compound at 100 µM concentration. All compounds tested, except of the standard frentizole, were found to be capable of markedly decreasing the activity of the ABAD enzyme, with nine coumpound (**49**, **51**, **52**, **55**, **56**, **58**–**61**) decreasing the activity by more than 50%. A subsequent compound screen was performed at 25 µM in an attempt to isolate the most potent inhibitors. At this lower concentration, compounds **49**, **52**, **56** and **59** were found to retain a similar level of inhibition as that seen at 100 µM, whilst the remaining inhibitors showed less marked inhibition (Table 6). Establishing of the SAR for the presented set of compounds was, however, a difficult task, as there were no clear correlations between the structure of compounds and their inhibitory activity. The only trend observed was that the thiourea derivatives showed mostly higher potency compared to the ureas and guanidines. Though, the best inhibiton was found for the guanidine **59**. Different susbstitutions of the benzothiazole and/or phenyl moieties of the parent frentizole had their effects on the compounds' activity, but without logical order.

Table 6: Prepared frentizole analogues and their ABAD inhibitory activity.

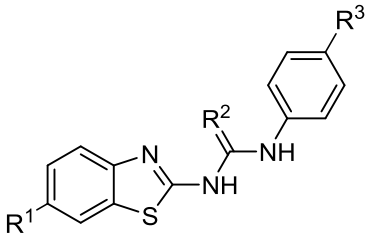

Compound	R^1	R^2	R^3	100 µM (% of Control ± SEM)	25 µM (% of Control ± SEM)
control	---	---	---	100.0 ± 0.11	100.0 ± 0.20
frentizole (**6**)	OMe	O	---	102.9 ± 2.98	97.4 ± 0.82
49	OMe	S	---	34.8 ± 1.42	39.8 ± 0.44
50	OMe	NH	---	61.8 ± 5.87	57.9 ± 3.91
51	F	O	---	41.0 ± 0.61	69.2 ± 0.40
52	F	S	---	23.9 ± 0.69	29.0 ± 0.23
53	F	NH	---	81.0 ± 4.78	86.6 ± 1.43
54	COOEt	O	---	64.3 ± 1.56	79.2 ± 1.60
55	COOEt	S	---	36.6 ± 0.33	45.5 ± 0.33
56	COOEt	NH	---	35.6 ± 2.45	32.0 ± 3.00
57	OMe	O	OMe	62.2 ± 0.93	69.7 ± 0.42
58	OMe	S	OMe	46.9 ± 1.50	60.9 ± 0.74
59	OMe	NH	OMe	17.9 ± 0.71	17.0 ± 0.09
60	OMe	O	COOH	41.1 ± 0.47	62.4 ± 0.29
61	OMe	S	COOH	29.3 ± 0.76	47.0 ± 0.34
62	OMe	NH	COOH	86.0 ± 6.23	104.2 ± 4.32

To further assess the potency of the two most active inhibitors, compounds **52** and **59**, ABAD activity was measured in the presence of increasing concentrations of the two inhibitors and their IC_{50} values calculated using GraphPad Prism. Relative IC_{50} value of 3.062 µM (95% confidence interval 2.692 – 3.483) was found for compounds **59** (Fig. 17).

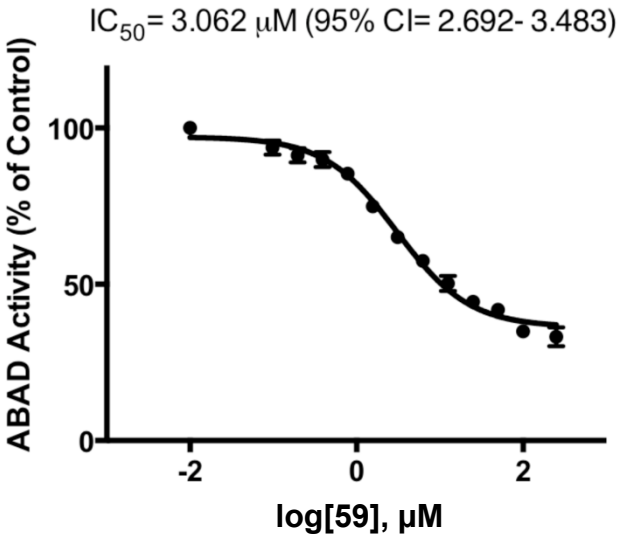

Figure 17: IC_{50} determination for compound **59**.

Compound **52** produced an inconclusive dose response curve and a relative IC_{50} value was unable to be calculated for this compound. Further analysis of this compound revealed that the inhibition was reversed upon the addition of dithiothreitol (DTT), indicating the inhibition is likely due to the formation of a disulphide bond to an active site cysteine residue (Fig. 18). The DMSO control and **59** showed little change in ABAD activity with inhibition remaining constant under the addition of DTT. However compound **52** showed a reversal in ABAD inhibition upon the addition of DTT with activity values nearly returning to the control levels. As many other enzymes exhibit similar properties containing active site cysteine residues this could prove difficult to obtain any compound specificity for ABAD. From this point of view, the thiourea moiety seems to be unlikely used for further design of ABAD inhibitors for the lack of specificity.

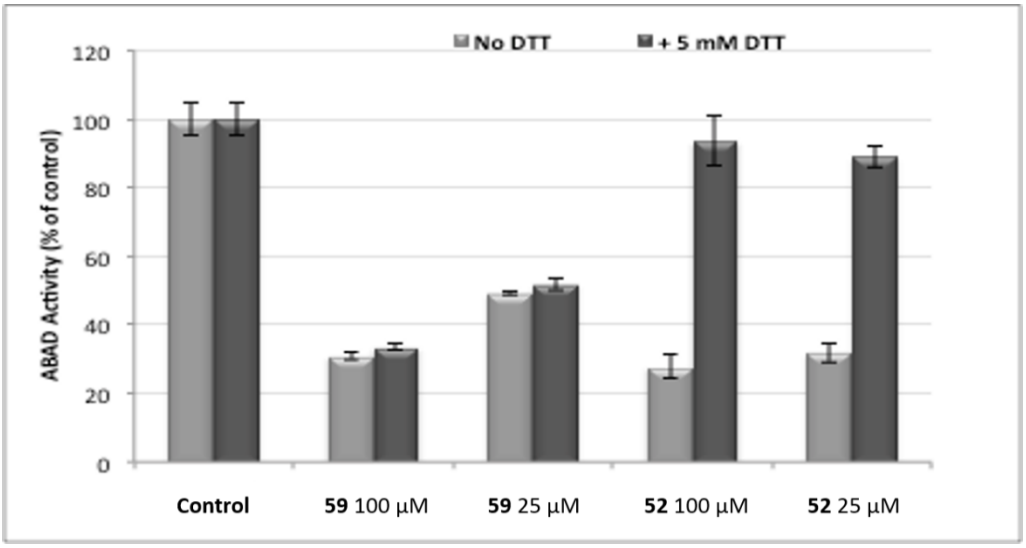

Figure 18: Relative ABAD activity in the presence of each compound at concentrations of 25 µM and 100 µM with and without the addition of 5 mM DTT (presented as % of control ± SEM).

The cytotoxicity of the two most potent inhibitors **52** and **59** was assessed using LDH and MTT assays. Cytotoxicity assessment revealed that compound **59** is one order of magnitude less toxic when compared to **52** using two different assays and that its toxicity is at similar level compared to parent frentizole (Table 7). Similar IC_{50} values obtained for **52** with both methods suggests that the compound does not affect the electron transport chain (ETC) of mitochondria. In the case of **59**, the IC_{50} value obtained via a MTT assay was lower than when compared to the LDH assay result, which could be hypothesized to its influence of ETC. However, only small differences between both assays were found that plausibly means only minor influence of mitochondrial ETC and should be further explored.

Table 7: Cytotoxicity assessment of frentizole and the most promising inhibitors **52** and **59**.

Compound	IC_{50} (µM ± SEM)	
	LDH	MTT
frentizole	46 ± 6	38 ± 4.9
52	3.5 ± 0.2	3.1 ± 0.4
59	51 ± 11	23 ± 6

The physical-chemical properties were calculated (ACDLabs PhysChemSuite 2014 [93]) and/or experimentally measured [94] for the two most potent compounds **52** and **59** and the parent compound frentizole (Table 8). The obtained data were compared with optimal properties for CNS targeted drugs [79–81]. All compounds complied with the optimal values for molecular weight, H-bond acceptor/donor numbers, number of rotatable bonds and logP value. $LogD_{7.4}$ values slightly

diverged from the optimal range in case of **52** and **59** and all three compounds showed higher than optimal values of total polar surface area (tPSA). Regarding solubility, then only compound **52** did not fit the optimal range for the calculated $logS_{7.4}$. Generally, a good correlation between the experimental and calculated logP and $loD_{7.4}$ values was found. Taken together, these data suggest that the compounds could penetrate the blood-brain barrier and so act within the CNS. However, for future structure design, it will be advantageous to improve some of the physical-chemical properties, especially the tPSA.

Table 8: Physical-chemical properties of frentizole and the most potent inhibitors **52** and **59** compared to optimal values for CNS targeted drugs [79–81].

Compound	M_w	H-bond acceptor/donor	Rot. bonds	tPSA (Å^2)	ClogP	ELogP±SD	$ClogD_{7.4}$	$ELogD_{7.4}$ ± SD	$ClogS_{7.4}$
optimum	≤450	≤7/≤3	<8	≤(60-70)	1-5	1-5	0-3	0-3	>(-4.5)
frentizole	299.35	5/2	3	91.49	3.2	nd	2.5	nd	-3.7
52	303.38	3/2	4	97.28	3.5	4.1 ± 0.4‰	3.5	4.1 ± 1.2‰	-4.6
59	328.39	6/3	6	107.50	3.3	3.4 ± 0.5‰	3.2	3.4 ± 0.1‰	-3.6

3.2.4 Conclusion

In summary, a series of novel ABAD inhibitors, analogues of frentizole, have been designed, synthesized and evaluated *in vitro*. Among the 15 prepared compounds **59** was found the most promising hit with good inhibitory activity (IC_{50} = 3.06 μM) and suitable cytotoxicity profile comparable to the parent frentizole. Together with satisfying physical-chemical properties suggesting its capability to permeate through BBB, **59** presents a novel lead structure for further development and testing. On the other hand, compounds encompassing the thiourea linker in their structure were found to be improper leads for further development despite their good inhibitory activity as they were suggested to act via an unspecific manner possibly creating a disulfide bond with the protein's cysteine residues.

3.3 Further development of the best hit: Modifications to the structure of compound 14

Based on the previous results we decided to work on with the most promising inhibitor, compound **14** (Table 7), and further explore its SAR when making changes to the benzothiazole moiety and to the urea linker connecting the two aromatic moieties. However, compounds presented in this chapter have been currently undergoing the *in vitro* evaluation and thus no inhibition data are yet available.

19 compounds within this chapter (namely **63**, **67**–**76**, **79**, **82**–**87** and **91**) have been prepared by the pregraduate student Vendula Králová participating on this project. Detailed synthetic procedure and characterization of these compounds are not mentioned in this work as they are going to be presented in her thesis.

3.3.1 Different positioning of chloro-substitution on the benzothiazole moiety

3.3.1.1 Design

Compound **14** possess chlorine substitution in position 6 of the benzothiazole moiety, therefore, we decided to prepare 4, 5 and 7 chloro-substituted analogues to compare their inhibitory activity (Table 9).

Table 9: Analogues of compound **14** with various positioning of the chloro-substitution on the benzothiazole moiety.

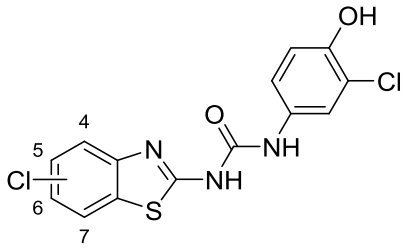

Compound	Cl-substitution
14	6-Cl
63	4-Cl
64	5-Cl
65	7-Cl

Additionally, the 6-chlorobenzothiazole (**66**) was prepared to find whether the sole benzothiazole moiety is capable of ABAD inhibition (Fig. 19).

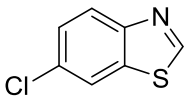

Figure 19: Structure of compound **66**.

3.3.1.2 Synthesis

7-Chlorobenzo[*d*]thiazol-2-amine was prepared from 7-chlorobenzo[*d*]thiazole-2-thiol in two steps (scheme 7). First, the five membered ring was cleaved by heating in hydrazine hydrate to give corresponding 2-aminobenzenethiol which was then treated with di(1*H*-imidazol-1-yl)methanimine to give the desired product [95]. The di(1*H*-imidazol-1-yl)methanimine was prepared beforehand according to the literature [96]. 5-Chlorobenzo[*d*]thiazol-2-amine was prepared from corresponding 2-aminobenzenethiol in reaction with BrCN (Scheme 7).

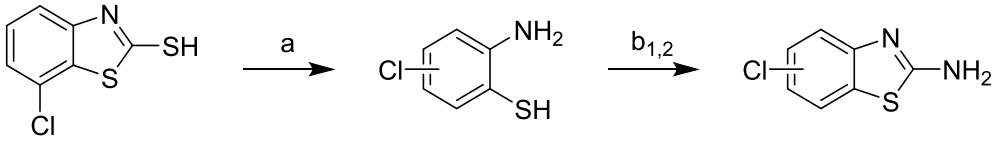

Scheme 7: Synthesis of benzothiazoles with chloro-substitution in different positions of the benzene ring. Reagents and conditions: (a) hydrazine hydrate, 110°C; (b_1) BrCN, water/MeOH, rt; (b_2) di(1*H*-imidazol-1-yl)methanimine, dioxane, reflux.

Further, the synthesis of **63**–**65** proceeded according to the general procedure using CDI as described in previous chapters. Compound **66** was prepared from 6-chlorobenzo[*d*]thiazol-2-amine in reaction with amylnitrite [97].

3.3.2 Different substitutions at position 6 of the benzothiazole moiety

3.3.2.1 Design

In next series, a broad range of different substitutions was introduced mainly to the position 6 of the benzothiazole moiety (Table 10) in order to find promising hits plausibly better than the original 6-chloro-substitution of compound **14**.

Table 10: Analogues of **14** with different substitution in position 6 of the benzothiazole moiety and their preliminary inhibitory data.

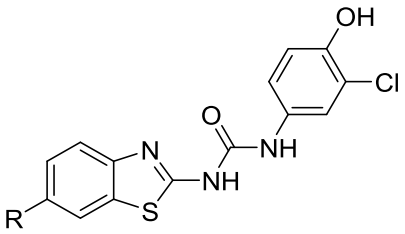

Compound	R	25 µM (% of Control ± SEM)	Compound	R	25 µM (% of Control ± SEM)
67	---	20.0 ± 0.61	**77**	NH_2	nd
68	5-Br	9.8 ± 0.18	**78**	OH	nd
69	Br	13.6 ± 0.25	**79**	*i*-Pr	36.5 ± 0.54
70	Me	25.6 ± 0.47	**80**	*t*-butyl	34.0 ± 2.44
71	CF_3	9.7 ± 0.41	**81**	I	76.7 ± 3.76
72	OMe	10.0 ± 0.39	**82**	OEt	28.7 ± 0.38
73	COMe	48.3 ± 0.63	**83**	SCF_3	50.5 ± 1.25
74	COOMe	18.1 ± 0.59	**84**	SCN	37.8 ± 0.35
75	CN	10.7 ± 0.25	**85**	SO_2Me	21.6 ± 0.21
76	NO_2	23.0 ± 0.37	**86**	SO_2CF_3	29.1 ± 0.32

3.3.2.2 Synthesis

If necessary, the 6-substituted benzothiazoles were prepared from the corresponding 4-substituted anilines in reaction with potassium isocyanate and bromine or potassium isocyanate and tetramethylammonium dichloroiodate (Scheme 8). Method using bromine as the oxidant was generally employed as bromine is significantly cheaper. Tetramethylammonium dichloroiodate was used when high yields were required and in case of 6-iodobenzo[*d*]thiazol-2-amine preparation, which in the bromine setup gave 6-isothiocyanate instead of the desired 6-iodo substitution (Scheme 8). Further, the synthesis proceeded according to the general procedure using CDI.

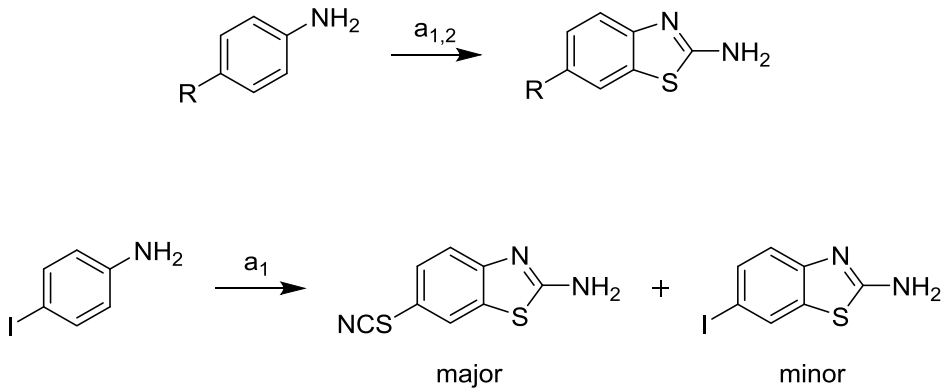

Scheme 8: Synthesis of 6-substituted benzothiazoles. Reagents and conditions: (a_1) KSCN, Br_2, acetic acid, 10°C–rt; (a_2) KSCN, tetramethylammonium dichloroiodate, DMSO/water, rt–70°C.

Compound **77** was prepared from the corresponding 6-nitro substituted compound (**76)** by reduction with iron powder and ammonium chloride (Scheme 9). Compound **78** was prepared from compound **48** by demethylation of its methoxy group using $AlCl_3$ (reaction conditions similar to Scheme 4, step a).

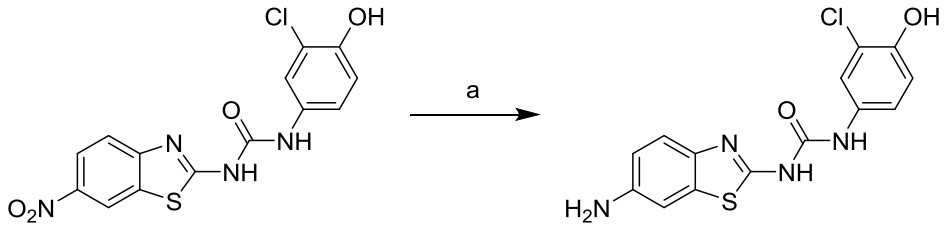

Scheme 9: Synthesis of compound **77**. Reagents and conditions: (a) Fe, NH4Cl, THF/MeOH/water, 50°C.

Preliminary data for this series of compounds indicate that the type of substitution in the position 6 has only limited influence on the inhibitory activity. Thus, for the following series we used mainly 6-methoxy substitution, which showed improved inhibitory potency compared to parent compound 14 and for which the synthetic precursors were easier to obtain. However, the original 6-chloro substitution was also employed in some cases as well as the unsubstituted benzothiazole as they were more suitable for certain synthetic approaches.

3.3.3 Alternatives to the benzothiazole heterocycle

3.3.3.1 Design

The benzothiazole heterocycle itself was also subject of modifications as indicated in the Table 11 beneath. The sulphur atom in the thiazole ring was replaced to obtain the benzoxazole (**89**, **90**) or benzimidazole (**87**, **88**) analogues, the benzene ring was replaced with saturated cycloxane (**94**), estranged (**95**) or removed at all (**93**), the thiazole ring was replaced with aliphatic cyclopentane (**96**) or reduced to an ethylene bridge (**97**). Moreover, the symmetric derivative **98** was prepared to see, whether the dimerized phenyl moiety alone is sufficient for ABAD inhibition.

Table 11: Analogues of **14** with modified benzothiazole moiety.

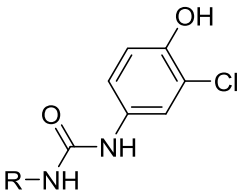

Compound	R	Compound	R
87	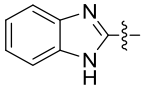	**93**	
88	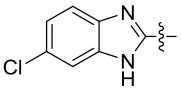	**94**	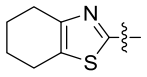
89	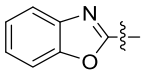	**95**	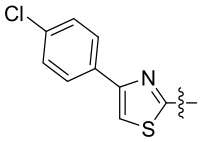
90	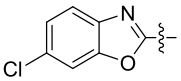	**96**	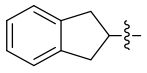
91	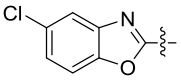	**97**	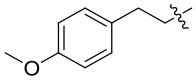
92	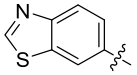	**98**	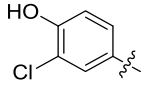

3.3.3.2 Synthesis

Both, 2-aminobenzoxazoles and 2-aminobenzimidazoles were prepared in reaction with BrCN (Scheme 10), however, different reaction conditions were used for each heterocycle.

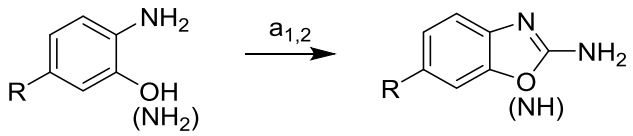

Scheme 10: Synthesis of benzoxazole and benzimidazole intermediates. Reagents and conditions: (a_1=benzoxazoles) BrCN, THF, rt; (a_2=benzimidazoles) BrCN, MeOH/H_2O, rt.

The next reaction step using CDI followed the general procedure described earlier in the text only in the case of compounds comprising the 2-aminothiazole core. In case of compounds **92**, **96** and **97** the procedure had to be updated due to increased solubility of imidazolecarboxamide intermediates, which did not allow their simple isolation by filtration in satisfactory yields. Therefore, after the activation of starting compound with CDI was finished, 4-amino-2-chlorophenol was added directly to the current reaction mixture (Scheme 11).

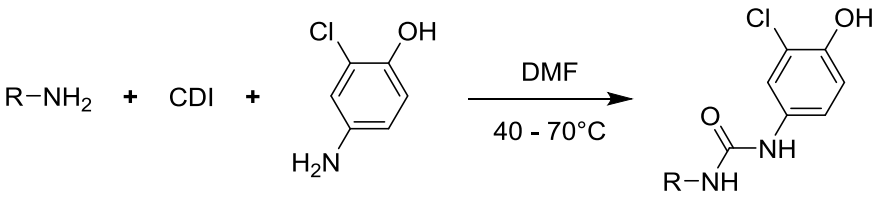

Scheme 11: One-pot synthesis of phenylureas **92**, **96** and **97**.

The symmetric 1,3-bis(3-chloro-4-hydroxyphenyl)urea (**98**) was prepared in two steps (Scheme 12). First 3-chloro-4-methoxyaniline was treated with CDI to give 1,3-bis(3-chloro-4-methoxyphenyl)urea, which was then demethylated in reaction with $AlCl_3$.

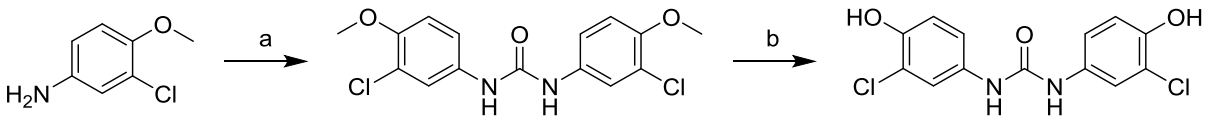

Scheme 12: Synthesis of symmetric urea derivative **98**. Reagents and conditions: (a) CDI, DMF, 60°C; (b) $AlCl_3$, toluene, reflux.

3.3.4 Modifications of the urea linker

3.3.4.1 Design

The original urea linker became a subject of modification, too (Table 12). It was replaced with analogous thiourea (**99**) and guanidine (**100**) linkers, the shorter amide (in both possible orientations;

compounds **102**, **103**) and secondary amine (**101**) linkers or it was also prolonged by one methylene group on the phenyl side of the molecule (**104**, **105**). Finally, methylation of the either one (**106**–**108**) or both nitrogen atoms (**109**) of the urea linker was conducted with aim of constraining the conjugation between the two aromatic moieties.

Table 12: Analogues of **14** with alternative linkers connecting the two aromatic moieties.

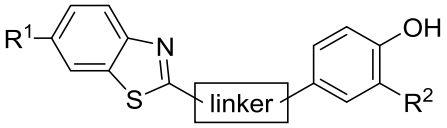

Compound	R^1	Linker	R^2	Compound	R^1	Linker	R^2
99	Cl	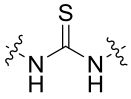	Cl	**105**	OMe	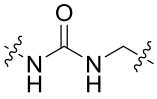	OH
100	Cl	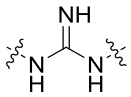	Cl	**106**	---	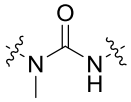	Cl
101	Cl		Cl	**107**	---	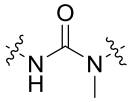	Cl
102	OMe	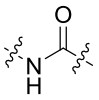	Cl	**108**	OMe	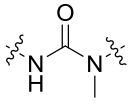	Cl
103	OMe	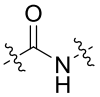	Cl	**109**	---	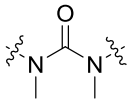	Cl
104	OMe	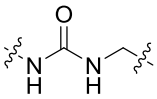	Cl				

3.3.4.2 Synthesis

Thiourea analogue **99** was prepared in similar manner to the parent **14** just instead of CDI was for the reaction used thiocarbonyldiimidazole (SCDI) and the procedure was slightly updated (already described in Scheme 5). Consequently guanidine analogue **100** was prepared from thiurea **99** in reaction with ammonia and mercury oxide as described previously (Scheme 6). Compounds **104** and **105** were prepared using the general procedure with CDI. In case of compound **104** synthesis, the corresponding benzylamine intermediate was prepared from its methoxy analogue by demethylation using $AlCl_3$ (reaction conditions similar to Scheme 4, step a). Compound **101** with

linker consisting of secondary amine group was prepared by mean of simple alkylation and amides **102** and **103** were prepared in reaction of corresponding carboxylic acid with CDI and corresponding amine (Scheme 13).

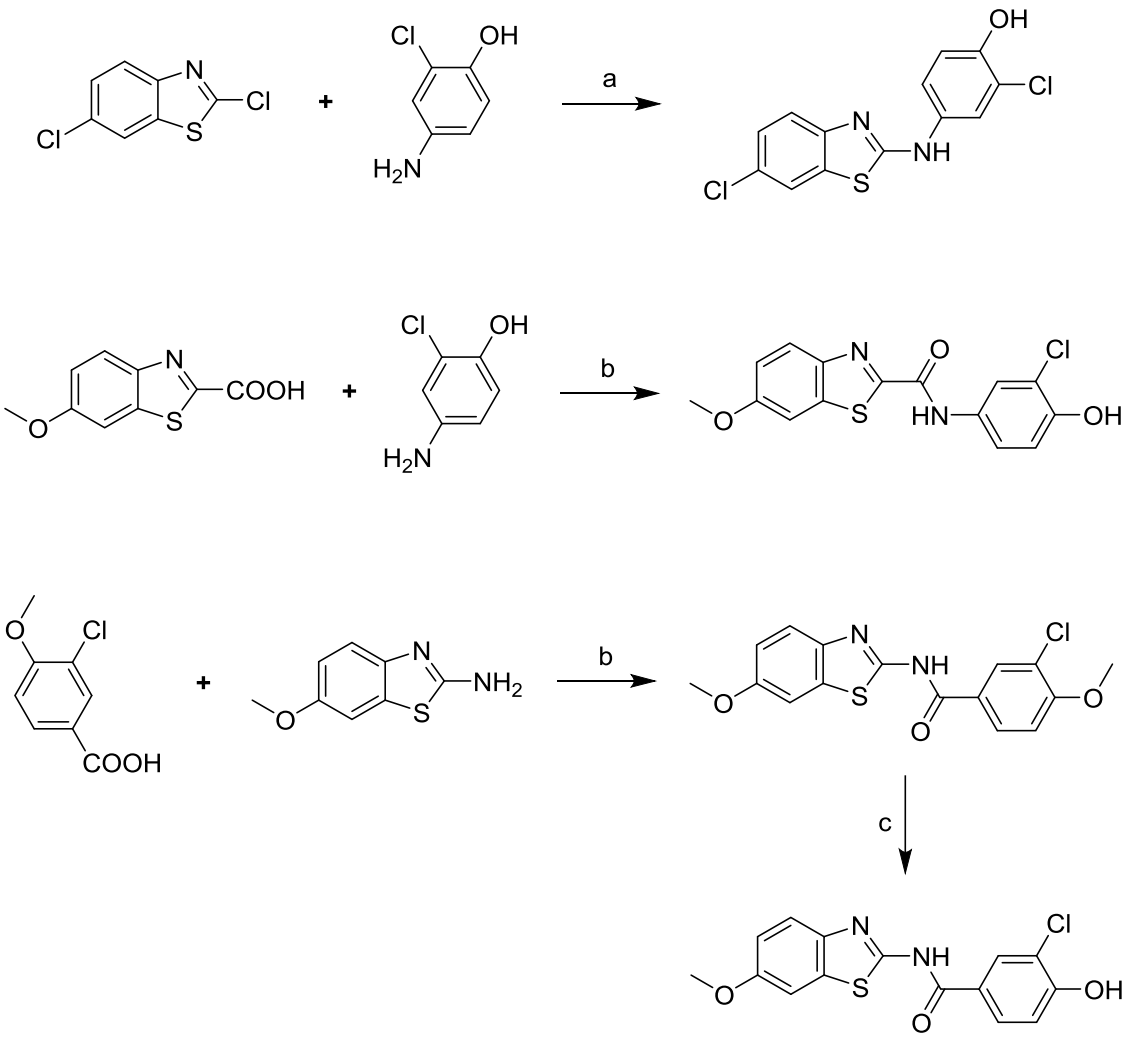

Scheme 13: Synthesis of compounds **101–103**. Reagents and conditions: (a) NMP, 160°C; (b) CDI, anh. DMF, rt; (c) $AlCl_3$, DCM, reflux.

Compound **106** was prepared in 4 steps (Scheme 14). The benzothiazole moiety was prepared from 2-iodoaniline in reaction with methylisothiocynate and tetrabutylammonium bromide catalysed by copper (I) chloride [98]. 3-chloro-4-methoxyaniline was treated with triphosgene to give the isocyanate intermediate, which was then reacted with the benzothiazole moiety and the resulting methoxy derivative was demethylated using $AlCl_3$ to give compound **106**.

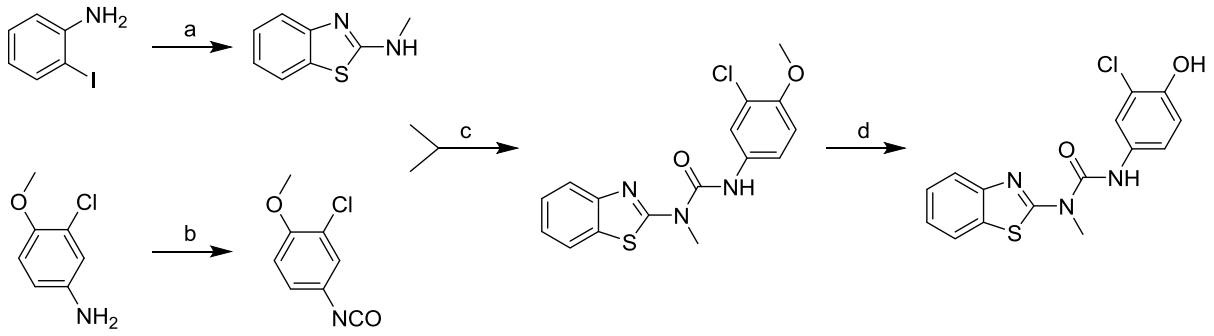

Scheme 14: Synthesis of compound **106**. Reagents and conditions: (a) MeNCS, TBABr, CuCl, DMSO, 60–80°C; (b) triphosgene, Et_3N, DCM, 0°C–reflux; (c) THF, rt; (d) $AlCl_3$, toluene, reflux.

The first step in the synthesis of compounds **107–109** was preparation of corresponding methylated phenyl moieties in one (*N*-methylation with methyl iodide) resp. two steps (*O*-demethylation using $AlCl_3$) as shown in Scheme 15.

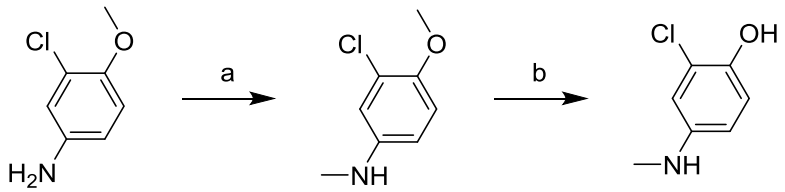

Scheme 15: Synthesis of *N*-methylated aniline derivatives. Reagents and conditions: (a) CH_3I, NaH, THF, 0°C–rt; (b) $AlCl_3$, toluene, reflux.

2-chloro-4-(methylamino)phenol was used for synthesis of **107** and **108** according to the general procedure employing CDI. Synthesis of compound **109** started with preparation of 3-(benzo[*d*]thiazol-2-yl)-1-(3-chloro-4-methoxyphenyl)-1-methylurea from 2-aminobeznothiazole and previously prepared 3-chloro-4-methoxy-*N*-methylaniline according to the general CDI procedure. The product was then treated with methyl iodide to methylate the second nitrogen of the urea linker. Finally, the *O*-demethylation using $AlCl_3$ gave the desired product (Scheme 16).

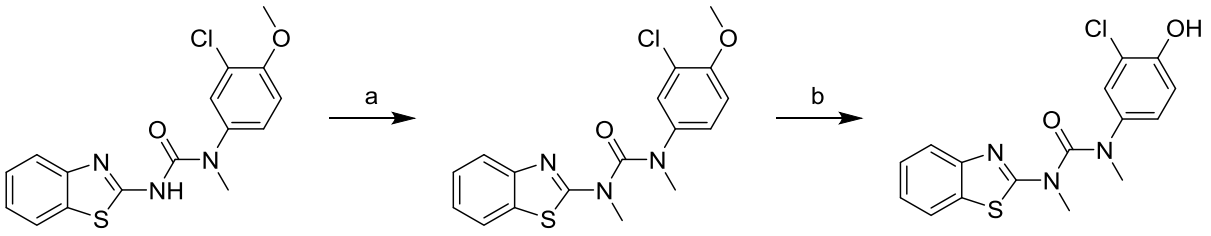

Scheme 16: Synthesis of compound **109**. Reagents and conditions: (a) NMP, 160°C; (b) $AlCl_3$, toluene, reflux.

3.4 Conclusion for the ABAD inhibitors development section

Taken together 103 (plus 3 standards) potential ABAD inhibitors have been designed and synthesized (including 19 compounds prepared by pregraduate student). Although the biological assessment of these compounds is still ongoing, several promising hits have already been identified, namely compounds **13**, **14** and **39**, which all showed IC_{50} values around 2 µM (Fig. 20). Common structural features of the novel inhibitors are two aromatic moieties connected through the urea linker. The best inhibition ability was observed for the benzothiazol-2-yl moiety with fluorine or chlorine substitution in position 6 plus the phenyl moiety with hydroxyl substitution in position 4 and chlorine substitution in position 3 resp. 3 and 5. Especially the 4-positionned hydroxyl group seems to be crucial for retaining inhibitory activity as omission of this substitution or substitution in position 4 with other group lead to drop-off in activity. Possible explanation for this observation could be that the hydroxyl group creates a crucial hydrogen bond with the enzyme, which significantly contributes to the overall affinity of the respective inhibitors. Also compound **59** showed promising inhibitory activity, with IC_{50} value 3 µM (Fig. 20). Interestingly, this compound does not follow the aforementioned SAR and requires (together with the whole 2nd series) further exploration.

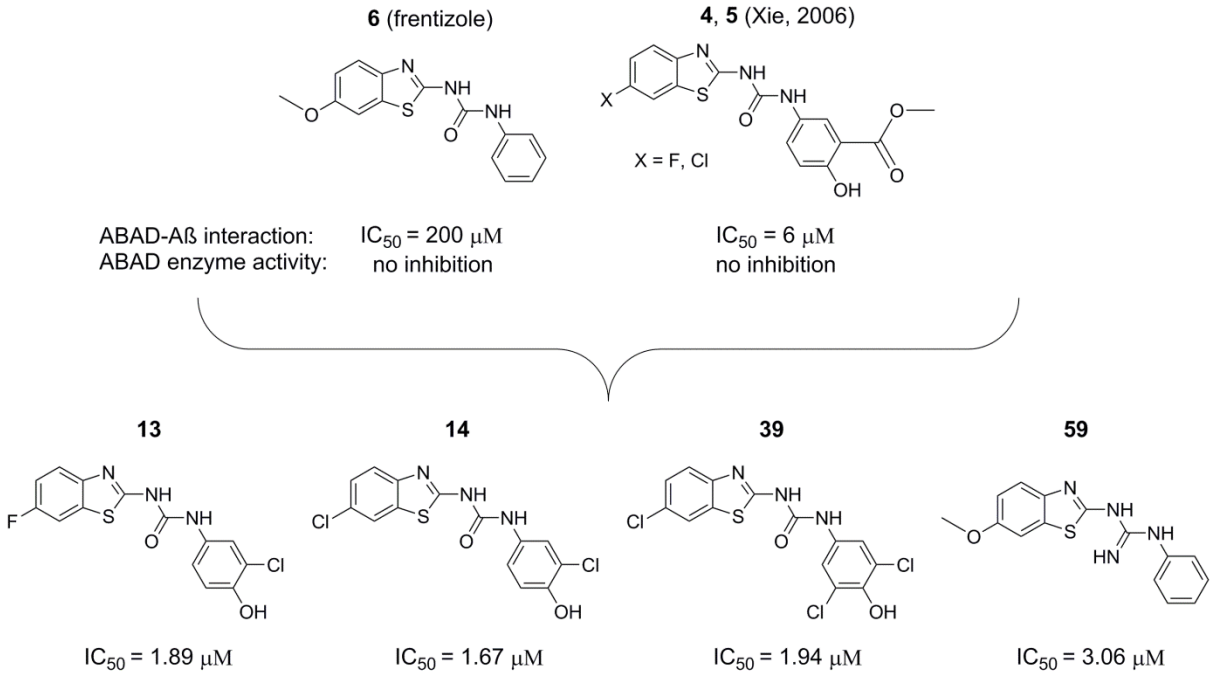

Figure 20: Development of novel ABAD inhibitors based on the structure of parent frentizole (**6**) and other inhibitors of ABAD-A*β* interaction (**4**, **5**).

The priority now is to finish the biological assessment. Consequently, the best compounds with highest inhibitory activity, plausible cytotoxicity and potential to cross the BBB (PAMPA assay) will undergone more detailed evaluation including *in vivo* testing on mouse model of AD. Moreover, such a wide set of compounds with its biological data could be used for pharmacophore modelling and 3D-QSAR studies in order to further rationalize the future design of ABAD inhibitors. It would be also of merit to find out, whether the novel compounds retained the inhibitory activity towards ABAD-A*β* interaction (Fig. 20). Such activity would further increase their therapeutical potential to ameliorate A*β*-induced mitochondrial dysfunction in the course of AD.

3.5 Design, synthesis and *in vitro* evaluation of indolotacrine analogues as multi-target-directed ligands for the treatment of Alzheimer's disease

(based on attachement IV)

The aim of this study was to develop novel multi-target-directed ligands (MTDLs) acting primarily as MAO and cholinesterase inhibitors. For this purpose we chose structural motifs contained in previously described MAO and/or ChEIs and incorporate them into the scaffold of the novel compounds. Two distinct series of molecules have been designed. The first series containing 2-aminoindole-3-carbonitrile structural scaffold (further referred as *"indole"* series; compounds **110**–**112** and **113**) employs an indole ring, that is a structural core in several MAOIs or dual-acting compounds targeting both MAO and ChEs, such MBA236 (Fig. 21) [99, 100], and the *β*-aminonitrile motif found in some previously identified MAOI [101]. Compounds **111**, **112** also contains the propargylamine moiety, which is an essential part of many neuroprotective, irreversible MAOIs (Fig. 21) [102]. Originally, only compounds **110**, **111** had been designed, however, during the synthesis of **111** a side-product **112** was isolated. Because of the low yield obtained, **112** was tested only for its inhibitory activity against MAO. Compound **113** was synthesized later on to explore, whether the *N*-allyl or *N*-propargyl substitution on the amino group in position two is important for MAO inhibition and also to validate the importance of the phenolic group for the antioxidant activity of other compounds in the series (discussed later in the text).

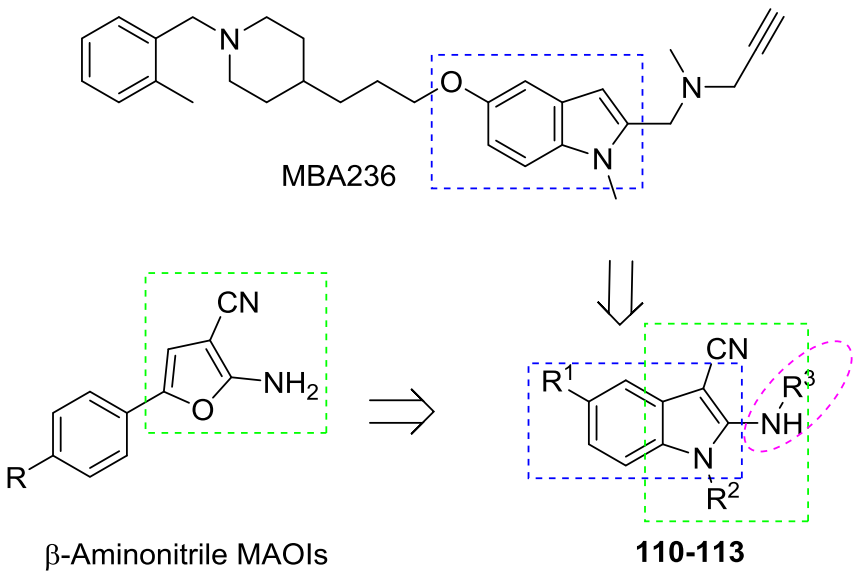

Figure 21: Design of *indole* series.

The second series was then designed employing the 2,3,4,6-tetrahydro-1*H*-indolo[2,3-*b*]quinolin-11-amine structural scaffold (described hereafter as the *"indolotacrine"* series;

compounds **114**, **115** and **116**) to improve the unsatisfactory anti-ChE activity of the *indole* series. For this purpose the 2-aminoindole-3-carbonitrile scaffold of the *indole* series was fused with the structure of potent ChEI tacrine or 7-methoxytacrine (7-MEOTA). Moreover, the resulting indolotacrines also resemble *β*-carboline alkaloids (e.g. harmine), which are known MAOI (Fig. 22) [103, 104]. Since compound **112** with *N*-propargyl substitution in position 1 was found the most potent MAOI within the indole series, it was decided to preserve this potentially favourable motif when designing compound **116** with benzyl substitution analogous to former *N*-propargyl moiety.

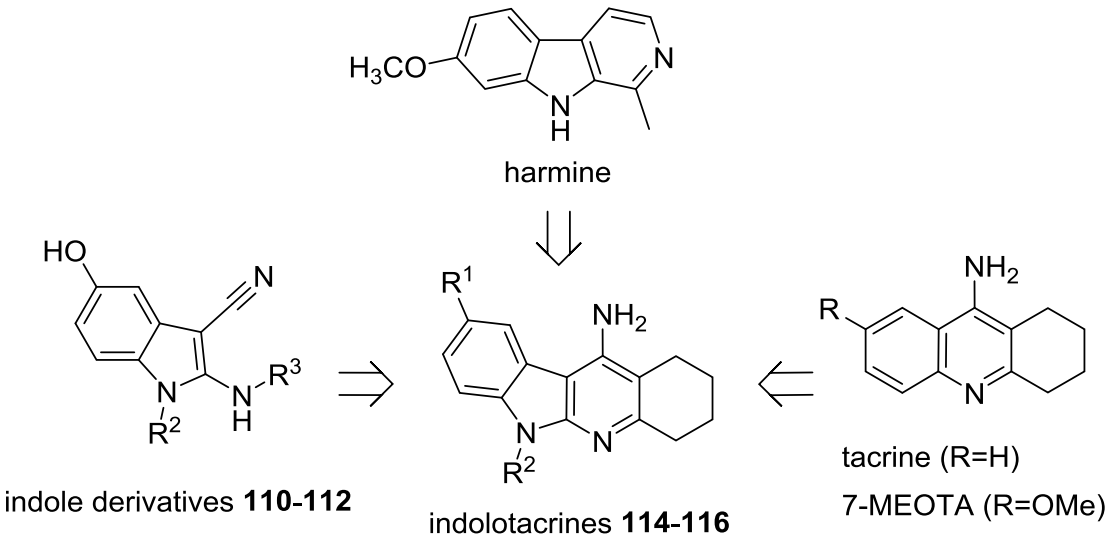

Figure 22: Design of *indolotacrine* series.

5-Hydroxy-1*H*-indole-3-carbonitrile derivatives **110–112** were prepared in three steps (Scheme 17). At first malononitrile was treated with ethanol in diethyl ether saturated with HCl (g) to obtain 3-amino-3-ethoxyacrylonitrile. In next step the 3-amino-3-ethoxyacrylonitrile was treated with the corresponding alkylamine to give *N*-alkylated 3,3-diaminoacrylonitriles. Lastly, diaminoacrylonitriles were treated with *p*-benzoquinone to give 2-(alkylamino)-5-hydroxy-1*H*-indole-3-carbonitriles **110**, **111** [105]. Moreover, a by-product, whose structure was assigned as the alkylated in position 1 (**112**), was also isolated from the reaction of 3-amino-3-(prop-2-yn-1-ylamino)acrylonitrile.

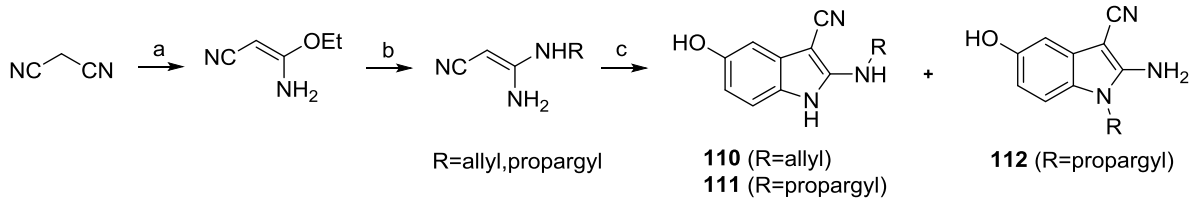

Scheme 17: Synthesis of indole series (**110**–**112**). Reagents and conditions: (a) HCl, EtOH, Et_2O, 0˚C–rt; (b) alkylamine, EtOH, rt; (c) *p*-benzoquinone, EtOH, rt.

Indole **113** and indolotacrines **114**, **115** were prepared in two to four steps using a similar synthetic approach (Scheme 18). The synthesis of compound **115** started from commercial 2-iodo-4-methoxy-1-nitrobenzene, which was reduced using Fe powder and ammonium chloride to the corresponding aniline derivative. The other two aniline intermediates were obtained as commercial chemicals. Further, the synthesis proceeded identically for three compounds. Corresponding 2-iodoaniline derivatives were treated with trifluoroacetic anhydride to give the trifluoracetamides, which were then used for the copper iodide catalysed cyclization with malononitrile to obtain corresponding indole derivatives including the end product, compound **113** [106]. Finally, indolotacrines **114** and **115** were prepared using microwave-assisted Friedländer reaction [107] of corresponding indole derivatives with cyclohexanone.

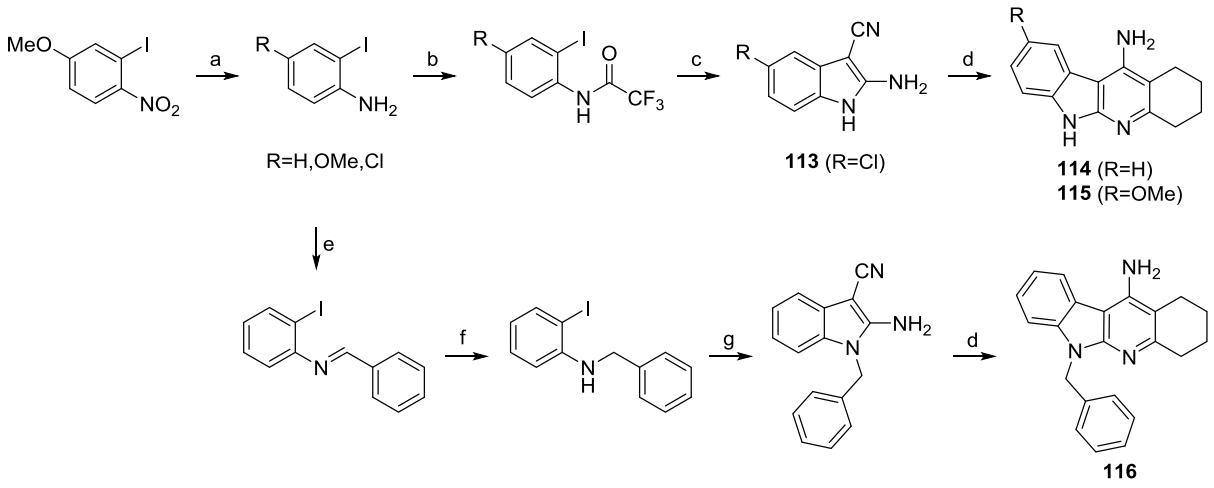

Scheme 18: Synthesis of indolotacrines **114**–**116** and indole **113**. Reagents and conditions: (a) Fe, NH_4Cl, MeOH/H_2O (3:1), 50˚C; (b) trifluoroacetic anhydride, Et_3N, THF, -7˚C–rt; (c) malononitrile, L-proline, K_2CO_3, CuI, DMSO/H_2O (1:1), 60˚C; (d) cyclohexanone, $AlCl_3$, 1,2-dichloroethane, microwave irradiation, 95˚C; (e) benzaldehyde, MeOH, rt; (f) $NaBH_3CN$, AcOH/MeOH, 0˚C–rt; (g) malononitrile, picolinic acid, K_2CO_3, CuI, DMSO, microwave irradiation, 90˚C.

Indolotacrine **116** was prepared by a slightly different synthetic procedure in four steps (Scheme 2). Firstly, 2-iodoaniline was treated with benzaldehyde to give *N*-(2-iodophenyl)-1-phenylmethanimine, which was then reduced to corresponding amine using $NaBH_3CN$. In next step cyclization of this amine with malononitrile gave 2-amino-1-benzyl-1*H*-indole-3-carbonitrile [108], which in the Friedländer reaction [107] with cyklohexanone gave indolotacrine **116**.

For the biological evaluation, all final products (Fig. 23) were transformed into better water-soluble hydrochlorides by stirring them in diethyl ether saturated with HCl (g).

A

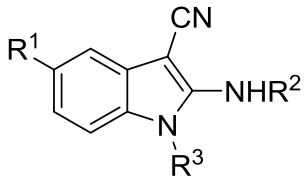

110 R^1=OH, R^2=allyl, R^3=H
111 R^1=OH, R^2=propargyl, R^3=H
112 R^1=OH, R^2=H, R^3=propargyl
113 R^1=Cl, R^2=H, R^3=H

B

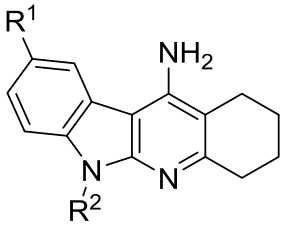

114 R^1=H, R^2=H
115 R^1=OMe, R^2=H
116 R^1=H, R^2=benzyl

Figure 23: Indole (**A**) and indolotacrine (**B**) analogues prepared in this study.

Both series were assayed *in vitro* for their inhibitory activity against membrane-bound MAO A and MAO B (Table 13). All the *indoles* were potent and unselective MAOIs, with **112** being the best inhibitor of both isoenzymes in the series. Indoles **110**–**112** were evaluated for irreversible inhibition and, unexpectedly, none of compounds showed significantly lower IC_{50} value after 30 min pre-incubation with enzyme, despite compounds **111**, **112** have the *N*-propargylamine moiety, which is present in many known irreversible MAOIs (e.g. deprenyl, clorgyline or rasagiline). This could be due to the change in the electron density on the triple bond of the *N*-propargyl motif, as its connecting nitrogen atom is here part of the aromatic system, in contrast to the known irreversible inhibitors where the *N*-propargylamine moiety is separated from the aromatic system usually by an alkyl linker. Alternatively, steric hindrance from the carbonitrile substituent could prevent the generation of the reactive intermediate or its modification of the enzyme. Based on this finding, we decided to investigate whether the *N*-allyl or *N*-propargyl substitution is necessary for MAO inhibition and so we synthesized compound **113**. Evaluation revealed that indole **113** devoid of any *N*-alkyl substitution on the amino group at position 2 retained the inhibitory activity at level similar to other indoles, showing that the propargyl moiety does not contribute to the binding.

Indolotacrine **115** retained the inhibitory activity for both MAO isoenzymes, however, **114** inhibited only MAO A and **116** with an extra *N*-benzyl substitution showed no inhibition of either MAO isoenzyme. It could be assumed that the extended spatial size of **116** would prevent entry into the active site of MAO enzymes [109]. In addition, compound **114** was used for inactivation studies with MAO A and showed the expected reversible mode of inhibition. Unlike the unselective indole analogues, indolotacrines **114**, **115** both exerted some selectivity towards MAO A inhibition with **115** being the most potent MAO A inhibitor among all the compounds tested (IC_{50} = 0.49 μM). Standards tacrine and 7-MEOTA showed only moderate activity being worse inhibitors of both MAO isoenzymes compared to the indolotacrine **115**.

Table 13: Inhibition of MAO A and MAO B.

Compound	MAO A IC_{50} ± SD (μM)	MAO B IC_{50} ± SD (μM)	SI[b]	MAO A 30'[c] IC_{50} ± SE (μM)	MAO B 30'[c] IC_{50} ± SE (μM)
110	2.32 ± 0.26	2.02 ± 0.56	0.9	1.78 ± 0.33	10.86 ± 0.78
111	1.32 ± 0.12	1.70 ± 0.40	1.3	1.80 ± 0.56	2.48 ± 0.32
112	0.68 ± 0.08	1.62 ± 0.35	2.4	0.45 ± 0.03	0.87 ± 0.10
113	2.80 ± 0.40	3.89 ± 0.02	1.4	-	-
114	11.40 ± 1.10	> 100	8.8	30.0 ± 1.9	-
115	0.49 ± 0.05	53.90 ± 10.70	110.0	-	-
116	> 100	> 100	-	-	-
tacrine	14.07 ± 1.47	317.2 ± 201.0	22.5	-	-
7-MEOTA	7.10 ± 0.03	98.61 ± 14.63	13.9	-	-

[a] IC_{50} and SD/SE values were obtained as a mean of 2 independent measurements
[b] selectivity index = IC_{50} MAO B / IC_{50} MAO A
[c] IC_{50} values after 30 min pre-incubation of enzyme with inhibitor

All final compounds with the exception of **112** (which was a by-product of synthesis and, due to low yield, was tested only for MAO inhibition) and **113** (prepared subsequently to enhance SAR on MAO inhibition and antioxidant activity) were assayed *in vitro* for their inhibitory activity against human recombinant acetylcholinesterase (AChE) and human plasma butyrylcholinesterase (BChE) (Table 14).

As preceded earlier in the text, no significant inhibitory activity against AChE or BChE was detected for *indoles* **110**, **111**. Both compounds exerted only poor inhibition of AChE in high micromolar range and were found inactive against BChE at the highest concentration tested. Possible explanation for this observation is that compounds **110**, **111** lack the structural complexity of other indoles or indanes, which are capable of ChEs inhibition (e.g. extra *N*-benzylpiperidine moiety

present in donepezil, ASS234 and MBA236 or carbamate moiety of ladostigil) [100]. Conversely, indolotacrines **114**, **115** were found potent unselective inhibitors of both enzymes with IC_{50} values in low micromolar range. Compound **116** was found to be a selective BChEI. None of the compounds were found superior compared to tacrine; however, compound **115** was found better inhibitor of both ChEs compared to 7-MEOTA. IC_{50} values obtained for standard inhibitors tacrine and 7-MEOTA were found in good correlation with previously published results [110].

Table 14: Inhibition of AChE and BChE.

Compound	AChE IC_{50} ± SEM (μM)	BChE IC_{50} ± SEM (μM)	SI[b]
110	319.2 ± 15.9	> 1000	3.1
111	101.9 ± 5.4	> 1000	9.8
114	11.6 ± 0.6	4.7 ± 0.1	0.4
115	1.5 ± 0.1	2.4 ± 0.1	1.6
116	> 1000	1.09 ± 0.07	0.001
tacrine	0.32 ± 0.01	0.088 ± 0.001	0.3
7-MEOTA	10.0 ± 1.0	17.6 ± 0.8	1.8

[a] IC_{50} and SEM values were obtained as a mean of 3 independent measurements
[b] selectivity index = IC_{50} BChE / IC_{50} AChE

Additionally, as ROS are likely to play a part in the development and progression of AD [111], the compounds were evaluated for their antioxidant activity using DPPH assay (Table 15). Indoles **110**, **111** showed promising antioxidant properties, similar to standard *N*-acetylcysteine and only slightly weaker than trolox. We hypothesized that this could be due to the presence of phenolic group, which is a key structural motif common of many antioxidants [112]. To prove this assumption we synthesized compound **113**, where the phenolic group was replaced with chlorine. Evaluation showed, in good correlation with our hypothesis, that indole **113** exerts more than 20 times weaker antioxidant activity compared to phenolic compounds **110** and **111**. Neither the indolotacrines nor tacrine or 7-MEOTA showed any significant antioxidant activity, which is not surprising, as they all lack the phenolic group responsible for this activity as demonstrated for the indoles. Introduction of the phenolic moiety therefore presents a possible improvement of the indolotacrine compounds for the future.

Table 15: Antioxidant activity and cytotoxicity of prepared compounds.

Compound	Antioxidant activity EC_{50} ± SEM (μM)	Cytotoxicity IC_{50} ± SEM (μM)
110	37.86 ± 5.01	> 1000
111	25.82 ± 1.35	> 1000
113	731.70 ± 27.17	113 ± 29
114	> 5000	13.0 ± 1.4
115	> 5000	5.5 ± 0.4
116	3827.0 ± 227.1	7.0 ± 0.7
tacrine	> 5000	248 ± 11
7-MEOTA	> 5000	63 ± 4
N-acetylcystein	27.91 ± 1.82	-
trolox	16.20 ± 0.42	-

[a] EC_{50}/IC_{50} and SEM values were obtained as a mean of 3 independent measurements

Next, the cytotoxicity of the compounds was evaluated using the MTT assay on the CHO-K1 cell line (Table 5). *Indoles* were found to possess very low toxicity with IC_{50} values above the measurable range (>1000 μM) in case of **110**, **111** and at high microlomolar range for **113**. All indolotacrines exerted similar level of cytotoxicity with IC_{50} values around 10 μM. Standards 7-MEOTA and tacrine were both found to be less toxic, with tacrine being the least toxic compound among the series *in vitro*. This could be considered quite a surprising result as it is known that *in vivo* tacrine is more toxic than 7-MEOTA [113].

Assuming the fact that the principal target of tacrine toxicity *in vivo* is liver, we decided to evaluate tacrine and 7-MEOTA together with the most promising indolotacrine **115** for their hepatotoxicity on the HepG2 cell line using the MTT assay (Table 16) [114]. Compound **115** was found slightly more hepatotoxic compared to 7-MEOTA and tacrine. As in cytotoxicity evaluation, tacrine showed lower *in vitro* hepatotoxicity compared to 7-MEOTA, which is at odds with the *in vivo* results [113]. A possible explanation for this peculiarity is that the hepatoxicity is not caused by tacrine itself but by its metabolites, products of cytochrome P450 oxidation [115]. Therefore it is hard to conclude about the compounds' toxicity *in vivo* (e.g. **115**) based on the results of *in vitro* testing and these cytotoxicity and hepatotoxicity assessments have, in this case, only generally informative character.

Table 16: Hepatotoxicity evaluation.

Compound	Hepatotoxicity IC_{50} ± SEM (μM)
115	1.22 ± 0.11
tacrine	17.28 ± 0.76
7-MEOTA	11.50 ± 0.77

[a] IC_{50} and SEM values were obtained as a mean of 3 independent measurements

Penetration across the blood-brain barrier (BBB) is an essential property for compounds targeting the CNS and should always be considered during the drug development. In order to predict passive BBB penetration, modification of the parallel artificial membrane permeation assay (PAMPA) has been used based on reported protocol [116]. As summarized in Table 17, it is obvious that compound **115** has a high potential to be available in the CNS. Data obtained for the new compound were correlated to standard drugs, where CNS availability is known and also reported using the PAMPA assay [116]. Our data show high resemblance with previously reported penetrations as well as with a general knowledge about the availability in the CNS of such standard drugs.

Table 17: Prediction of blood-brain barrier penetration of **115** and reference compounds.

Compound	BBB penetration estimation	
	P_e ± SEM (10^{-6} cm s^{-1})	CNS (+/-)[b]
115	6.6 ± 0.65	(+)
donepezil	7.3 ± 0.9	(+)
rivastigmine	6.6 ± 0.5	(+)
tacrine	5.3 ± 0.19	(+)
testosterone	11.3 ± 1.6	(+)
chlorpromazine	5.6 ± 0.6	(+)
hydrocortisone	2.85 ± 0.1	(+/-)
piroxicam	2.2 ± 0.15	(+/-)
theophyline	1.07 ± 0.18	(-)
atenolol	1.02 ± 0.37	(-)

[a] P_e and SEM values were obtained as a mean of 4 independent measurements

[b] (+) (high BBB permeation predicted) P_e (10^{-6} cm s^{-1}) > 4.0

(-) (low BBB permeation predicted) P_e (10^{-6} cm s^{-1}) < 2.0

(+/-) (BBB permeation uncertain) P_e (10^{-6} cm s^{-1}) = 2.0 – 4.0

In summary, in this chapter we have reported design, synthesis and *in vitro* evaluation of series of indoles and series of indolotacrine hybrid analogues as potential drugs for the treatment of AD. The novel compounds were designed as MTDLs targeting primarily ChEs and MAOs. In addition to ChE and MAO inhibition, the biological evaluation also involved determination of antioxidant, cytotoxic and hepatotoxic properties and permeability prediction (PAMPA assay). The most promising compound, indolotacrine **115** (Fig. 24), was found to be a potent inhibitor of AChE (IC_{50} = 1.5 µM), BChE (IC_{50} = 2.4 µM) and MAO A (IC_{50} = 0.49 µM) and weak inhibitor of MAO B (IC_{50} = 53.9 µM). The inhibitory activity of **115** against ChEs and MAOs therefore seems quite well balanced, which should enable the desired simultaneous multi-target directed action *in vivo*, however, the optimal inhibitory ability against the single targets and their balance in AD is still not known [117]. Although, the cytotoxic and hepatotoxic profile of **115** are slightly worse compared to standards tacrine and 7-MEOTA the overall improvement in the enzymatic inhibitory activities and potential to cross BBB make indolotacrine **115** a promising lead compound for further development and investigation.

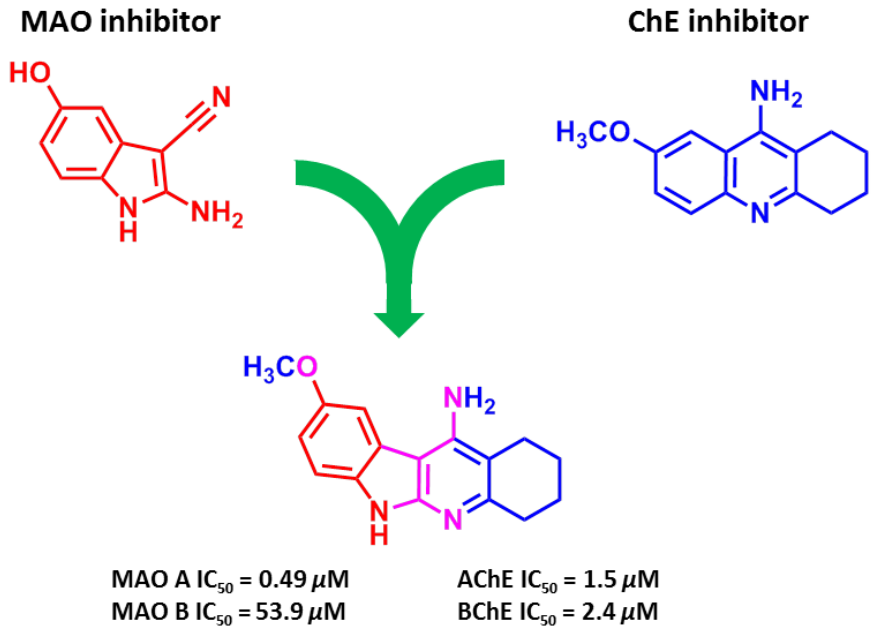

Figure 24: Design of indolotacrine **115** and its inhibitory potency against monoamine oxidases and cholinesterases.

4 Experimental part

4.1 Chemical preparation

4.1.1 General chemistry

Solvents and reagents were purchased from Fluka and Sigma-Aldrich (Czech Republic) and used without further purification. Reactions were monitored by thin layer chromatography (TLC) performed on aluminium sheets pre-coated with silica gel 60 F_{254} (Merck, Czech Republic) and detected under 254 nm UV light. Column chromatography was performed on silica gel 60 (230 mesh). Melting points were measured on Stuart SMP30 melting point apparatus (Bibby Scientific Limited, Staffordshire, UK) and are uncorrected.

NMR spectra were generally recorded at Varian Gemini 300 (^{1}H 300 MHz, ^{13}C 75 MHz, Palo Alto CA, USA) or Varian S500 (^{1}H 500 MHz, ^{13}C 126 MHz, Palo Alto CA, USA). In all cases, the chemical shift values for ^{1}H spectra are reported in ppm (δ) relative to residual $CHD_2SO_2CD_3$ (δ 2.50) or $CDCl_3$ (δ 7.27), shift values for ^{13}C spectra are reported in ppm (δ) relative to solvent peak dimethylsulfoxide-d_6 (δ 39.52) or $CDCl_3$ (δ 77.2). The assignment of chemical shifts was based on standard NMR experiments (^{1}H, ^{13}C, ^{1}H–^{1}H COSY, ^{1}H–^{13}C HSQC, HMBC). The measurments were performed at Faculty of Pharmacy in Hradec Králové by assoc. prof. Jiří Kuneš and his group.

Mass spectra (MS, respectively, multiple stage MS) were recorded on a LTQ XL linear ion trap mass spectrometer and evaluated using Xcalibur v 2.5.0 software (both Thermo Fisher Scientific, San Jose, CA, USA). The samples were dissolved in methanol (HPLC grade; Sigma-Aldrich, Prague, Czech Republic) and injected continuously (10 µL/min) using a Hamilton syringe into the electrospray ion source. The parameters of the electrospray were set up as follows: sheath gas flow rate 20 arbitrary units, aux gas flow rate 10 arbitrary units, sweep gas flow rate 0 arbitrary units, spray voltage 4.5 kV, capillary temperature 275 °C, capillary voltage 13 V, tube lens 100 V. The measurments were performed at Faculty of Military Healt Sciences in Hradec Králové by assoc. prof. Daniel Jun and his group.

For HRMS determination, a Dionex UltiMate 3000 analytical LC-MS system coupled with a Q Exactive Plus hybrid quadrupole-orbitrap spectrometer (both produced by ThermoFisher Scientific, Bremen, Germany) was used. The LC-MS system consisted of a binary pump HPG-3400RS connected to a vacuum degasser, a heated column compartment TCC-3000, an autosampler WTS-3000 equipped with a 25 µL loop and a VWD-3000 ultraviolet detector. A Waters Atlantis dC18 100Å (2.1 x 100mm/3µm) column was used as the stationary phase. The analytical column was protected against mechanical particles by an in-line filter (Vici Jour) with a frit of 0.5 µm pores. Water (MFA) and acetonitrile (MFB) used in the analyses were acidified with 0.1% (v/v) of formic acid. Ions for mass spectrometry (MS) were generated by heated electro-spray ionization source (HESI) working in

positive mode, with the following settings: sheath gas flow rate 40, aux gas flow rate 10, sweep gas flow rate 2, spray voltage 3.2 kV, capillary temperature 350 °C, aux gas temperature 300 °C, S-lens RF level 50, microscans 1, maximal injection time 35 ms, resolution 140 000. The full-scan MS analyses monitored ions within m/z range 100 – 1500. The studied compounds were dissolved in methanol and 1 μL of the solution was injected into the LC-MS system. For elution, following ramp-gradient program was used: 0 – 1 min: 10% MFB, 1 – 4 min: 10% – 100% MFB, 4 – 5 min: 100% MFB, 5 – 7.5 min: 10% MFB. The flow-rate in the gradient elution was set to 0.4 mL/min. To increase the accuracy of HRMS, internal lock-mass calibration was employed using polysiloxane traces of m/z = 445.12003 ($[M+H]^+$, $[C_2H_6SiO]_6$) present in the mobile phases. The chromatograms and mass spectra were processed in Chromeleon 6.80 and Xcalibur 3.0.63 software, respectively. The measurments were performed at University Hospital in Hradec Králové by dr. Rafael Doležal and his group.

Elemental analysis (EA) was measured at Perkin-Elmer CHN Analyser 2400 Series II apparatus. The measurments were performed at Faculty of Pharmacy in Hradec Králové by prof. Martin Doležal and his group.

4.1.2 Detailed description of synthetic procedures

General procedure for synthesis of N-(benzo[d]thiazol-2-yl)-1H-imidazole-1-carboxamides

Corresponding benzo[*d*]thiazol-2-amine (1 eq.) was dissolved in a mixture of dichloromethane (DCM) and dimethylformamide (DMF) (6:1; 12 mL/mmol). 1,1'-carbonyldiimidazole (CDI; 1.2 eq.) was added and the reaction mixture was vigorously stirred at reflux overnight. The resulting precipitate was collected by filtration, washed with DCM and dried under reduced pressure to obtain corresponding *N*-(benzo[*d*]thiazol-2-yl)-1*H*-imidazole-1-carboxamide in good to excellent yield (80-95%).

General procedure for synthesis of N-(benzo[d]thiazol-2-yl)-1H-imidazole-1-carbothioamides

Corresponding benzo[*d*]thiazol-2-amine (1 eq.) was dissolved in acetonitrile (MeCN; 5 mL/mmol), then 1,1'-thiocarbonyldiimidazole (SCDI; 1.2 eq.) was added and the reaction mixture was stirred at reflux overnight. The resulting precipitate was collected by filtration, washed with DCM and dried under reduced pressure to obtain corresponding *N*-(benzo[*d*]thiazol-2-yl)-1*H*-imidazole-1-carbothioamide in medium to excellent yield (65-95%).

*General procedure for synthesis of 1-(benzo[d]thiazol-2-yl)-3-phenylureas, -3-benzylureas and -3-phenylthioureas (**4–47**, **49**, **51**, **52**, **54**, **55**, **57**, **58**, **60**, **61**, **64, 65**, **80**, **81**, **88–91**, **93–95**, **99**, **104**, **105**, **107**, **108**)*

Corresponding *N*-(benzo[*d*]thiazol-2-yl)-1*H*-imidazole-1-carboxamide resp. *N*-(benzo[*d*]thiazol-2-yl)-1*H*-imidazole-1-carbothioamide (1 eq.) was dissolved in DMF (8 mL/mmol), the corresponding aniline / fenylmethanamine derivative (1.1 eq.) was added and the reaction mixture was stirred at 60 °C overnight.

When the corresponding fenylmethanamine was available in the form of hydrochloride, it was first converted to a free amine by stirring with trimethylamine in DMF at 60°C for 2h, before the activated benzothiazol was added to the reaction mixture.

After the reaction was completed (monitored by TLC), 1M aq. HCl was poured to the reaction mixture. The resulting precipitate was collected by filtration, washed with water, MeCN and dried to obtain corresponding 1-(benzo[*d*]thiazol-2-yl)-3-phenylurea or 1-(benzo[*d*]thiazol-2-yl)-3-phenylthiourea. In cases, where further purification was required, the procedure is described together with the respective compound's characterization.

3-chloro-2-methoxy-5-nitrobenzoic acid

3-chloro-2-methoxybenzoic acid (1 eq.) was dissolved in 96% sulphuric acid (3.1 mL/mmol). The solution was cooled in an ice bath and 69% nitric acid (3.2 eq.) was added dropwise. The reaction mixture was warmed to rt and stirred for 3 h. After the reaction was completed (monitored by TLC), reaction mixture was slowly poured into ice cold water and the mixture was stirred for 30 mins. The resulting precipitate was collected by filtration, dried under reduced pressure and used for the next step without further purification.

^{1}H NMR (300 MHz, DMSO-d_6): δ (ppm) 8.51 (dd, *J* = 2.9, 0.6 Hz, 1H), 8.41 (dd, *J* = 2.8, 0.7 Hz, 1H), 3.94 (d, *J* = 0.5 Hz, 3H).

3-chloro-2-hydroxy-5-nitrobenzoic acid

3-chloro-2-methoxy-5-nitrobenzoic acid (1 eq.) was dissolved in anhydrous DCM (9 mL/mmol), aluminium chloride (3.5 eq.) was added and the reaction mixture was stirred at reflux overnight. After the reaction was completed (monitored by TLC), 1M aq. HCl was slowly poured in and reaction mixture was stirred for another 15 mins and then the product was extracted to DCM. Organic layer was washed with brine, dried with anhydrous Na_2SO_4 and concentrated under reduced pressure to obtain in 3-chloro-2-hydroxy-5-nitrobenzoic acid quantitative yield.

^{1}H NMR (300 MHz, DMSO-d_6): δ (ppm) 12.66 (br s, 2H), 8.48 (dd, *J* = 2.5, 0.9 Hz, 1H), 8.41 (dd, *J* = 2.9, 0.5 Hz, 1H).

General procedure for synthesis of anilines by palladium catalysed reduction of nitrobenzenes

Corresponding nitrobenzene derivative (1 eq.) was dissolved in EtOAc (10 mL/mmol), 10% Pd on carbon (0.01 eq.) was added and the reaction mixture was stirred at rt under hydrogen atmosphere overnight. After the reaction was completed (monitored by TLC), reaction mixture was filtered over Celite, filter was washed sufficiently with suitable solvent (usually EtOAc, MeOH or THF) and filtrate was concentrated under reduced pressure to obtain the crude product, which was either further purified (described separately for respective compounds) or used as such.

5-amino-3-chloro-2-methoxybenzoic acid (100%)

^{1}H NMR (300 MHz, DMSO-d_6): δ (ppm) 6.83 (d, *J* = 2.8 Hz, 1H), 6.78 (d, *J* = 2.8 Hz, 1H), 3.67 (s, 3H).

5-amino-3-chloro-2-hydroxybenzoic acid

The crude product was recrystallized from Et_2O to obtain 5-amino-3-chloro-2-hydroxybenzoic acid in 58% yield.

^{1}H NMR (300 MHz, DMSO-d_6): δ (ppm) 7.19 (d, *J* = 2.8 Hz, 1H), 7.05 (d, *J* = 2.8 Hz, 1H).

4-amino-2-methoxyphenol (100%)

^{1}H NMR (300 MHz, DMSO-d_6): δ (ppm) 7.79 (br s, 1H), 6.46 (d, *J* = 8.3 Hz, 1H), 6.23 (d, *J* = 2.5 Hz, 1H), 5.98 (dd, *J* = 8.3, 2.4 Hz, 1H), 4.44 (br s, 2H), 3.66 (s, 3H).

4-aminobenzene-1,2-diol (100%)

2-aminobenzo[d]thiazol-6-ol

2-aminobenzo[*d*]thiazol-6-ol was prepared according to the generel procedure for demethylation of methoxy group using aluminium chloride ($AlCl_3$).

Corresponding phenylmethylether (1 eq.) was dissolved/dispersed in anhydrous toluene (12 mL/mmol), aluminium chloride (3.5 eq.) was added and the reaction mixture was stirred at reflux overnight. After the reaction was completed (monitored by TLC), water was slowly poured in and the reaction mixture was stirred for another 15 mins. Then the product was extracted to EtOAc, organic layer was washed with brine, dried with anhydrous Na_2SO_4 and evaporated. The crude product was either further purified (described separately for respective compounds) or used as such.

The crude product was recrystallized from Et_2O to obtain 2-aminobenzo[*d*]thiazol-6-ol in 80% yield.

^{1}H NMR (500 MHz, DMSO-d_6): δ (ppm) 9.09 (br s, 1H), 7.13 (d, *J* = 8.6 Hz, 1H), 7.09 (br s, 2H), 7.03 (d, *J* = 2.5 Hz, 1H), 6.65 (dd, *J* = 8.6, 2.5 Hz, 1H).

*1-(3-chloro-4-methoxyphenyl)-3-(6-hydroxybenzo[d]thiazol-2-yl)urea (**48**)*

3-chloro-4-methoxyaniline (1 eq.) was dissolved in DMF (3 mL/mmol), CDI (1.1 eq.) was added and the reaction mixture was stirred at 35 °C for 6 h. Then 2-aminobenzo[*d*]thiazol-6-ol (1.1 eq.) was added and the reaction was stirred at 60 °C overnight. After the reaction was completed (monitored by TLC), 1M aq. HCl was added to the reaction mixture and resulting precipitate was collected by filtration. The crude product was purified using column chromatography to obtain the product **48** in 31% yield.

*General procedure for synthesis of guanidines from thioureas using mercury oxide (**50**, **53**, **56**, **59**, **62**, **100**)*

The corresponding thiourea (1 eq.) was dissolved in 7N methanolic ammonia solution (12 mL/mmol), mercury oxide (3 eq.) was added and the reaction mixture was stirred at room temperature overnight. After the reaction was completed (monitored by TLC), the reaction mixture was filtered over Celite and washed with either THF or MeOH (40 mL/mmol). Evaporation of the filtrate gave corresponding guanidine in poor to good yield (10–79 %). In cases, where further purification was required, the procedure is described together with the respective compound's characterization.

2-aminobenzo[d]thiazole-6-carboxylate

Ethyl 4-aminobenzoate (1 eq.) and KSCN (4 eq.) were dissolved in acetic acid (4 mL/mmol) and stirred at rt for 20 mins. Then the reaction mixture was cooled to 10 °C and bromine (2 eq.) dissolved in small amount of acetic acid was added dropwise. Afterwards the reaction mixture was left to warm up to rt and stirred overnight. After the reaction was completed (monitored by TLC), reaction mixture was added dropwise into the sat. aq. NH_3 solution (15 mL/mmol) while cooling in an ice bath. The product was extracted to EtOAc and the organic layer was washed with $Na_2S_2O_3$, sat. aq. $NaHCO_3$ and brine, dried using anhydrous Na_2SO_4 and concentrated under reduced pressure. The crude product was either recrystallized from diethylether to obtain ethyl 2-aminobenzo[*d*]thiazole-6-carboxylate in 69% yield.

^{1}H NMR (500 MHz, DMSO-d_6): δ (ppm) 8.27 (d, *J* = 1.8 Hz, 1H), 7.88 (s, 2H), 7.81 (dd, *J* = 8.4, 1.8 Hz, 1H), 7.36 (d, *J* = 8.4 Hz, 1H), 4.27 (q, *J* = 7.1 Hz, 2H), 1.30 (t, *J* = 7.1 Hz, 3H).

5-chlorobenzo[*d*]*thiazol-2-amine*

BrCN (1.5 eq.) was dissolved in mixture MeOH/H_2O of (2:1; 4 mL/mmol), then 2-amino-4-chlorobenzenethiol (1 eq.) dissolved in MeOH was added dropwise and the reaction mixture was stirred at rt overnight. The next day another 0.3 eq. of BrCN was added and reaction was stirred for 3

more days. After the reaction was completed (monitored by TLC), EtOAc was poured into the reaction and extracted with sat. aq. $NaHCO_3$ and brine, dried using anhydrous Na_2SO_4 and concentrated under reduced pressure. The crude product was purified by column chromatography to obtain 5-chlorobenzo[*d*]thiazol-2-amine in 31% yield.

^{1}H NMR (500 MHz, DMSO-d_6): δ (ppm) 7.68 (br s, 2H), 7.66 (d, *J* = 8.4 Hz, 1H), 7.34 (d, *J* = 2.0 Hz, 1H), 7.02 (dd, *J* = 8.3, 2.0 Hz, 1H).

di(1H-imidazol-1-yl)methanimine

Imidazole (3 eq.) and BrCN (1 eq.) were dissolved DCM (5 mL/mmol) and stirred at reflux for 30 mins. Then the reaction mixture was cooled to rt and filtered. Filtrate was concentrated under reduced pressure to 1/10 of its original volume and left to crystallize in freezer overnight. Resulting precipitate was collected by filtration to obtain the di(1*H*-imidazol-1-yl)methanimine in 76% yield.

^{1}H NMR (500 MHz, DMSO-d_6): δ (ppm) 10.20 (br s, 1H), 8.08 (d, *J* = 26.0 Hz, 2H), 7.56 (d, *J* = 36.6 Hz, 2H), 7.12 (d, *J* = 7.8 Hz, 2H).

2-amino-6-chlorobenzenethiol

7-chlorobenzo[*d*]thiazole-2-thiol (1 eq.) was dissolved in 50% aq. hydrazine solution (2 mL/mmol) and stirred at 110 °C overnight. After the reaction was completed (monitored by TLC), water was poured into the reaction, pH was adjusted to 7 using 1M HCl and the product was extracted to Et_2O. Organic layer was washed brine, dried using anhydrous Na_2SO_4 and concentrated under reduced pressure. The crude product was purified by column chromatography to obtain 2-amino-6-chlorobenzenethiol in 65% yield.

^{1}H NMR (300 MHz, DMSO-d_6): δ (ppm) 7.02 (t, *J* = 8.0 Hz, 1H), 6.64 (dd, *J* = 8.3, 1.3 Hz, 1H), 6.57 (dd, *J* = 7.7, 1.2 Hz, 1H), 5.78 (br s, 2H).

7-chlorobenzo[*d*]*thiazol-2-amine*

2-amino-6-chlorobenzenethiol (1 eq.) and di(1*H*-imidazol-1-yl)methanimine (1.1 eq.) were dissolved in 1,4-dioxane (4 mL/mmol) and the reaction mixture was stirred at reflux for 3 days. Then water was added to quench the reaction and product was extracted to EtOAc. Organic layer was washed with brine, dried with anhydrous Na_2SO_4 and concentrated under reduced pressure. The crude product was purified by column chromatography to obtain 7-chlorobenzo[*d*]thiazol-2-amine in 17% yield.

^{1}H NMR (500 MHz, DMSO-d_6): δ (ppm) 7.73 (br s, 2H), 7.28 (dd, *J* = 8.0, 1.0 Hz, 1H), 7.23 (t, *J* = 7.9 Hz, 1H), 7.08 (dd, *J* = 7.8, 1.0 Hz, 1H).

*6-chlorobenzo[d]thiazole (**66**)*

6-chlorobenzo[*d*]thiazol-2-amine (1 eq.) was dissolved in THF (2.5 mL/mmol), amylnitrite (2.2 eq.) was added dropwise and the reaction mixture was stirred at reflux for 30 mins. After the reaction was completed (monitored by TLC), the solvent was evaporated and the residue was partitioned between EtOAc and water. The organic layer was washed with 15% citric acid and brine, dried with anhydrous Na_2SO_4 and evaporated. The crude product was purified by column chromatography to obtain 6-chlorobenzo[*d*]thiazole in 82% yield.

*1-(6-aminobenzo[d]thiazol-2-yl)-3-(3-chloro-4-hydroxyphenyl)urea (**77**)*

1-(3-chloro-4-hydroxyphenyl)-3-(6-nitrobenzo[*d*]thiazol-2-yl)urea (1 eq.) was dissolved in mixture of THF/ MeOH /water (2:1:1; 12 mL/mmol), iron powder (10 eq.) and ammonium chloride (4 eq.) were added and the reaction mixture was stirred at 50 °C overnight. After the reaction was completed (monitored by TLC), the reaction mixture was filtered over Celite, washed with THF and concentrated. The product was precipitated from the residual liquid by addition of water, filtered and dried under reduced pressure. Recrystallization from Et_2O gave 1-(6-aminobenzo[*d*]thiazol-2-yl)-3-(3-chloro-4-hydroxyphenyl)urea in 77% yield.

*1-(3-chloro-4-hydroxyphenyl)-3-(6-hydroxybenzo[d]thiazol-2-yl)urea (**78**)*

1-(3-chloro-4-hydroxyphenyl)-3-(6-hydroxybenzo[*d*]thiazol-2-yl)urea was prepared from 1-(3-chloro-4-methoxyphenyl)-3-(6-hydroxybenzo[*d*]thiazol-2-yl)urea (**48**) according to the General demethylation procedure using $AlCl_3$ described above (see 2-aminobenzo[*d*]thiazol-6-ol synthesis).

The crude product was purified using column chromatography (85%).

General procedure for synthesis of benzo[d]thiazol-2-amines substituted in position 6 using tetramethylammonium dichloroiodate

Corresponding 6-substituted aniline (1 eq.) and KSCN (7 eq.) were dissolved in mixture of DMSO/H_2O (9:1; 10 mL/mmol). Tetramethylammonium dichloroiodate (3 eq.) was added and the reaction mixture stirred at rt for 5 mins and then at 70 °C overnight. After the reaction was completed (monitored by TLC), water was poured into the reaction and the product extracted to EtOAc. The organic layer was washed with $Na_2S_2O_3$, sat. aq. $NaHCO_3$ and brine, dried using anhydrous Na_2SO_4 and concentrated under reduced pressure. The crude product was used without further purification or purified by column chromatography.

6-(tert-butyl)benzo[d]thiazol-2-amine

The crude product was used for the next step without further purification (98%).

^{1}H NMR (500 MHz, DMSO-d_6): δ (ppm) 7.65 (m, 1H), 7.33 (br s, 2H), 7.25 – 7.22 (m, 2H), 1.28 (s, 9H).

6-iodobenzo[d]thiazol-2-amine

The crude product was purified using column chromatography (36%).

^{1}H NMR (500 MHz, DMSO-d_6): δ (ppm) 8.00 (d, *J* = 1.8 Hz, 1H), 7.58 (br s, 2H), 7.48 (dd, *J* = 8.4, 1.9 Hz, 1H), 7.12 (d, *J* = 8.4 Hz, 1H).

6-chloro-1H-benzo[*d*]*imidazol-2-amine*

BrCN (1.1 eq.) was dissolved in mixture MeCN/H_2O of (1:10; 3 mL/mmol), then 4-chlorobenzene-1,2-diamine (1 eq.) dissolved in MeOH was added dropwise and the reaction mixture was stirred at rt for 2 h. After the reaction was completed (monitored by TLC), EtOAc was poured into the reaction and extracted with sat. aq. $NaHCO_3$ and brine, dried using anhydrous Na_2SO_4 and concentrated under reduced pressure. The crude product was purified by column chromatography to obtain 6-chloro-1*H*-benzo[*d*]imidazol-2-amine in 71% yield.

^{1}H NMR (300 MHz, DMSO-d_6): δ (ppm) 10.75 (br s, 1H), 7.09 (d, *J* = 2.0 Hz, 1H), 7.06 (d, *J* = 8.3 Hz, 1H), 6.84 (dd, *J* = 8.3, 2.1 Hz, 1H), 6.33 (br s, 2H).

General procedure for synthesis of benzo[d]oxazol-2-amines from 2-aminophenols using cyanic bromide

Corresponding 2-aminophenol (1 eq.) was dissolved in THF (4 mL/mmol), cyanic bromide (1.8 eq.; BrCN) was added and the reaction mixture was stirred at rt overnight. The next day another 0.35 eq of BrCN was added and reaction was stirred for 3 more days. After the reaction was completed (monitored by TLC), EtOAc was poured into the reaction and extracted with sat. aq. $NaHCO_3$ and brine, dried using anhydrous Na_2SO_4 and concentrated under reduced pressure. The crude product was purified by column chromatography to obtain the corresponding benzo[*d*]oxazol-2-amine.

benzo[d]oxazol-2-amine (87%)

^{1}H NMR (300 MHz, DMSO-d_6): δ (ppm) 7.37 (br s, 2H), 7.30 (d, *J* = 7.7 Hz, 1H), 7.19 (d, *J* = 7.0 Hz, 1H), 7.08 (td, *J* = 7.6, 1.2 Hz, 1H), 6.95 (td, *J* = 7.7, 1.3 Hz, 1H).

6-chlorobenzo[d]oxazol-2-amine (73%)

^{1}H NMR (500 MHz, DMSO-d_6): δ (ppm) 7.53 (s, 2H), 7.47 (d, *J* = 1.9 Hz, 1H), 7.17 (d, *J* = 8.3 Hz, 1H), 7.12 (dd, *J* = 8.3, 1.9 Hz, 1H).

*1-(benzo[d]thiazol-6-yl)-3-(3-chloro-4-hydroxyphenyl)urea (**92**)*

Benzo[*d*]thiazol-6-amine was dissolved in a mixture of DCM and DMF (6:1; 12 mL/mmol). CDI (1.1 eq.) was added and the reaction mixture was stirred at reflux overnight. The resulting precipitate

was collected by filtration and removed. Filtrate was concentrated, dissolved in MeCN (10 mL/mmol), 4-amino-2-chlorophenol (1.1 eq.) was added and the reaction was stirred at reflux overnight. After the reaction was completed (monitored by TLC), 1M aq. HCl was added to the reaction mixture and resulting precipitate was collected by filtration. The crude product was purified using column chromatography to obtain 1-(benzo[*d*]thiazol-6-yl)-3-(3-chloro-4-hydroxyphenyl)urea in 25% yield.

*1-(3-chloro-4-hydroxyphenyl)-3-(2,3-dihydro-1H-inden-2-yl)urea (**96**)*

2,3-dihydro-1*H*-inden-2-amine (1 eq.) was dissolved in DMF (3 mL/mmol), CDI (1.1 eq.) was added and the reaction mixture was stirred at 50 °C for 6 h. Then 4-amino-2-chlorophenol (1.1 eq.) was added and the reaction was stirred at 70 °C overnight. After the reaction was completed (monitored by TLC), 1M aq. HCl was added to the reaction mixture and resulting precipitate was collected by filtration. The crude product was purified using column chromatography to obtain *N*-(3-chloro-4-hydroxyphenyl)-6-methoxybenzo[*d*]thiazole-2-carboxamide in 21% yield.

*1-(3-chloro-4-hydroxyphenyl)-3-(4-methoxyphenethyl)urea (**97**)*

2-(4-methoxyphenyl)ethan-1-amine (1 eq.) was dissolved in DMF (7 mL/mmol), CDI (1.1 eq.) was added and the reaction mixture was stirred at 45 °C for 6 h. Then 4-amino-2-chlorophenol (1.1 eq.) was added and the reaction was stirred at 70 °C overnight. After the reaction was completed (monitored by TLC), 1M aq. HCl was added to the reaction mixture and resulting precipitate was collected by filtration. The crude product was purified using column chromatography to obtain 1-(3-chloro-4-hydroxyphenyl)-3-(4-methoxyphenethyl)urea in 21% yield.

1,3-bis(3-chloro-4-methoxyphenyl)urea

3-chloro-4-methoxyaniline (2 eq.) was dissolved in DMF (3 mL/mmol), CDI (1 eq.) was added and the reaction mixture was stirred at 60°C overnight. After the reaction was completed (monitored by TLC), 1M aq. HCl was added to the reaction mixture and resulting precipitate was collected by filtration, washed with water and dried to give 1,3-bis(3-chloro-4-methoxyphenyl)urea in 90% yield.

^{1}H NMR (300 MHz, DMSO-d_6): δ (ppm) 8.62 (br s, 2H), 7.64 (d, *J* = 2.2 Hz, 2H), 7.25 (dd, *J* = 8.9, 2.2 Hz, 2H), 7.07 (d, *J* = 8.9 Hz, 2H), 3.80 (s, 6H).

*1,3-bis(3-chloro-4-hydroxyphenyl)urea (**98**)*

1,3-bis(3-chloro-4-hydroxyphenyl)urea was prepared from 1,3-bis(3-chloro-4-methoxyphenyl)urea according to the General demethylation procedure using $AlCl_3$ described above (see 2-aminobenzo[*d*]thiazol-6-ol synthesis).

The crude product was recrystallized from Et_2O to obtain compound **98** in 94% yield.

*2-chloro-4-((6-chlorobenzo[d]thiazol-2-yl)amino)phenol (**101**)*

2,6-dichlorobenzo[*d*]thiazole (1 eq.) and 4-amino-2-chlorophenol (1.05 eq.) were dissolved in *N*-methyl-2-pyrrolidone (NMP; 3mL/mmol) and the reaction mixture was stirred at 160°C overnight. After the reaction was completed (monitored by TLC), 1M aq. HCl was added to the reaction mixture and the water layer was extracted with EtOAc. The water layer was adjusted to pH=7 and extracted with EtOAc. The organic layer was evaporated and the crude residue was purified using column chromatography to obtain the product in 30% yield.

3-chloro-4-methoxy-N-(6-methoxybenzo[d]thiazol-2-yl)benzamide

3-chloro-4-methoxybenzoic acid (1 eq.) was dissolved in anhydrous DMF (7 mL/mmol), CDI (1.1 eq.) was added and the reaction mixture was stirred at rt for 2 h. Then 6-methoxybenzo[*d*]thiazol-2-amine (1.1 eq.) was added and the reaction was stirred at rt overnight. After the reaction was completed (monitored by TLC), 1M aq. HCl was added to the reaction mixture and the resulting precipitate was collected by filtration and dried. The crude product was purified by column chromatography to obtain 3-chloro-4-methoxy-*N*-(6-methoxybenzo[*d*]thiazol-2-yl)benzamide in 34% yield.

*3-Chloro-4-hydroxy-N-(6-methoxybenzo[d]thiazol-2-yl)benzamide (**102**)*

3-chloro-4-hydroxy-*N*-(6-methoxybenzo[*d*]thiazol-2-yl)benzamide was prepared from 3-chloro-4-methoxy-*N*-(6-methoxybenzo[*d*]thiazol-2-yl)benzamide according to the General demethylation procedure using $AlCl_3$ described above (see 2-aminobenzo[*d*]thiazol-6-ol synthesis).

The crude product was purified by column chromatography to obtain compound **102** in 69% yield.

*N-(3-chloro-4-hydroxyphenyl)-6-methoxybenzo[d]thiazole-2-carboxamide (**103**)*

6-methoxybenzo[*d*]thiazole-2-carboxylic acid (1 eq.) was dissolved in anhydrous DMF (7 mL/mmol), CDI (1.1 eq.) was added and the reaction mixture was stirred at rt for 1 h. Then 4-amino-2-chlorophenol (1.1 eq.) was added and the reaction was stirred at rt overnight. After the reaction was completed (monitored by TLC), 1M aq. HCl was added to the reaction mixture, resulting precipitate was collected by filtration and recryctallized from MeCN to obtain *N*-(3-chloro-4-hydroxyphenyl)-6-methoxybenzo[*d*]thiazole-2-carboxamide in 58% yield.

4-(aminomethyl)-2-chlorophenol

4-(aminomethyl)-2-chlorophenol was prepared from (3-chloro-4-methoxyphenyl)methanaminium chloride according to the General demethylation procedure using $AlCl_3$ described above (see 2-aminobenzo[*d*]thiazol-6-ol synthesis).

After the reaction was completed (monitored by TLC), water was slowly poured in and the reaction mixture was stirred for another 15 mins. The organic layer was removed and the water layer was filtered and the filtrate evaporated. The solid residue was dispersed in acetone using the ultrasound bath and filtered. Filtrate was evaporated to give 4-(aminomethyl)-2-chlorophenol (92%), which was used for the next step without further purification.

N-methylbenzo[d]thiazol-2-amine

2-iodoaniline (1 eq.), methylisothiocyanate (1 eq.), tetrabutylammonium bromide (1 eq.) and copper (I) chloride (0.01 eq.) were dissolved in DMSO (7 mL/mmol) and the reaction mixture was stirred at 80°C overnight. After the reaction was completed (monitored by TLC), water was added to the reaction mixture and the product was extracted to Et_2O. Organic layer was washed with brine, dried using anhydrous Na_2SO_4 and concentrated under reduced pressure. The crude product was purified by column chromatography to obtain *N*-methylbenzo[*d*]thiazol-2-amine in 40% yield.

^{1}H NMR (500 MHz, DMSO-d_6): δ (ppm) 7.91 (d, *J* = 4.4 Hz, 1H), 7.65 (dd, *J* = 7.8, 0.9 Hz, 1H), 7.39 (dd, *J* = 8.0, 0.6 Hz, 1H), 7.21 (ddd, *J* = 8.1, 7.4, 1.3 Hz, 1H), 7.05 – 6.96 (m, 1H), 2.93 (d, *J* = 4.7 Hz, 3H).

2-chloro-4-isocyanato-1-methoxybenzene

Triphosgene (1 eq.) was dissolved in anh. DCM (3.5 mL/mmol) at 0 °C and 3-chloro-4-methoxyaniline (1 eq.), dissolved in anh. DCM, was added dropwise. Consequently, Et_3N (0.3 mL/mmol) was added dropwise and the reaction mixture was stirred at reflux for 1 h. Then the reaction was cooled to the room temperature, Et_2O was added, the mixture was filtered and washed with Et_2O. The filtrate was concentrated under reduced pressure to obtain the crude product (100%), which was used without further purification for the next step.

1-(benzo[d]thiazol-2-yl)-3-(3-chloro-4-methoxyphenyl)-1-methylurea

N-methylbenzo[*d*]thiazol-2-amine (1 eq.) was dissolved in anh. THF (6 mL/mmol), 2-chloro-4-isocyanato-1-methoxybenzene (0.95 eq.), dissolved in anh. THF, was added dropwise and the reaction mixture was stirred at reflux overnight. After the reaction was completed (monitored by TLC), 1M aq. HCl (1 mL/mmol) was added dropwise and the reaction mixture was evaporated to

dryness under reduced pressure. The crude residue was dispersed in MeOH in the ultrasound bath, filtered and washed with MeOH to give the product in 67% yield.

^{1}H NMR (500 MHz, DMSO-d_6): δ (ppm) 9.54 (s, 1H), 7.91 (dd, *J* = 7.8, 0.6 Hz, 1H), 7.75 (d, *J* = 8.0 Hz, 1H), 7.69 (d, *J* = 2.6 Hz, 1H), 7.49 (dd, *J* = 8.9, 2.6 Hz, 1H), 7.44 – 7.37 (m, 1H), 7.30 – 7.23 (m, 1H), 7.16 (d, *J* = 9.0 Hz, 1H), 3.85 (s, 3H), 3.76 (s, 3H).

*1-(benzo[d]thiazol-2-yl)-3-(3-chloro-4-hydroxyphenyl)-1-methylurea (**106**)*

Compound **106** was prepared from 1-(benzo[*d*]thiazol-2-yl)-3-(3-chloro-4-methoxyphenyl)-1-methylurea according to the General demethylation procedure using $AlCl_3$ described above (see 2-aminobenzo[*d*]thiazol-6-ol synthesis).

The crude product was purified by column chromatography to obtain compound **106** in 83% yield.

3-chloro-4-methoxy-N-methylaniline

3-chloro-4-methoxyaniline (1 eq.) was dissolved in anh. THF (4 mL/mmol), sodium hydride (1.5 eq.) was added at 0°C and the reaction mixture was stirred for 30 mins. Then methyl iodide (1.1 eq.) was added and the reaction was allowed to warm up to rt and stirred overnight. After the reaction was completed (monitored by TLC), water was slowly added into the reaction and product was extracted to EtOAc. The organic layer was washed with brine, dried using anhydrous Na_2SO_4 and concentrated under reduced pressure. The crude product was purified by column chromatography to obtain 3-chloro-4-methoxy-*N*-methylaniline in 28% yield.

^{1}H NMR (500 MHz, $CDCl_3$): δ (ppm) 6.82 (d, *J* = 8.8 Hz, 1H), 6.68 (d, *J* = 2.7 Hz, 1H), 6.50 (dd, *J* = 8.8, 2.7 Hz, 1H), 3.82 (s, 3H), 2.79 (s, 3H).

2-chloro-4-(methylamino)phenol

2-chloro-4-(methylamino)phenol was prepared from 3-chloro-4-methoxy-*N*-methylaniline according to the General demethylation procedure using $AlCl_3$ described above (see 2-aminobenzo[*d*]thiazol-6-ol synthesis).

The crude product was purified by column chromatography to obtain the product in 74% yield.

^{1}H NMR (500 MHz, $CDCl_3$): δ (ppm) 6.86 (d, *J* = 8.7 Hz, 1H), 6.59 (d, *J* = 2.8 Hz, 1H), 6.48 (dd, *J* = 8.7, 2.8 Hz, 1H), 2.78 (s, 3H).

3-(benzo[d]thiazol-2-yl)-1-(3-chloro-4-methoxyphenyl)-1-methylurea

3-(benzo[*d*]thiazol-2-yl)-1-(3-chloro-4-methoxyphenyl)-1-methylurea was prepared from benzo[*d*]thiazol-2-amine and 3-chloro-4-methoxy-*N*-methylaniline in two steps according to the general procedure for synthesis of urea derivatives employing CDI (described earlier in this chapter).

1-(benzo[d]thiazol-2-yl)-3-(3-chloro-4-methoxyphenyl)-1,3-dimethylurea

3-(benzo[*d*]thiazol-2-yl)-1-(3-chloro-4-methoxyphenyl)-1-methylurea (1 eq.) was dissolved in anh. DMF (10 mL/mmol), sodium hydride (1.2 eq.) was added at 0°C and the reaction mixture was stirred for 30 mins. Then methyl iodide (2.2 eq.) was added and the reaction was allowed to warm up to rt and stirred overnight. After the reaction was completed (monitored by TLC), water was slowly added and product was extracted to EtOAc. The organic layer was washed with brine, dried using anhydrous Na_2SO_4 and concentrated under reduced pressure. The crude product was recrystallized from MeOH to obtain the product in 77% yield.

^{1}H NMR (500 MHz, DMSO-d_6): δ (ppm) 7.76 (d, *J* = 7.7 Hz, 1H), 7.49 (d, *J* = 2.6 Hz, 1H), 7.48 – 7.39 (m, 2H), 7.31 (dd, *J* = 8.8, 2.5 Hz, 1H), 7.25 (t, *J* = 8.0 Hz, 1H), 7.13 (d, *J* = 8.9 Hz, 1H), 3.87 (s, 3H).

*1-(benzo[d]thiazol-2-yl)-3-(3-chloro-4-hydroxyphenyl)-1,3-dimethylurea (**109**)*

1-(benzo[*d*]thiazol-2-yl)-3-(3-chloro-4-hydroxyphenyl)-1,3-dimethylurea was prepared from 1-(benzo[*d*]thiazol-2-yl)-3-(3-chloro-4-methoxyphenyl)-1,3-dimethylurea according to the General demethylation procedure using $AlCl_3$ described above (see 2-aminobenzo[*d*]thiazol-6-ol synthesis).

The crude product was purified by column chromatography to obtain compound **109** in 65% yield.

*Detailed synthesis of indole analogues **110 – 112** (respective steps according to Scheme 17 in the manuscript).*

a) Malononitrile (1 eq) and EtOH (1.1 eq) were dissolved in Et_2O saturated with HCl gas (0.8 mL/mmol) at 0˚C under argon atmosphere. Reaction mixture was allowed to warm to RT and stirred for 4 h. Precipitate was filtered off and washed extensively with Et_2O. Free base was obtained by addition of K_2CO_3 saturated aq. solution and extraction into Et_2O. Organic layer was then dried with brine and Na_2SO_4 and evaporated to obtain 3-amino-3-ethoxyacrylonitrile as white solid (18%), which was used for the next step without further purification.

b) 3-amino-3-ethoxyacrylonitrile (1 eq) was dissolved in EtOH (1 mL/mmol) under argon atmosphere, corresponding amine (1.2 eq) was added and reaction mixture stirred at RT overnight. Solvent was evaporated and product isolated by flash chromatography (hex/EtOAc) to obtain

product 3-(allylamino)-3-aminoacrylonitrile (R_f = 0.30, EtOAc) as yellow oil (61%) or 3-amino-3-(prop-2-yn-1-ylamino)acrylonitrile (R_f = 0.30, EtOAc) as orange oil (77%).

3-(allylamino)-3-aminoacrylonitrile

^{1}H NMR (300 MHz, DMSO-d_6): δ (ppm) 6.12 (t, *J* = 5.2 Hz, 1H), 5.89 – 5.70 (m, 1H), 5.53 (s, 2H), 5.24 – 5.13 (m, 1H), 5.13 – 5.07 (m, 1H), 3.53 (t, *J* = 5.5 Hz, 2H), 2.85 (s, 1H).

3-amino-3-(prop-2-yn-1-ylamino)acrylonitrile

^{1}H NMR (300 MHz, DMSO-d_6): δ (ppm) 6.25 (t, *J* = 5.7 Hz, 1H), 5.62 (s, 2H), 3.74 (dd, *J* = 5.8, 2.5 Hz, 2H), 3.20 (t, *J* = 2.5 Hz, 1H), 2.93 (s, 1H).

c) Corresponding *N*-substituted 3,3-diaminoacrylonitrile (**3**) (1 eq) was dissolved in EtOH (4 mL/mmol) under argon atmosphere, *p*-benzoquinone (1.2 eq) was added and reaction mixture stirred at RT for 1 h. Solvent was evaporated and product (**4**) isolated by flash chromatography (hex/EtOAc). 2-(allylamino)-5-hydroxy-1*H*-indole-3-carbonitrile (**4a**) (R_f = 0.40, hex/EtOAc, 40%) was obtained as brown solid (22%). Recrystallization from EtOAc/hex gave beige crystals. Mixture of 5-hydroxy-2-(prop-2-yn-1-ylamino)-1*H*-indole-3-carbonitrile (**4b**) and 2-amino-5-hydroxy-1-(prop-2-yn-1-yl)-1*H*-indole-3-carbonitrile (**4c**) was obtained as brown oil. Repeated flash chromatography DCM/MeOH with SiO_2 neutralized by washing with Et_3N resulted in isolation of the products as brown oils. Recrystallization from EtOAc/hexane gave **4b** (R_f = 0.10, DCM/MeOH, 5%) as white crystals (10%) and **4c** (R_f = 0.15, DCM/MeOH, 5%) as off-white crystals (14%).

*Detailed synthesis of indolotacrine analogues (**114 – 116**) and indole analogue **113** (respective steps according to Scheme 18 in the manuscript).*

a) 2-iodo-4-methoxy-1-nitrobenzene (1 eq), Fe powder (10 eq) and NH_4Cl (4 eq) were dissolved/dispersed in MeOH/H_2O (3:1; 14 mL/mmol) and stirred at 50˚C for 2 h. The mixture was filtered and washed extensively with MeOH. The filtrate was concentrated under vacuum, resulting liquid diluted with water and extracted with EtOAc. Organic layer was washed with brine, dried over Na_2SO_4 and evaporated. 2-iodo-4-methoxyaniline (R_f = 0.25, hex/DCM, 5%) was isolated by flash chromatography (hex/DCM) as light orange oil (79%). Compounds 2-iodoaniline and 4-chloro-2-iodoaniline were purchased commercially.

2-iodo-4-methoxyaniline

^{1}H NMR (300 MHz, $CDCl_3$): δ (ppm) 7.21 (d, *J* = 2.7 Hz, 1H), 6.77 (dd, *J* = 8.7, 2.7 Hz, 1H), 6.70 (d, *J* = 8.7 Hz, 1H), 3.79 (s, 2H), 3.72 (s, 3H).

b) Corresponding 2-iodoaniline derivative (1 eq) was dissolved in dry THF (2.5 mL/mmol), Et_3N (1.2 eq) was added and resulting solution cooled down to -7˚C. Trifluroacetic anhydride (1.2 eq) dissolved in dry THF was added dropwise within 20 min and then the reaction was allowed to warm up to RT and was stirred overnight. After completion the reaction was diluted with water and the product extracted to EtOAc. Organic layer was washed with brine, dried over Na_2SO_4 and evaporated to obtain 2,2,2-trifluoro-*N*-(2-iodophenyl)acetamide (R_f = 0.40, hept/EtOAc, 25%) as light pink solid (99%), 2,2,2-trifluoro-*N*-(2-iodo-4-methoxyphenyl)acetamide (R_f = 0.30, hex/DCM, 50%) as off-white crystals (97%) or 2,2,2-trifluoro-*N*-(2-iodo-4-chlorophenyl)acetamide (R_f = 0.50, hept/EtOAc, 25%) as pink solid (98%). Products were used for the next step without further purification.

c) Corresponding 2,2,2-trifluoro-*N*-(2-iodophenyl)acetamide derivative (1 eq), malononitrile (1.2 eq), K_2CO_3 (2 eq) and *L*-proline (0.2 eq) were dispersed in DMSO/H_2O (1:1; 2 mL/mmol) and stirred for 15 min at RT. Then CuI (0.1 eq) was added and the reaction mixture stirred at 60˚C overnight. After completion the reaction mixture was filtrated and filter washed extensively with MeOH. The filtrate was concentrated and resulting liquid diluted with water and extracted with Et_2O. Organic layer was washed with brine, dried over Na_2SO_4 and evaporated to obtain 2-amino-5-methoxy-1*H*-indole-3-carbonitrile (R_f = 0.25, hex/EtOAc, 50%) as beige solid (90%). In case of 2-amino-1*H*-indole-3-carbonitrile and 2-amino-5-chloro-1*H*-indole-3-carbonitrile (**113**) the crude product was purified by flash chromatography (hex/EtOAc) to afford (R_f = 0.30, hex/EtOAc, 50%) as beige solid (56%) and **113** (R_f = 0.35, hex/EtOAc, 50%) as brown solid (48%).

2-amino-1H-indole-3-carbonitrile

^{1}H NMR (500 MHz, DMSO-d_6): δ (ppm) 10.68 (br s, 1H), 7.13 (d, *J* = 8.6 Hz, 2H), 6.96 (t, *J* = 7.5 Hz, 1H), 6.90 (t, *J* = 7.5 Hz, 1H), 6.71 (s, 2H).

2-amino-5-methoxy-1H-indole-3-carbonitrile

^{1}H NMR (300 MHz, DMSO-d_6): δ (ppm) 10.49 (br s, 1H), 7.00 (d, *J* = 8.5 Hz, 1H), 6.65 (d, *J* = 2.0 Hz, 3H), 6.49 (dd, *J* = 8.5, 2.5 Hz, 1H), 3.72 (s, 3H).

d) $AlCl_3$ (1.5 eq) and corresponding 2-amino-1*H*-indole-3-carbonitrile derivative (1 eq) were loaded into a 10 mL microwave glass tube under argon atmosphere and dispersed in dry 1,2-dichloroethane (7 mL). Cyclohexanone (1.5 eq) was added and reaction exposed to microwave irradiation at 95˚C for 2 h. Reaction was quenched by adding THF/H_20 (2:1; 15 mL) dropwise at RT. An aqueous solution of NaOH (10%) was added dropwise to adjust pH 8-9. After stirring for 30 min, the mixture was extracted with DCM. The organic layer was washed with brine, dried over Na_2SO_4 and concentrated. The crude product was purified by flash chromatography (DCM/MeOH) to afford the 2,3,4,6-tetrahydro-1*H*-indolo[2,3-*b*]quinolin-11-amine (**114**) (R_f = 0.20, DCM/MeOH, 10%) as beige

solid (25%), 9-methoxy-2,3,4,6-tetrahydro-1*H*-indolo[2,3-*b*]quinolin-11-amine (**115**) (R_f = 0.20, DCM/MeOH, 10%) as beige solid (16%) or 6-benzyl-2,3,4,6-tetrahydro-1*H*-indolo[2,3-*b*]quinolin-11-amine (**116**) (R_f = 0.60, DCM/MeOH, 10%) as beige solid (54%). Recrystallization from EtOH gave beige crystals in all cases.

e) 2-iodoaniline (1 eq) and benzaldehyde (1 eq) were dissolved in MeOH (2 mL/mmol) and stirred at RT overnight. Evaporation of solvent gave crude product (*E*)-*N*-(2-iodophenyl)-1-phenylmethanimine (R_f = 0.70, hex/EtOAc, 25%) as brown oil (97%). The crude product was used for the next step without further purification.

(E)-N-(2-iodophenyl)-1-phenylmethanimine

^{1}H NMR (300 MHz, DMSO-d_6): δ (ppm) 8.48 (s, 1H), 8.10 – 7.96 (m, 2H), 7.91 (d, *J* = 7.9 Hz, 1H), 7.64 – 7.51 (m, 3H), 7.45 (t, *J* = 7.6 Hz, 1H), 7.20 (d, *J* = 7.8 Hz, 1H), 7.00 (t, *J* = 7.6 Hz, 1H).

f) (*E*)-*N*-(2-iodophenyl)-1-phenylmethanimine (1 eq) was dissolved in MeOH (15 mL/mmol), resulting solution was acidified with acetic acid (2 drops/mmol) and cooled to 0˚C. $NaBH_3CN$ (1.1 eq) was added at 0 ˚C and the reaction was allowed to warm up to RT and stirred overnight. After completion the reaction was quenched with few drops of 1 M NaOH aq. solution (pH 8) and the product *N*-benzyl-2-iodoaniline (R_f = 0.65, hex/EtOAc, 20%) isolated by flash chromatography (hex/EtOAc) as light yellow oil (75%).

N-benzyl-2-iodoaniline

^{1}H NMR (300 MHz, $CDCl_3$): δ (ppm) 7.68 (dd, *J* = 7.8, 1.5 Hz, 1H), 7.43 – 7.27 (m, 5H), 7.20 – 7.11 (m, 1H), 6.54 (dd, *J* = 8.2, 1.3 Hz, 1H), 6.48 – 6.42 (m, 1H), 4.63 (br s, 1H), 4.41 (d, *J* = 4.2 Hz, 2H).

g) Malononitrile (1.2 eq), picolinic acid (0.2 eq), K_2CO_3 (3 eq) and CuI (0.1 eq) were charged into microwave vessel under argon atmosphere. *N*-benzyl-2-iodoaniline (1 eq) dissolved in dry DMSO was added and the reaction mixture was exposed to microwave irradiation at 90˚C for 12 h. After completion the reaction mixture was diluted with water and the product extracted to Et_2O. Organic layer was washed with brine, dried over Na_2SO_4 and evaporated. 2-amino-1-benzyl-1*H*-indole-3-carbonitrile (R_f = 0.60, hex/EtOAc, 50%) was isolated by flash chromatography (hex/EtOAc) as yellow-brown solid (26%).

2-amino-1-benzyl-1H-indole-3-carbonitrile

^{1}H NMR (300 MHz, DMSO-d_6): δ (ppm) 7.38 – 7.06 (m, 9H), 7.05 – 6.96 (m, 1H), 6.94 – 6.86 (m, 1H), 5.33 (s, 2H).

Hydrochlorides of final products were prepared by dissolving the compounds in a minimal volume of EtOAc and adding dropwise a saturated solution of HCl (g) in diethyl ether. A white solid was formed, that was separated by filtration, washed with diethyl ether and dried under reduced pressure.

4.2 Final products and their characterization

Yields are given for the last step of synthesis resp. last 2 steps in case that the synthesis followed the general procedure employing CDI for preparation of urea derivatives.

Compound 4 (standard 5h)[51]

methyl 5-(3-(6-fluorobenzo[*d*]thiazol-2-yl)ureido)-2-hydroxybenzoate

M.p. 277–279 °C. Yield 81 %.^{1}H NMR (500 MHz, DMSO-d_6): δ (ppm) 10.28 (br s, 1H), 9.09 (br s, 1H), 8.04 (d, *J* = 2.6 Hz, 1H), 7.82 (dd, *J* = 8.7, 2.6 Hz, 1H), 7.68 – 7.60 (m, 1H), 7.55 (dd, *J* = 8.9, 2.7 Hz, 1H), 7.23 (td, *J* = 9.1, 2.7 Hz, 1H), 6.98 (d, *J* = 9.0 Hz, 1H), 3.92 (s, 3H). ^{13}C NMR (126 MHz, DMSO-d_6): δ (ppm) 168.94, 159.54, 158.29 (d, *J* = 239.0 Hz), 155.98, 152.11, 132.43, 130.19, 127.59, 120.38, 120.13, 117.80, 113.80 (d, *J* = 24.4 Hz), 112.71, 108.09 (d, *J* = 26.9 Hz), 52.55. ESI-MS: *m/z* 362 [M+H$^+$] (calc. for $C_{16}H_{12}FN_3O_4S$: 361.05). EA: calc. C 53.18; H 3.35; N 11.63; S 8.87. Found: C 52.90; H 2.96; N 11.28; S 9.15.

Compound 5 (standard 5l)[51]

methyl 5-(3-(6-chlorobenzo[*d*]thiazol-2-yl)ureido)-2-hydroxybenzoate

M.p. 278–280 °C. Yield 80 %.^{1}H NMR (500 MHz, DMSO-d_6): δ (ppm) 10.29 (br s, 1H), 9.11 (br s, 1H), 8.08 – 8.00 (m, 2H), 7.62 (d, *J* = 9.0 Hz, 1H), 7.55 (dd, *J* = 9.6, 2.3 Hz, 1H), 7.39 (dd, *J* = 9.0, 2.1 Hz, 1H), 6.98 (d, *J* = 9.7 Hz, 1H), 3.92 (s, 3H). ^{13}C NMR (126 MHz, DMSO-d_6): δ (ppm) 168.94, 160.46, 156.00, 152.24, 147.04, 132.88, 130.15, 127.59, 126.89, 126.20, 121.21, 120.13, 117.80, 112.69, 52.55. ESI-MS: *m/z* 378 [M+H$^+$] (calc. for $C_{16}H_{12}ClN_3O_4S$: 377.02). EA: calc. C 50.87; H 3.20; N 11.12; S 8.49. Found: C 50.57; H 3.47; N 10.88; S, 8.52.

Compound 6 (frentizole)

1-(6-methoxybenzo[*d*]thiazol-2-yl)-3-phenylurea

M.p. 328–330 °C. Yield 91 %. ^{1}H NMR (500 MHz, DMSO-d_6): δ (ppm) 10.68 (br s, 1H), 9.13 (br s, 1H), 7.56 (d, *J* = 8.8 Hz, 1H), 7.54 – 7.47 (m, 3H), 7.33 (t, *J* = 7.9 Hz, 2H), 7.05 (t, *J* = 7.3 Hz, 1H), 6.98 (dd, *J* = 8.8, 2.6 Hz, 1H), 3.79 (s, 3H). ^{13}C NMR (126 MHz, DMSO-d_6): δ (ppm) 157.68, 155.87, 152.01, 142.82, 138.66, 132.61, 129.10, 123.08, 120.29, 118.95, 114.55, 105.12, 55.78. ESI-MS: *m/z* 300 [M+H]$^+$ (calc. for $C_{15}H_{13}N_3O_2S$: 399.07). EA: calc. C, 60.19; H, 4.38; N, 14.04; S, 10.71. Found: C, 60.31; H, 4.20; N, 14.53; S, 10.71.

Compound 7

1-(6-fluorobenzo[*d*]thiazol-2-yl)-3-(4-hydroxyphenyl)urea

M.p. 250 °C decomp. Yield 90 %.^{1}H NMR (500 MHz, DMSO-d_6): δ (ppm) 8.85 (br s, 1H), 7.81 (dd, *J* = 8.7, 2.7 Hz, 1H), 7.67 – 7.60 (m, 1H), 7.30 – 7.25 (m, 2H), 7.21 (td, *J* = 9.1, 2.7 Hz, 1H), 6.76 – 6.71 (m, 2H). ^{13}C NMR (126 MHz, DMSO-d_6): δ (ppm) 159.64, 158.26 (d, *J* = 238.9 Hz), 153.51, 151.97, 145.48, 132.62 (d, *J* = 11.0 Hz), 129.65, 121.22, 120.52, 115.37, 113.72 (d, *J* = 24.3 Hz), 108.03 (d, *J* = 26.9 Hz). ESI-MS: *m/z* 304 [M+H$^+$] (calc. for $C_{14}H_{10}FN_3O_2S$: 303.05). EA: calc. C 55.44; H 3.32; N 13.85; S 10.57. Found: C 55.22; H 3.50; N 13.55; S 10.48.

Compound 8

1-(6-chlorobenzo[*d*]thiazol-2-yl)-3-(4-hydroxyphenyl)urea

M.p. 285 °C decomp. Yield 58 %.^{1}H NMR (300 MHz, DMSO-d_6): δ (ppm) 9.25 (br s, 1H), 8.83 (br s, 1H), 8.03 (d, *J* = 2.1 Hz, 1H), 7.63 (d, *J* = 8.6 Hz, 1H), 7.39 (dd, *J* = 8.6, 2.2 Hz, 1H), 7.33 – 7.22 (m, 2H), 6.80 – 6.68 (m, 2H). ^{13}C NMR (75 MHz, DMSO-d_6): δ (ppm) 160.33, 153.55, 151.77, 147.74, 133.15, 129.57, 126.81, 126.16, 121.21, 120.81, 115.37. ESI-MS: *m/z* 320 [M+H$^+$] (calc. for $C_{14}H_{10}ClN_3O_2S$: 319.02). EA: calc. C 52.59; H 3.15; N 13.14; S 10.03. Found: C 52.34; H 3.45; N 12.90; S 9.81.

Compound 9

1-(6-fluorobenzo[*d*]thiazol-2-yl)-3-(3-hydroxyphenyl)urea

M.p. 298–300 °C. Yield 49 %.^{1}H NMR (500 MHz, DMSO-d_6): δ (ppm) 9.45 (br s, 1H), 9.02 (br s, 1H), 7.83 (dd, *J* = 8.7, 2.5 Hz, 1H), 7.71 – 7.60 (m, 1H), 7.23 (td, *J* = 9.1, 2.7 Hz, 1H), 7.14 – 7.06 (m, 2H), 6.84 (d, *J* = 8.0 Hz, 1H), 6.47 (dd, *J* = 8.1, 1.7 Hz, 1H). ^{13}C NMR (126 MHz, DMSO-d_6): δ (ppm) 158.29 (d, *J* = 239.0 Hz), 157.85, 151.41, 145.58, 139.33, 132.60, 129.66, 120.80, 113.80 (d, *J* = 24.3 Hz), 110.19, 109.45, 108.06 (d, *J* = 26.9 Hz), 105.80. ESI-MS: *m/z* 304 [M+H$^+$] (calc. for $C_{14}H_{10}FN_3O_2S$: 303.05). EA: calc. C 55.44; H 3.32; N 13.85; S 10.57. Found: C 55.15; H 3.66; N 13.59; S 10.27.

Compound 10

1-(6-chlorobenzo[*d*]thiazol-2-yl)-3-(3-hydroxyphenyl)urea

M.p. 294–296 °C. Yield 36 %.^{1}H NMR (300 MHz, DMSO-d_6): δ (ppm) 9.47 (br s, 1H), 9.05 (br s, 1H), 8.05 (d, *J* = 2.1 Hz, 1H), 7.64 (d, *J* = 8.7 Hz, 1H), 7.40 (dd, *J* = 8.7, 2.2 Hz, 1H), 7.18 – 7.03 (m, 2H), 6.85 (d, *J* = 8.4 Hz, 1H), 6.47 (dd, *J* = 8.0, 1.9 Hz, 1H). ^{13}C NMR (75 MHz, DMSO-d_6): δ (ppm) 160.21, 157.89, 151.59, 139.33, 133.09, 129.72, 126.93, 126.24, 121.26, 120.81, 110.26, 109.48, 105.82. ESI-MS: *m/z* 320 [M+H$^+$] (calc. for $C_{14}H_{10}ClN_3O_2S$: 319.02). EA: calc. C 52.59; H 3.15; N 13.14; S 10.03. Found: C 52.30; H 3.38; N 12.88; S 10.32.

Compound 11

1-(6-fluorobenzo[*d*]thiazol-2-yl)-3-(2-hydroxyphenyl)urea

M.p. 228–230 °C. Yield 80 %.^{1}H NMR (500 MHz, DMSO-d_6): δ (ppm) 8.82 (br s, 1H), 8.04 (d, *J* = 8.0 Hz, 1H), 7.83 (dd, *J* = 8.7, 2.4 Hz, 1H), 7.69 – 7.63 (m, 1H), 7.23 (td, *J* = 9.0, 2.4 Hz, 1H), 6.88 (d, *J* = 4.3 Hz, 2H), 6.83 – 6.77 (m, 1H). ^{13}C NMR (126 MHz, DMSO-d_6): δ (ppm) 159.12, 158.28 (d, *J* = 238.9 Hz), 151.41, 146.17, 145.81, 132.74 (d, *J* = 11.1 Hz), 126.47, 123.11, 120.83, 119.21, 119.05, 114.63, 113.76 (d, *J* = 24.3 Hz), 108.04 (d, *J* = 27.0 Hz). ESI-MS: *m/z* 304 [M+H$^+$] (calc. for $C_{14}H_{10}FN_3O_2S$: 303.05). EA: calc. C 55.44; H 3.32; N 13.85; S 10.57. Found: C 55.21; H 3.69; N 13.47; S 10.23.

Compound 12

1-(6-chlorobenzo[*d*]thiazol-2-yl)-3-(2-hydroxyphenyl)urea

M.p. 216–218 °C. Yield 42 %.^{1}H NMR (500 MHz, DMSO-d_6): δ (ppm) 11.30 (br s, 1H), 10.12 (br s, 1H), 8.84 (br s, 1H), 8.04 (d, *J* = 1.8 Hz, 1H), 7.99 (d, *J* = 6.5 Hz, 1H), 7.64 (d, *J* = 8.6 Hz, 1H), 7.40 (dd, *J* = 8.6, 2.1 Hz, 1H), 6.93 – 6.88 (m, 2H), 6.85 – 6.77 (m, 1H). ^{13}C NMR (126 MHz, DMSO-d_6): δ (ppm) 160.77, 152.24, 148.09, 146.47, 133.35, 126.67, 126.54, 125.97, 123.13, 121.01, 120.77, 119.28, 119.06, 114.91. ESI-MS: *m/z* 320 [M+H$^+$] (calc. for $C_{14}H_{10}ClN_3O_2S$: 319.02). EA: calc. C 52.59; H, 3.15; N 13.14; S 10.03. Found: C 52.72; H 3.27; N 13.09; S 10.07.

Compound 13

1-(3-chloro-4-hydroxyphenyl)-3-(6-fluorobenzo[*d*]thiazol-2-yl)urea

M.p. 298–299.5 °C. Yield 74 %.^{1}H NMR (500 MHz, DMSO-d_6): δ (ppm) 9.94 (br s, 1H), 8.98 (br s, 1H), 7.82 (dd, *J* = 8.6, 2.6 Hz, 1H), 7.69 – 7.61 (m, 1H), 7.59 (d, *J* = 2.5 Hz, 1H), 7.22 (td, *J* = 9.1, 2.7 Hz, 1H), 7.18 (dd, *J* = 8.7, 2.5 Hz, 1H), 6.94 (d, *J* = 8.7 Hz, 1H). ^{13}C NMR (126 MHz, DMSO-d_6): δ (ppm) 159.42, 158.29 (d, *J* = 239.1 Hz), 151.83, 149.05, 145.57, 132.52, 130.60, 120.92, 120.57, 119.59, 119.36, 116.67, 113.80 (d, *J* = 24.4 Hz), 108.11 (d, *J* = 27.0 Hz). ESI-MS: *m/z* 338 [M+H$^+$] (calc. for $C_{14}H_9ClFN_3O_2S$: 337.01). EA: calc. C 49.78; H 2.69; N 12.44; S 9.49. Found: C 47.39; H 2.89; N 12.12; S 9.15.

Compound 14

1-(3-chloro-4-hydroxyphenyl)-3-(6-chlorobenzo[*d*]thiazol-2-yl)urea

M.p. 283.5–285 °C. Yield 30 %.^{1}H NMR (300 MHz, DMSO-d_6): δ (ppm) 9.95 (br s, 1H), 9.01 (br s, 1H), 8.04 (d, *J* = 2.1 Hz, 1H), 7.70 – 7.56 (m, 2H), 7.40 (dd, *J* = 8.6, 2.2 Hz, 1H), 7.19 (dd, *J* = 8.8, 2.5 Hz, 1H), 6.94 (d, *J* = 8.7 Hz, 1H). ^{13}C NMR (75 MHz, DMSO-d_6): δ (ppm) 160.40, 151.93, 149.07, 132.94, 130.55, 126.88, 126.20, 121.24, 120.93, 119.60, 119.34, 116.66. ESI-MS: *m/z* 354 [M+H$^+$] (calc. for $C_{14}H_9Cl_2N_3O_2S$: 352.98). EA: calc. C 47.47; H 2.56; N 11.86; S 9.05. Found: C 47.12; H 2.96; N 11.49; S 9.33.

Compound 15

5-(3-(6-fluorobenzo[*d*]thiazol-2-yl)ureido)-2-hydroxybenzoic acid

M.p. 304–305 °C. Yield 70 %.^{1}H NMR (500 MHz, DMSO-d_6): δ (ppm) 9.13 (br s, 1H), 8.01 (d, *J* = 2.7 Hz, 1H), 7.82 (dd, *J* = 8.7, 2.7 Hz, 1H), 7.69 – 7.61 (m, 1H), 7.58 (dd, *J* = 8.8, 2.7 Hz, 1H), 7.22 (td, *J* = 9.1, 2.7 Hz, 1H), 6.95 (d, *J* = 8.9 Hz, 1H). ^{13}C NMR (126 MHz, DMSO-d_6): δ (ppm) 171.60, 159.58, 158.29 (d, *J* = 239.1 Hz), 157.09, 152.26, 144.93, 132.45 (d, *J* = 11.3 Hz), 129.97, 127.69, 120.52, 120.42, 117.45, 113.79 (d, *J* = 24.2 Hz), 112.65, 108.09 (d, *J* = 26.9 Hz). ESI-MS: *m/z* 348 [M+H$^+$] (calc. for $C_{15}H_{10}FN_3O_4S$: 347.04). EA: calc. C 51.87; H 2.90; N 12.10; S 9.23. Found: C 51.52; H 2.66; N 12.02; S 8.99.

Compound 16

5-(3-(6-chlorobenzo[*d*]thiazol-2-yl)ureido)-2-hydroxybenzoic acid

M.p. 285–287 °C. Yield 61 %.^{1}H NMR (300 MHz, DMSO-d_6): δ (ppm) 9.10 (br s, 1H), 8.05 (d, *J* = 2.1 Hz, 1H), 8.01 (d, *J* = 2.7 Hz, 1H), 7.63 (d, *J* = 8.6 Hz, 1H), 7.57 (dd, *J* = 8.8, 2.5 Hz, 1H), 7.40 (ddd, *J* = 8.6, 2.2, 0.7 Hz, 1H), 6.95 (d, *J* = 8.9 Hz, 1H). ^{13}C NMR (75 MHz, DMSO-d_6): δ (ppm) 189.75, 171.62, 160.45, 157.14, 152.28, 147.04 132.94, 129.93, 127.74, 126.90, 126.22, 121.24, 120.58, 117.47, 112.66. ESI-MS: *m/z* 364 [M+H$^+$] (calc. for $C_{15}H_{10}ClN_3O_4S$: 363.01). EA: calc. C 49.53; H 2.77; N 11.55; S 8.81. Found: C 49.39; H 2.89; N 11.40; S 8.78.

Compound 17

1-(6-fluorobenzo[*d*]thiazol-2-yl)-3-(4-methoxyphenyl)urea

M.p. 331–333 °C. Yield 70 %.^{1}H NMR (500 MHz, DMSO-d_6): δ (ppm) 8.95 (br s, 1H), 7.82 (dd, *J* = 8.6, 2.4 Hz, 1H), 7.69 – 7.61 (m, 1H), 7.41 (d, *J* = 8.9 Hz, 2H), 7.22 (td, *J* = 9.1, 2.7 Hz, 1H), 6.91 (d, *J* = 9.0 Hz, 2H), 3.73 (s, 3H). ^{13}C NMR (126 MHz, DMSO-d_6): δ (ppm) 159.44, 158.26 (d, *J* = 239.0 Hz), 155.30, 151.85, 145.47, 132.62, 131.22, 120.82, 120.70, 114.11, 113.75 (d, *J* = 24.3 Hz), 108.05 (d, *J* = 26.8 Hz), 55.21. ESI-MS: *m/z* 318 [M+H$^+$] (calc. for $C_{15}H_{12}FN_3O_2S$: 317.06). EA: calc. C 56.77; H 3.81; N 13.24; S 10.10. Found: C 56.59; H 3.41; N 12.92; S 9.87.

Compound 18

1-(6-chlorobenzo[*d*]thiazol-2-yl)-3-(4-methoxyphenyl)urea

M.p. 280–282 °C. Yield 92 %.^{1}H NMR (300 MHz, DMSO-d_6): δ (ppm) 8.96 (br s, 1H), 8.04 (d, *J* = 2.1 Hz, 1H), 7.63 (d, *J* = 8.6 Hz, 1H), 7.45 – 7.36 (m, 3H), 6.95 – 6.88 (m, 2H), 3.73 (s, 3H). ^{13}C NMR (75 MHz, DMSO-d_6): δ (ppm) 160.31, 155.33, 151.83, 147.59, 133.08, 131.18, 126.83, 126.16, 121.19, 120.83, 114.11, 55.21. ESI-MS: *m/z* 334 [M+H$^+$] (calc. for $C_{15}H_{12}ClN_3O_2S$: 333.03). EA: calc. C 53.97; H 3.62; N 12.59; S 9.61. Found: C 53.71; H3.95; N 12.21; S 9.30.

Compound 19

1-(3,4-dimethoxyphenyl)-3-(6-fluorobenzo[*d*]thiazol-2-yl)urea

M.p. 280–282 °C. Yield 84 %.^{1}H NMR (300 MHz, DMSO-d_6): δ (ppm) 8.97 (br s, 1H), 7.82 (dd, *J* = 8.7, 2.7 Hz, 1H), 7.73 – 7.59 (m, 1H), 7.28 – 7.17 (m, 2H), 6.97 (dd, *J* = 8.6, 2.3 Hz, 1H), 6.91 (d, *J* = 8.7 Hz, 1H), 3.76 (s, 3H), 3.73 (s, 3H). ^{13}C NMR (75 MHz, DMSO-d_6): δ (ppm) 159.47, 158.29 (d, *J* = 239.0 Hz), 148.81, 144.91, 132.53, 131.72, 120.54, 113.79 (d, *J* = 24.3 Hz), 112.28, 111.11, 108.07 (d, *J* = 26.9 Hz), 104.46, 55.78, 55.47. ESI-MS: *m/z* 348 [M+H$^+$] (calc. for $C_{16}H_{14}FN_3O_3S$: 347.07). EA: calc. C 55.32; H 4.06; N 12.10; S 9.23. Found: C 54.97; H 4.00; N 11.94; S 8.86.

Compound 20

1-(6-chlorobenzo[*d*]thiazol-2-yl)-3-(3,4-dimethoxyphenyl)urea

M.p. 280–282 °C. Yield 87 %.^{1}H NMR (500 MHz, DMSO-d_6): δ (ppm) 8.98 (br s, 1H), 8.03 (d, *J* = 2.1 Hz, 1H), 7.64 (d, *J* = 8.6 Hz, 1H), 7.40 (dd, *J* = 8.6, 2.2 Hz, 1H), 7.20 (d, *J* = 2.1 Hz, 1H), 6.97 (dd, *J* = 8.6, 2.3 Hz, 1H), 6.91 (d, *J* = 8.7 Hz, 1H), 3.76 (s, 3H), 3.73 (s, 3H). ^{13}C NMR (126 MHz, DMSO-d_6): δ (ppm) 160.27, 151.78, 148.80, 147.81, 144.94, 133.06, 131.66, 126.85, 126.18, 121.19, 120.76, 112.28, 111.12, 104.47, 55.78, 55.47. ESI-MS: *m/z* 364 [M+H$^+$] (calc. for $C_{16}H_{14}ClN_3O_3S$: 363.04). EA: calc. C 52.82; H 3.88; N 11.55; S 8.81. Found: C 52.38; H 4.26; N 10.97; S 8.37.

Compound 21

5-(3-(6-fluorobenzo[*d*]thiazol-2-yl)ureido)-2-methoxybenzoic acid

M.p. 278–279 °C. Yield 47 %.^{1}H NMR (500 MHz, DMSO-d_6): δ (ppm) 9.13 (br s, 1H), 7.85 – 7.80 (m, 2H), 7.68 – 7.62 (m, 1H), 7.60 (dd, *J* = 8.9, 2.8 Hz, 1H), 7.23 (td, *J* = 9.1, 2.7 Hz, 1H), 7.11 (d, *J* = 9.0 Hz, 1H), 3.80 (s, 3H). ^{13}C NMR (126 MHz, DMSO-d_6): δ (ppm) 166.97, 159.56, 158.30 (d, *J* = 239.0 Hz), 154.11, 152.22, 144.87, 132.44 (d, *J* = 12.1 Hz), 130.95, 124.02, 121.71, 121.27, 120.41, 113.80 (d, *J* = 24.3 Hz), 113.17, 108.10 (d, *J* = 26.9 Hz), 56.05. ESI-MS: *m/z* 362 [M+H$^+$] (calc. for $C_{16}H_{12}FN_3O_4S$: 361.05). EA: calc. C 53.18; H 3.35; N 11.63; S 8.87. Found: C 52.83; H 2.96; N 11.59; S 8.48.

Compound 22

5-(3-(6-chlorobenzo[*d*]thiazol-2-yl)ureido)-2-methoxybenzoic acid

M.p. 268.5–270.5 °C. Yield 56 %.^{1}H NMR (500 MHz, DMSO-d_6): δ (ppm) 9.12 (br s, 1H), 8.05 (d, *J* = 1.9 Hz, 1H), 7.82 (d, *J* = 2.7 Hz, 1H), 7.63 (d, *J* = 8.6 Hz, 1H), 7.60 (dd, *J* = 9.0, 2.7 Hz, 1H), 7.40 (dd, *J* = 8.6, 2.1 Hz, 1H), 7.11 (d, *J* = 9.0 Hz, 1H), 3.80 (s, 3H). ^{13}C NMR (126 MHz, DMSO-d_6): δ (ppm) 166.95, 160.44, 154.13, 152.22, 132.92, 130.89, 126.89, 126.20, 124.04, 121.74, 121.26, 121.23, 120.49,

113.16, 56.05. ESI-MS: *m/z* 378 [M+H$^+$] (calc. for $C_{16}H_{12}ClN_3O_4S$: 377.02). EA: calc. C 50.87; H 3.20; N 11.12; S 8.49. Found: C 50.37; H 3.31; N 10.79; S 8.97.

Compound 23

1-(6-fluorobenzo[*d*]thiazol-2-yl)-3-(4-phenoxyphenyl)urea

M.p. 305–307 °C. Yield 83 %.^{1}H NMR (500 MHz, DMSO-d_6): δ (ppm) 9.15 (br s, 1H), 7.82 (dd, *J* = 8.6, 2.2 Hz, 1H), 7.69 – 7.62 (m, 1H), 7.53 (d, *J* = 8.7 Hz, 2H), 7.37 (t, *J* = 7.8 Hz, 2H), 7.23 (td, *J* = 9.1, 2.5 Hz, 1H), 7.10 (t, *J* = 7.4 Hz, 1H), 7.02 (d, *J* = 8.8 Hz, 2H), 6.98 (d, *J* = 8.0 Hz, 2H). ^{13}C NMR (126 MHz, DMSO-d_6): δ (ppm) 158.29 (d, *J* = 238.4 Hz), 151.74, 134.16, 132.54, 129.96, 122.99, 120.79, 120.67, 119.67, 117.87, 113.80 (d, *J* = 24.3 Hz), 108.09 (d, *J* = 27.1 Hz). ESI-MS: *m/z* 380 [M+H$^+$] (calc. for $C_{20}H_{14}FN_3O_2S$: 379.08). EA: calc. C 63.31; H 3.72; N 11.08; S 8.45. Found: C 62.89; H 3.40; N 10.70; S 8.05.

Compound 24

1-(6-chlorobenzo[*d*]thiazol-2-yl)-3-(4-phenoxyphenyl)urea

M.p. 295–297 °C. Yield 88 %.^{1}H NMR (500 MHz, DMSO-d_6): δ (ppm) 9.15 (br s, 1H), 8.05 (d, *J* = 2.0 Hz, 1H), 7.64 (d, *J* = 8.9 Hz, 1H), 7.53 (d, *J* = 9.2 Hz, 2H), 7.41 (dd, *J* = 8.6, 2.2 Hz, 1H), 7.40 – 7.35 (m, 2H), 7.11 (t, *J* = 7.4 Hz, 1H), 7.03 (d, *J* = 8.9 Hz, 2H), 6.98 (d, *J* = 7.7 Hz, 2H). ^{13}C NMR (126 MHz, DMSO-d_6): δ (ppm) 160.31, 157.66, 157.33, 151.78, 150.59, 135.75, 134.12, 133.01, 129.97, 126.90, 126.21, 123.01, 122.73, 121.24, 120.81, 119.92, 119.79, 119.66, 117.89, 117.57. ESI-MS: *m/z* 396 [M+H$^+$] (calc. for $C_{20}H_{14}ClN_3O_2S$: 395.05). EA: calc. C 60.68; H 3.56; N 10.61; S 8.10. Found: C 60.33; H 3.94; N 10.30; S 7.85.

Compound 25

4-(3-(6-fluorobenzo[*d*]thiazol-2-yl)ureido)benzoic acid

M.p. 300 °C decomp. Yield 67 %.^{1}H NMR (500 MHz, DMSO-d_6): δ (ppm) 10.38 (br s, 1H), 7.91 (d, *J* = 8.7 Hz, 2H), 7.84 (dd, *J* = 8.7, 2.6 Hz, 1H), 7.69 – 7.65 (m, 1H), 7.63 (d, *J* = 8.8 Hz, 2H), 7.24 (td, *J* = 9.1, 2.7 Hz, 1H). ^{13}C NMR (126 MHz, DMSO-d_6): δ (ppm) 166.92, 162.31, 159.07, 158.36 (d, *J* = 239.1 Hz), 152.10, 144.90, 142.80, 132.50 (d, *J* = 11.0 Hz), 130.63, 120.57 (d, *J* = 9.0 Hz), 117.68, 113.89 (d, *J* = 24.2 Hz), 108.12 (d, *J* = 27.0 Hz). ESI-MS: *m/z* 332 [M+H$^+$] (calc. for $C_{15}H_{10}FN_3O_3S$: 331.04). EA: calc. C 54.38; H 3.04; N 12.68; S 9.68. Found: C 54.04; H 3.33; N 12.39; S 9.35.

Compound 26

4-(3-(6-chlorobenzo[*d*]thiazol-2-yl)ureido)benzoic acid

M.p. 300 °C decomp. Yield 35 %.^{1}H NMR (500 MHz, DMSO-d_6): δ (ppm) 9.76 (br s, 1H), 8.06 (d, *J* = 2.0 Hz, 1H), 7.92 (d, *J* = 8.6 Hz, 2H), 7.70 – 7.59 (m, 3H), 7.41 (dd, *J* = 8.6, 2.1 Hz, 1H). ^{13}C NMR (126 MHz, DMSO-d_6): δ (ppm) 166.90, 160.24, 152.21, 142.67, 132.81, 130.59, 127.04, 126.30, 124.82, 121.31, 120.48, 117.90. ESI-MS: *m/z* 348 [M+H$^+$] (calc. for $C_{15}H_{10}ClN_3O_3S$: 347.01). EA: calc. C 51.80; H 2.90; N 12.08; S 9.22. Found: C 51.41; H 3.13; N 11.80; S 8.91.

Compound 27

ethyl 4-(3-(6-fluorobenzo[*d*]thiazol-2-yl)ureido)benzoate

M.p. 333–335 °C. Yield 32 %.^{1}H NMR (500 MHz, DMSO-d_6): δ (ppm) 9.53 (br s, 1H), 7.99 – 7.79 (m, 3H), 7.72 – 7.56 (m, 3H), 7.29 – 7.20 (m, 1H), 4.33 – 4.25 (m, 2H), 1.31 (t, *J* = 6.5 Hz, 3H). ^{13}C NMR (126 MHz, DMSO-d_6): δ (ppm) 165.30, 158.36 (d, *J* = 237.5 Hz), 142.93, 130.39, 123.85, 118.02, 117.49, 113.94 (d, *J* = 23.6 Hz), 108.21 (d, *J* = 26.9 Hz), 60.44, 14.24. ESI-MS: *m/z* 360 [M+H$^+$] (calc. for $C_{17}H_{14}FN_3O_3S$: 359.07). EA: calc. C 56.82; H 3.93; N 11.69; S 8.92. Found: C 56.37; H 3.77; N 11.92; S 9.24.

Compound 28

ethyl 4-(3-(6-chlorobenzo[*d*]thiazol-2-yl)ureido)benzoate

M.p. 326–328 °C. Yield 45 %.^{1}H NMR (500 MHz, DMSO-d_6): δ (ppm) 9.19 (br s, 1H), 8.08 (s, 1H), 7.97 – 7.86 (m, 2H), 7.72 – 7.55 (m, 3H), 7.48 – 7.39 (m, 1H), 4.34 – 4.25 (m, 2H), 1.32 (t, *J* = 6.9 Hz, 3H). ^{13}C NMR (126 MHz, DMSO-d_6): δ (ppm) 165.27, 160.41, 151.78, 142.91, 132.73, 130.37, 127.04, 126.31, 123.86, 121.33, 118.03, 117.45, 60.45, 14.24.ESI-MS: *m/z* 376 [M+H$^+$] (calc. for $C_{17}H_{14}ClN_3O_3S$: 375.04). EA: calc. C 54.33; H 3.75; N 11.18; S 8.53. Found: C 54.01; H 3.89; N 11.50; S 8.82.

Compound 29

1-(4-acetylphenyl)-3-(6-fluorobenzo[*d*]thiazol-2-yl)urea

M.p. 308–310 °C. Yield 48 %. ^{1}H NMR (500 MHz, DMSO-d_6): δ (ppm) 9.53 (br s, 1H), 8.00 – 7.80 (m, 3H), 7.71 – 7.55 (m, 3H), 7.25 (t, *J* = 7.8 Hz, 1H), 2.53 (s, 3H). ^{13}C NMR (126 MHz, DMSO-d_6): δ (ppm) 196.41, 158.37 (d, *J* = 235.7 Hz), 151.85, 143.91, 143.02, 132.24, 131.36, 129.67, 120.45, 117.89, 117.38, 113.96 (d, *J* = 23.8 Hz), 108.26 (d, *J* = 27.9 Hz), 26.45. ESI-MS: *m/z* 330 [M+H$^+$] (calc. for $C_{16}H_{12}FN_3O_2S$: 329.06). EA: calc. C 58.35; H 3.67; N 12.76; S 9.74. Found: C 57.97; H 3.46; N 13.18; S 10.19.

Compound 30

1-(4-acetylphenyl)-3-(6-chlorobenzo[*d*]thiazol-2-yl)urea

M.p. 288–290 °C. Yield 38 %. ^{1}H NMR (300 MHz, DMSO-d_6): δ (ppm) 9.62 (br s, 1H), 8.20 – 7.80 (m, 3H), 7.66 (d, *J* = 13.9 Hz, 3H), 7.42 (d, *J* = 13.3 Hz, 1H), 2.53 (s, 3H). ^{13}C NMR (75 MHz, DMSO-d_6): δ (ppm) 196.40, 160.77, 152.56, 143.05, 132.72, 131.37, 129.63, 126.99, 126.29, 121.32, 120.32, 117.93, 117.38, 26.43. ESI-MS: *m/z* 346 [M+H$^+$] (calc. for $C_{16}H_{12}ClN_3O_2S$: 345.03). EA: calc. C 55.57; H 3.50; N 12.15; S 9.27. Found: C 55.29; H 3.88; N 12.22; S 9.49.

Compound 31

N-(4-(3-(6-fluorobenzo[*d*]thiazol-2-yl)ureido)phenyl)acetamide

M.p. 335–337 °C. Yield 85 %. ^{1}H NMR (500 MHz, DMSO-d_6): δ (ppm) 9.88 (br s, 1H), 9.03 (br s, 1H), 7.82 (dd, *J* = 8.6, 2.5 Hz, 1H), 7.69 – 7.62 (m, 1H), 7.54 (d, *J* = 8.9 Hz, 2H), 7.42 (d, *J* = 8.9 Hz, 2H), 7.23 (td, *J* = 9.1, 2.7 Hz, 1H), 2.03 (s, 3H). ^{13}C NMR (126 MHz, DMSO-d_6): δ (ppm) 167.94, 158.27 (d, *J* = 239.0 Hz), 151.64, 145.50, 134.84, 133.37, 132.52, 120.66, 119.60, 119.41, 118.52, 113.76 (d, *J* = 24.2 Hz), 108.05 (d, *J* = 26.8 Hz), 23.88. ESI-MS: *m/z* 345 [M+H$^+$] (calc. for $C_{16}H_{13}FN_4O_2S$: 344.07). EA: calc. C 55.80; H 3.81; N 16.27; S 9.31. Found: C 55.53; H 3.77; N 16.71; S 8.95.

Compound 32

N-(4-(3-(6-chlorobenzo[*d*]thiazol-2-yl)ureido)phenyl)acetamide

M.p. 335–337 °C. Yield 89 %. ^{1}H NMR (500 MHz, DMSO-d_6): δ (ppm) 9.89 (br s, 1H), 9.06 (br s, 1H), 8.04 (d, *J* = 1.9 Hz, 1H), 7.64 (d, *J* = 8.7 Hz, 1H), 7.54 (d, *J* = 9.2 Hz, 2H), 7.45 – 7.36 (m, 3H), 2.03 (s, 3H). ^{13}C NMR (126 MHz, DMSO-d_6): δ (ppm) 167.98, 160.25, 151.69, 134.89, 133.34, 126.87, 126.19, 121.21, 120.80, 119.60, 119.46, 23.90. ESI-MS: *m/z* 361 [M+H$^+$] (calc. for $C_{16}H_{13}ClN_4O_2S$: 360.04). EA: calc. C 53.26; H 3.63; N 15.53; S 8.89. Found: C 52.95; H, 3.95; N 15.22; S 8.48.

Compound 33

1-(6-chlorobenzo[*d*]thiazol-2-yl)-3-(3-chlorophenyl)urea

M.p. 351–353 °C. Yield 83 %. ^{1}H NMR (500 MHz, DMSO-d_6): δ (ppm) 11.07 (br s, 1H), 9.36 (br s, 1H), 8.04 (s, 1H), 7.73 (s, 1H), 7.63 (d, *J* = 8.4 Hz, 1H), 7.47 – 7.27 (m, 3H), 7.10 (d, *J* = 7.3 Hz, 1H). ^{13}C NMR (126 MHz, DMSO-d_6): δ (ppm) 160.42, 152.17, 146.76, 139.99, 133.28, 132.77, 130.54, 127.04, 126.30, 122.69, 121.32, 120.54, 118.29, 117.40. ESI-MS: *m/z* 338 [M+H$^+$] (calc. for $C_{14}H_9Cl_2N_3OS$: 336.98). EA: calc. C 49.72; H 2.68; N12.42; S 9.48. Found: C 49.29; H 2.76; N 12.53; S 9.81.

Compound 34

1-(6-chlorobenzo[*d*]thiazol-2-yl)-3-(4-chlorophenyl)urea

M.p. 335–337 °C. Yield 86 %. ^{1}H NMR (500 MHz, DMSO-d_6): δ (ppm) 10.98 (br s, 1H), 9.29 (br s, 1H), 8.04 (s, 1H), 7.63 (d, *J* = 8.3 Hz, 1H), 7.55 (d, *J* = 8.6 Hz, 2H), 7.47 – 7.27 (m, 3H). ^{13}C NMR (126 MHz,

DMSO-d_6): δ (ppm) 160.24, 152.01, 147.33, 137.40, 132.83, 128.79, 126.99, 126.68, 126.26, 121.28, 120.48. ESI-MS: *m/z* 338 [M+H$^+$] (calc. for $C_{14}H_9Cl_2N_3OS$: 336.98). EA: calc. C 49.72; H 2.68; N 12.42; S 9.48. Found: C 49.67; H 2.72; N 12.54; S 9.78.

Compound 35

1-(6-chlorobenzo[*d*]thiazol-2-yl)-3-(3,4-dichlorophenyl)urea

M.p. 334–336 °C. Yield 85 %. ^{1}H NMR (300 MHz, DMSO-d_6): δ (ppm) 11.25 (br s, 1H), 9.47 (br s, 1H), 8.03 (s, 1H), 7.90 (s, 1H), 7.77 – 7.19 (m, 4H). ^{13}C NMR (75 MHz, DMSO-d_6): δ (ppm) 160.70, 152.89, 145.92, 138.79, 132.47, 131.13, 130.66, 127.05, 126.31, 124.36, 121.35, 120.01, 119.01. ESI-MS: *m/z* 372 [M+H$^+$] (calc. for $C_{14}H_8Cl_3N_3OS$: 370.95). EA: calc. C 45.12; H 2.16; N 11.28; S 8.60. Found: C 44.91; H 2.20; N 11.39; S 9.01.

Compound 36

1-(2-chloro-4-hydroxyphenyl)-3-(6-chlorobenzo[*d*]thiazol-2-yl)urea

M.p. 283–285 °C. Yield 71 %. ^{1}H NMR (500 MHz, DMSO-d_6): δ (ppm) 11.29 (br s, 1H), 9.77 (br s, 1H), 8.74 (br s, 1H), 8.05 (d, *J* = 2.4 Hz, 1H), 7.73 (d, *J* = 8.9 Hz, 1H), 7.65 (d, *J* = 8.6 Hz, 1H), 7.40 (dd, *J* = 8.6, 2.4 Hz, 1H), 6.90 (d, *J* = 2.6 Hz, 1H), 6.77 (dd, *J* = 8.9, 2.5 Hz, 1H). ^{13}C NMR (126 MHz, DMSO-d_6): δ (ppm) 160.16, 154.72, 151.80, 147.81, 133.14, 126.94, 126.19, 125.94, 125.42, 125.04, 121.19, 121.00, 115.61, 114.65. ESI-MS: *m/z* 354 [M+H$^+$] (calc. for $C_{14}H_9Cl_2N_3O_2S$: 352.98). EA: calc. C 47.47; H 2.56; N 11.86; S 9.05. Found: C 47.10; H 2.74; N 11.90; S 9.17.

Compound 37

1-(3-chloro-4-methoxyphenyl)-3-(6-chlorobenzo[*d*]thiazol-2-yl)urea

M.p. 307–309 °C. Yield 93 %. ^{1}H NMR (500 MHz, DMSO-d_6): δ (ppm) 11.00 (br s, 1H), 9.12 (br s, 1H), 8.03 (d, *J* = 2.2 Hz, 1H), 7.68 (d, *J* = 2.4 Hz, 1H), 7.62 (d, *J* = 8.5 Hz, 1H), 7.39 (dd, *J* = 8.6, 2.2 Hz, 1H), 7.36 (dd, *J* = 8.9, 2.3 Hz, 1H), 7.11 (d, *J* = 9.0 Hz, 1H), 3.83 (s, 3H). ^{13}C NMR (126 MHz, DMSO-d_6): δ (ppm) 160.39, 152.14, 150.50, 147.12, 132.84, 131.96, 126.90, 126.20, 121.23, 120.86, 120.82, 119.16, 113.04, 56.20. ESI-MS: *m/z* 368 [M+H$^+$] (calc. for $C_{15}H_{11}Cl_2N_3O_2S$: 366.99). EA: calc. C 48.93; H 3.01; N 11.41; S 8.71. Found: C 48.84; H 3.13; N 11.89; S 8.65.

Compound 38

2-chloro-4-(3-(6-chlorobenzo[*d*]thiazol-2-yl)ureido)benzoic acid

M.p. 324–326 °C. Yield 83 %. ^{1}H NMR (300 MHz, DMSO-d_6): δ (ppm) 12.27 (br s, 1H), 9.69 (br s, 1H), 8.05 (d, *J* = 1.9 Hz, 1H), 7.92 – 7.77 (m, 2H), 7.62 (d, *J* = 8.6 Hz, 1H), 7.50 (dd, *J* = 8.6, 1.6 Hz, 1H), 7.41 (dd, *J* = 8.6, 2.0 Hz, 1H). ^{13}C NMR (75 MHz, DMSO-d_6): δ (ppm) 166.00, 160.99, 152.98, 145.64,

142.54, 133.30, 132.53, 132.40, 127.13, 126.40, 124.12, 121.43, 119.90, 119.74, 116.74. ESI-MS: *m/z* 382 [M+H$^+$] (calc. for $C_{15}H_9Cl_2N_3O_3S$: 380.97). EA: calc. C 47.14; H 2.37; N 10.99; S 8.39. Found: C 47.05; H 2.49; N 11.12; S 8.66.

Compound 39

1-(6-chlorobenzo[*d*]thiazol-2-yl)-3-(3,5-dichloro-4-hydroxyphenyl)urea

M.p. 300 °C decomp. Yield 69 %. ^{1}H NMR (300 MHz, DMSO-d_6): δ (ppm) 10.61 (br s, 1H), 9.19 (br s, 1H), 8.03 (d, *J* = 2.1 Hz, 1H), 7.61 (d, *J* = 8.6 Hz, 1H), 7.55 (s, 2H), 7.39 (dd, *J* = 8.6, 2.2 Hz, 1H). ^{13}C NMR (75 MHz, DMSO-d_6): δ (ppm) 160.83, 152.82, 146.07, 144.82, 132.58, 131.55, 126.97, 126.28, 122.42, 121.33, 120.06, 119.41. ESI-MS: *m/z* 388 [M+H$^+$] (calc. for $C_{14}H_8Cl_3N_3O_2S$: 386.94). EA: calc. C 43.27; H 2.07; N 10.81; S 8.25. Found: C 42.92; H 2.32; N 10.60; S 8.09.

Compound 40

1-(6-chlorobenzo[*d*]thiazol-2-yl)-3-(3,5-dichloro-4-methoxyphenyl)urea

M.p. 290 °C decomp. Yield 90 %. ^{1}H NMR (500 MHz, DMSO-d_6): δ (ppm) 11.26 (br s, 1H), 9.39 (br s, 1H), 8.02 (d, *J* = 2.0 Hz, 1H), 7.65 (s, 2H), 7.60 (d, *J* = 8.6 Hz, 1H), 7.40 (dd, *J* = 8.7, 2.0 Hz, 1H), 3.79 (s, 3H). ^{13}C NMR (126 MHz, DMSO-d_6): δ (ppm) 146.74, 135.97, 132.25, 128.14, 127.03, 126.31, 121.36, 119.07, 60.64. ESI-MS: *m/z* 402 [M+H$^+$] (calc. for $C_{15}H_{10}Cl_3N_3O_2S$: 400.96). EA: calc. C 44.74; H 2.50; N 10.44; S 7.96. Found: C 45.10; H 2.58; N 10.90; S 8.26.

Compound 41

3-chloro-5-(3-(6-chlorobenzo[*d*]thiazol-2-yl)ureido)-2-hydroxybenzoic acid

M.p. 268–270 °C. Yield 68 %. ^{1}H NMR (300 MHz, DMSO-d_6): δ (ppm) 11.34 (br s, 1H), 9.23 (br s, 1H), 8.03 (d, *J* = 2.1 Hz, 1H), 7.93 (d, *J* = 2.6 Hz, 1H), 7.87 (d, *J* = 2.7 Hz, 1H), 7.61 (d, *J* = 8.6 Hz, 1H), 7.39 (dd, *J* = 8.6, 2.2 Hz, 1H). ^{13}C NMR (75 MHz, DMSO-d_6): δ (ppm) 171.37, 160.76, 152.64, 146.45, 132.67, 130.24, 126.97, 126.73, 126.28, 121.30, 120.47, 119.53, 114.20. ESI-MS: *m/z* 398 [M+H$^+$] (calc. for $C_{15}H_9Cl_2N_3O_4S$: 396.97). EA: calc. C 45.24; H 2.28; N 10.55; S 8.05. Found: C 44.83; H 2.69; N 10.19; S 7.89.

Compound 42

3-chloro-5-(3-(6-chlorobenzo[*d*]thiazol-2-yl)ureido)-2-methoxybenzoic acid

M.p. 263.6–265 °C. Yield 60 %. ^{1}H NMR (500 MHz, DMSO-d_6): δ (ppm) 12.10 (br s, 1H), 9.41 (br s, 1H), 8.04 (d, *J* = 2.1 Hz, 1H), 7.89 (d, *J* = 2.7 Hz, 1H), 7.79 (d, *J* = 2.7 Hz, 1H), 7.61 (d, *J* = 8.6 Hz, 1H), 7.40 (dd, *J* = 8.6, 2.2 Hz, 1H), 3.80 (s, 3H). ^{13}C NMR (126 MHz, DMSO-d_6): δ (ppm) 166.11, 160.84, 152.95, 149.82, 145.83, 135.06, 132.50, 128.18, 128.02, 127.04, 126.31, 123.23, 121.34, 119.79, 61.67. ESI-

MS: *m/z* 412 [M+H$^+$] (calc. for $C_{16}H_{11}Cl_2N_3O_4S$: 410.98). EA: calc. C 46.62; H 2.69; N 10.19; S 7.78. Found: C 46.12; H 3.08; N 9.72; S 7.68.

Compound 43

1-(6-chlorobenzo[*d*]thiazol-2-yl)-3-(2,4-dihydroxyphenyl)urea

M.p. 241–243 °C. Yield 81 %. ^{1}H NMR (500 MHz, DMSO-d_6): δ (ppm) 8.60 (br s, 1H), 8.03 (d, *J* = 2.1 Hz, 1H), 7.72 – 7.53 (m, 2H), 7.38 (dd, *J* = 8.6, 2.1 Hz, 1H), 6.42 (d, *J* = 2.6 Hz, 1H), 6.21 (dd, *J* = 8.7, 2.5 Hz, 1H). ^{13}C NMR (126 MHz, DMSO-d_6): δ (ppm) 160.33, 153.99, 151.53, 148.23, 147.76, 133.19, 126.78, 126.16, 121.37, 121.15, 120.81, 117.75, 105.63, 102.57. ESI-MS: *m/z* 336 [M+H$^+$] (calc. for $C_{14}H_{10}ClN_3O_3S$: 335.01). EA: calc. C 50.08; H 3.00; N 12.52; S 9.55. Found: C 49.77; H 3.48; N 12.30; S 9.22.

Compound 44

1-(6-chlorobenzo[*d*]thiazol-2-yl)-3-phenylurea

M.p. 360–362 °C. Yield 71 %. ^{1}H NMR (500 MHz, DMSO-d_6): δ (ppm) 10.87 (br s, 1H), 9.14 (br s, 1H), 8.05 (d, *J* = 1.9 Hz, 1H), 7.64 (d, *J* = 10.0 Hz, 1H), 7.51 (d, *J* = 9.9 Hz, 2H), 7.40 (dd, *J* = 10.0, 2.0 Hz, 1H), 7.34 (m, 2H), 7.06 (t, *J* = 7.1 Hz, 1H). ^{13}C NMR (126 MHz, DMSO-d_6): δ (ppm) 160.13, 151.70, 147.51, 138.27, 133.02, 128.95, 126.91, 126.20, 123.09, 121.22, 120.83, 118.89; ESI-MS: *m/z* 304 [M+H$^+$] (calc. for $C_{14}H_{10}ClN_3OS$: 303.02). EA: calc. C 55.36; H 3.32; N 13.83; S 10.55. Found: C 54.91; H 3.56; N 13.43; S 10.59.

Compound 45

1-(6-chlorobenzo[*d*]thiazol-2-yl)-3-(3,4-dihydroxyphenyl)urea

M.p. 257–259 °C. Yield 27%. ^{1}H NMR (500 MHz DMSO-d_6): δ (ppm) 9.18 (s, 1H), 8.03 (d, *J* = 2.2 Hz, 1H), 7.63 (d, *J* = 8.6 Hz, 1H), 7.38 (ddd, *J* = 8.6, 2.2, 0.5 Hz, 1H), 7.03 (d, *J* = 2.1 Hz, 1H), 6.73 – 6.64 (m, 2H). ^{13}C NMR (126 MHz, DMSO-d_6): δ (ppm) 160.17, 151.60, 147.56, 145.29, 141.39, 133.14, 130.10, 126.75, 126.13, 121.13, 120.70, 115.58, 110.12, 107.69. ESI-HRMS: *m/z* 336.02020 [M+H]$^+$ (calc. for $C_{14}H_{10}ClN_3O_3S$: 336.02042 [M+H]$^+$).

Compound 46

1-(6-chlorobenzo[*d*]thiazol-2-yl)-3-(4-hydroxy-3-methoxyphenyl)urea

M.p. 257–259 °C. Yield 90%. ^{1}H NMR (500 MHz, DMSO-d_6): δ (ppm) 9.42 (s, 1H), 8.03 (d, *J* = 2.2 Hz, 1H), 7.63 (d, *J* = 8.6 Hz, 1H), 7.39 (dd, *J* = 8.6, 2.2 Hz, 1H), 7.17 (d, *J* = 2.4 Hz, 1H), 6.82 (dd, *J* = 8.5, 2.4 Hz, 1H), 6.73 (d, *J* = 8.4 Hz, 1H), 3.77 (s, 3H). ^{13}C NMR (126 MHz, DMSO-d_6): δ (ppm) 160.19, 151.85,

147.51, 147.47, 142.61, 133.11, 130.21, 126.78, 126.16, 121.15, 120.68, 115.45, 111.74, 104.76, 55.61. ESI-HRMS: *m/z* 350.03568 $[M+H]^+$ (calc. for $C_{15}H_{12}ClN_3O_3S$: 350.03607 $[M+H]^+$).

Compound 47

1-(6-chlorobenzo[*d*]thiazol-2-yl)-3-(3-hydroxy-4-methoxyphenyl)urea

M.p. 281–283 °C. Yield 75%. ^{1}H NMR (500 MHz, DMSO-d_6): δ (ppm) 10.77 (s, 1H), 9.12 (s, 1H), 8.88 (s, 1H), 8.04 (d, *J* = 2.1 Hz, 1H), 7.63 (d, *J* = 8.7 Hz, 1H), 7.39 (dd, *J* = 8.7, 2.2 Hz, 1H), 7.07 (d, *J* = 2.4 Hz, 1H), 6.86 (d, *J* = 8.8 Hz, 1H), 6.82 (dd, *J* = 8.7, 2.4 Hz, 1H), 3.73 (s, 3H). ^{13}C NMR (126 MHz, DMSO-d_6): δ (ppm) 160.23, 151.67, 147.38, 146.73, 143.85, 133.06, 131.68, 126.81, 126.15, 121.16, 120.65, 112.81, 109.67, 107.56, 55.96. ESI-HRMS: *m/z* 350.03589 $[M+H]^+$ (calc. for $C_{15}H_{12}ClN_3O_3S$: 350.03607 $[M+H]^+$).

Compound 48

1-(3-chloro-4-methoxyphenyl)-3-(6-hydroxybenzo[*d*]thiazol-2-yl)urea

M.p. 290–292 °C. Yield 31%. ^{1}H NMR (500 MHz, DMSO-d_6): δ (ppm) 10.68 (s, 1H), 9.43 (s, 1H), 9.09 (s, 1H), 7.69 (d, *J* = 2.6 Hz, 1H), 7.45 (d, *J* = 8.6 Hz, 1H), 7.35 (dd, *J* = 8.9, 2.5 Hz, 1H), 7.22 (d, *J* = 2.4 Hz, 1H), 7.11 (d, *J* = 9.0 Hz, 1H), 6.84 (dd, *J* = 8.6, 2.4 Hz, 1H), 3.83 (s, 3H). ^{13}C NMR (126 MHz, DMSO-d_6): δ (ppm) 157.00, 153.67, 152.21, 150.31, 141.07, 132.26, 120.82, 120.67, 119.86, 118.95, 114.74, 113.09, 106.68, 56.20. ESI-HRMS: *m/z* 350.03540 $[M+H]^+$ (calc. for $C_{15}H_{12}ClN_3O_3S$: 350.03607 $[M+H]^+$).

Compound 49

1-(6-methoxybenzo[*d*]thiazol-2-yl)-3-phenylthiourea

M.p. 198–200 °C. Yield 88 %. ^{1}H NMR (500 MHz, DMSO-d_6): δ (ppm) 12.51 (br s, 1H), 10.80 (br s, 1H), 7.70 (d, *J* = 7.9 Hz, 2H), 7.49 (m, 2H), 7.35 (t, *J* = 7.4 Hz, 2H), 7.14 (s, 1H), 7.02 (dd, *J* = 8.8, 2.3 Hz, 1H), 3.79 (s, 3H); ^{13}C NMR (126 MHz, DMSO-d_6): δ (ppm) 181.42, 156.09, 139.38, 128.44, 124.17, 122.87, 114.74, 105.93, 55.68; ESI-MS: *m/z* 316 $[M+H]^+$ (calc. for $C_{15}H_{13}N_3OS_2$: 315.05); EA: calc. C, 57.12; H, 4.15; N, 13.32; S, 20.33. Found: C, 57.28; H, 4.17; N, 13.61; S, 20.73.

Compound 50

The crude product was recrystallized from petroleum ether.

1-(6-methoxybenzo[*d*]thiazol-2-yl)-3-phenylguanidine

M.p. 129.5–131 °C. Yield 79 %. ^{1}H NMR (500 MHz, DMSO-d_6): δ (ppm) 9.04 (br s, 1H), 7.96 (br s, 2H), 7.48 (dd, *J* = 8.5, 0.9 Hz, 2H), 7.46 (d, *J* = 8.8 Hz, 1H), 7.37 (d, *J* = 2.6 Hz, 1H), 7.35 – 7.30 (m, 2H), 7.08 – 7.01 (m, 1H), 6.90 (dd, *J* = 8.8, 2.7 Hz, 1H), 3.77 (s, 3H). ^{13}C NMR (126 MHz, DMSO-d_6): δ (ppm)

171.47, 155.27, 153.69, 145.64, 138.93, 131.80, 128.82, 122.83, 120.68, 119.53, 113.54, 104.94, 55.52. ESI-HRMS: *m/z* 299.09564 $[M+H]^+$ (calc. for $C_{15}H_{14}N_4OS$: 299.09611 $[M+H]^+$).

Compound 51

1-(6-fluorobenzo[*d*]thiazol-2-yl)-3-phenylurea

M.p. 362.5–364.4 °C. Yield 76 %. ^{1}H NMR (500 MHz, DMSO-d_6): δ (ppm) 10.77 (br s, 1H), 9.06 (br s, 1H), 7.79 (dd, *J* = 8.7, 2.6 Hz, 1H), 7.71 – 7.61 (m, 1H), 7.51 (d, *J* = 7.8 Hz, 2H), 7.34 (t, *J* = 7.9 Hz, 2H), 7.21 (td, *J* = 9.2, 2.7 Hz, 1H), 7.07 (t, *J* = 7.4 Hz, 1H). ^{13}C NMR (126 MHz, DMSO-d_6): δ (ppm) 159.20, 158.14 (d, *J* = 239.3 Hz), 151.64, 144.93, 138.10, 132.39, 128.63 (d, *J* = 15.5 Hz), 122.84 (d, *J* = 8.3 Hz), 120.28, 118.79 (d, *J* = 16.6 Hz), 113.48 (dd, *J* = 24.3, 14.2 Hz), 107.70 (dd, *J* = 26.9, 13.5 Hz). ESI-MS: *m/z* 288 $[M+H]^+$ (calc. for $C_{14}H_{10}FN_3OS$: 287.05). EA: calc. C, 58.53; H, 3.51; N, 14.63; S, 11.16. Found: C, 58.12; H, 3.69; N, 14.71; S, 11.57.

Compound 52

1-(6-fluorobenzo[*d*]thiazol-2-yl)-3-phenylthiourea

M.p. 302 °C decomp. Yield 84 %. ^{1}H NMR (300 MHz, DMSO-d_6): δ (ppm) 12.52 (br s, 1H), 10.81 (br s, 1H), 7.81 (dd, *J* = 9.0, 2.1 Hz, 1H), 7.69 (d, *J* = 8.4 Hz, 2H), 7.55 (s, 1H), 7.36 (t, *J* = 7.9 Hz, 2H), 7.27 (td, *J* = 9.2, 2.5 Hz, 1H), 7.21 – 7.06 (m, 1H); ^{13}C NMR (75 MHz, DMSO-d_6): δ (ppm) 180.89, 158.50 (d, *J* = 239.2 Hz), 157.48, 139.25, 128.48, 124.52, 123.21, 114.37 (d, *J* = 24.6 Hz), 108.97 (d, *J* = 27.2 Hz); ESI-MS: *m/z* 304 $[M+H]^+$ (calc. for $C_{14}H_{10}FN_3S_2$: 303.03); EA: calc. C, 55.43; H, 3.32; N, 13.85; S, 21.14. Found: C, 55.13; H, 3.14; N, 14.10; S, 20.80.

Compound 53

The crude product was recrystallized from petroleum ether/heptan.

1-(6-fluorobenzo[*d*]thiazol-2-yl)-3-phenylguanidine

M.p. 166–168 °C. Yield 32 %. ^{1}H NMR (500 MHz, CD_3OD): δ (ppm) 7.51 (dd, *J* = 8.8, 4.8 Hz, 1H), 7.44 – 7.33 (m, 5H), 7.15 (tt, *J* = 7.4, 1.3 Hz, 1H), 7.03 (td, *J* = 9.1, 2.7 Hz, 1H). ^{13}C NMR (126 MHz, CD_3OD): δ (ppm) 174.60, 160.27 (d, *J* = 239.6 Hz), 156.54, 149.69, 139.25, 133.70 (d, *J* = 10.7 Hz), 130.28, 125.78, 123.96, 121.04 (d, *J* = 8.9 Hz), 114.00 (d, *J* = 24.3 Hz), 108.14 (d, *J* = 27.0 Hz). ESI-HRMS: *m/z* 287.07584 $[M+H]^+$ (calc. for $C_{14}H_{11}FN_4S$: 287.07612 $[M+H]^+$).

Compound 54

ethyl 2-(3-phenylureido)benzo[*d*]thiazole-6-carboxylate

M.p. 314–316 °C. Yield 59 %. ^{1}H NMR (500 MHz, DMSO-d_6): δ (ppm) 11.12 (br s, 1H), 9.23 (br s, 1H), 8.56 (d, *J* = 0.8 Hz, 1H), 7.97 (dd, *J* = 8.5, 1.8 Hz, 1H), 7.72 (d, *J* = 8.4 Hz, 1H), 7.53 (d, *J* = 7.7 Hz, 2H),

7.34 (t, *J* = 7.9 Hz, 2H), 7.07 (t, *J* = 7.4 Hz, 1H), 4.33 (q, *J* = 7.1 Hz, 2H), 1.34 (t, *J* = 7.1 Hz, 3H). ^{13}C NMR (126 MHz, DMSO-d_6): δ (ppm) 165.49, 162.76, 151.89, 138.25, 131.45, 128.93, 127.06, 124.17, 123.41, 123.13, 119.08, 118.88, 60.64, 14.23. ESI-HRMS: *m/z* 342.09009 $[M+H]^+$ (calc. for $C_{17}H_{15}N_3O_3S$: 342.09069 $[M+H]^+$)

Compound 55

ethyl 2-(3-phenylthioureido)benzo[*d*]thiazole-6-carboxylate

M.p. 207.5–208.8 °C. Yield 88 %. ^{1}H NMR (500 MHz, DMSO-d_6): δ (ppm) 10.61 (s, 1H), 8.48 (s, 1H), 7.99 (dd, *J* = 8.4, 1.6 Hz, 1H), 7.69 (d, *J* = 7.9 Hz, 2H), 7.60 (s, 1H), 7.37 (t, *J* = 6.9 Hz, 2H), 7.16 (s, 1H), 4.33 (q, *J* = 7.1 Hz, 2H), 1.33 (t, *J* = 7.1 Hz, 3H). ^{13}C NMR (126 MHz, DMSO-d_6): δ (ppm) 181.89, 165.35, 156.99, 139.18, 128.55, 128.48, 127.74, 124.73, 124.01, 123.41, 112.48, 60.79, 14.27. ESI-MS: *m/z* 358 $[M+H]^+$ (calc. for $C_{17}H_{15}N_3O_2S_2$: 357.06). EA: calc. C, 57.12; H, 4.23; N, 11.76; S, 17.94. Found: C, 56.85; H, 3.92; N, 11.60; 17.52.

Compound 56

The crude product was recrystallized from petroleum ether/heptan.

ethyl 2-(3-phenylguanidino)benzo[*d*]thiazole-6-carboxylate

M.p. 134–136 °C. Yield 28 % ^{1}H NMR (500 MHz, DMSO-d_6): δ (ppm) 9.31 (br s, 1H), 8.36 (s, 1H), 8.14 (br s, 1H), 7.89 (d, *J* = 8.2 Hz, 1H), 7.59 (d, *J* = 8.4 Hz, 1H), 7.46 (d, *J* = 7.1 Hz, 2H), 7.36 (t, *J* = 7.7 Hz, 2H), 7.10 (t, *J* = 7.1 Hz, 1H), 4.31 (dd, *J* = 14.0, 6.9 Hz, 2H), 1.33 (t, *J* = 7.1 Hz, 3H). ^{13}C NMR (126 MHz, DMSO-d_6): δ (ppm) 176.24, 165.56, 155.35, 154.57, 138.31, 130.74, 128.93, 126.78, 123.54, 122.58, 121.43, 118.38, 60.49, 14.23. ESI-HRMS: *m/z* 341.10617 $[M+H]^+$ (calc. for $C_{17}H_{16}N_4O_2S$: 341.10667 $[M+H]^+$).

Compound 57

1-(6-methoxybenzo[*d*]thiazol-2-yl)-3-(4-methoxyphenyl)urea

M.p. 316–318 °C. Yield 87 %. ^{1}H NMR (500 MHz, DMSO-d_6): δ (ppm) 10.59 (br s, 1H), 8.94 (br s, 1H), 7.55 (d, *J* = 8.7 Hz, 1H), 7.50 (d, *J* = 2.3 Hz, 1H), 7.41 (d, *J* = 8.7 Hz, 2H), 6.98 (dd, *J* = 8.7, 2.2 Hz, 1H), 6.91 (d, *J* = 8.8 Hz, 2H), 3.79 (s, 3H), 3.73 (s, 3H). ^{13}C NMR (126 MHz, DMSO-d_6): δ (ppm) 157.57, 155.64, 155.20, 151.87, 142.77, 132.48, 131.38, 120.70, 120.16, 114.30, 114.09, 104.92, 55.59, 55.20. ESI-MS: *m/z* 330 $[M+H]^+$ (calc. for $C_{16}H_{15}N_3O_3S$: 329.08); EA: calc. C, 58.35; H, 4.59; N, 12.76; S, 9.73. Found: C, 58.36; H, 4.66; N, 13.09; S, 9.59.

Compound 58

1-(6-methoxybenzo[*d*]thiazol-2-yl)-3-(4-methoxyphenyl)thiourea

M.p. 202.2–202.7 °C. Yield 90 %. ^{1}H NMR (500 MHz, DMSO-d_6): δ 12.33 (br s, 1H), 11.04 (br s, 1H), 7.60 – 7.40 (m, 4H), 7.01 (dd, *J* = 8.8, 2.6 Hz, 1H), 6.93 (d, *J* = 8.8 Hz, 2H), 3.79 (s, 3H), 3.76 (s, 3H). ^{13}C NMR (126 MHz, DMSO-d_6): δ (ppm) 179.76, 160.68, 156.49, 156.06, 138.31, 132.03, 129.52, 125.22, 118.05, 114.61, 113.63, 105.76, 55.66, 55.24. ESI-MS: *m/z* 346 $[M+H]^+$ (calc. for $C_{16}H_{15}N_3O_2S_2$: 345.06). EA: calc. C, 55.63; H, 4.38; N, 12.16; S, 18.56. Found: C, 55.21; H, 4.41; N, 12.40; S, 18.82.

Compound 59

1-(6-methoxybenzo[*d*]thiazol-2-yl)-3-(4-methoxyphenyl)guanidine

M.p. 160.5–161.7 °C. Yield 72 %. ^{1}H NMR (500 MHz, DMSO-d_6): δ (ppm) 8.96 (br s, 1H), 7.82 (s, 1H), 7.43 (d, *J* = 8.8 Hz, 1H), 7.37 – 7.29 (m, 3H), 6.96 – 6.91 (m, 2H), 6.89 (dd, *J* = 8.8, 2.6 Hz, 1H), 3.76 (s, 3H), 3.74 (s, 3H). ^{13}C NMR (126 MHz, DMSO-d_6): δ (ppm) 171.74, 155.71, 155.14, 154.33, 145.77, 131.66, 131.35, 123.57, 119.28, 114.15, 113.37, 104.97, 55.51, 55.22. ESI-MS: *m/z* 329 $[M+H]^+$ (calc. for $C_{16}H_{16}N_4O_2S$: 328.10).; EA: calc. C, 58.52; H, 4.91; N, 17.06; S, 9.76. Found: C, 58.15; H, 4.60; N, 16.62; S, 9.37.

Compound 60

4-(3-(6-methoxybenzo[*d*]thiazol-2-yl)ureido)benzoic acid

M.p. 295 °C decomp. Yield 96 %. ^{1}H NMR (500 MHz, DMSO-d_6): δ (ppm) 10.52 (br s, 1H), 8.75 (br s, 1H), 7.94 – 7.89 (m, 2H), 7.67 – 7.61 (m, 2H), 7.57 (d, *J* = 8.8 Hz, 1H), 7.53 (d, *J* = 2.6 Hz, 1H), 7.00 (dd, *J* = 8.8, 2.6 Hz, 1H), 3.80 (s, 3H). ^{13}C NMR (126 MHz, DMSO-d_6): δ (ppm) 166.96, 157.31, 155.83, 152.10, 142.98, 141.94, 132.38, 130.65, 124.57, 120.06, 117.58, 114.56, 104.99, 55.67. ESI-MS: *m/z* 344 $[M+H]^+$ (calc. for $C_{16}H_{13}N_3O_4S$: 343.06). EA: calc. C, 55.97; H, 3.82; N, 12.24; S, 9.34. Found: C, 55.54; H, 3.92; N, 11.83; S, 8.86.

Compound 61

4-(3-(6-methoxybenzo[*d*]thiazol-2-yl)thioureido)benzoic acid

M.p. 278 °C decomp. Yield 95 %. ^{1}H NMR (500 MHz, DMSO-d_6): δ (ppm) 12.67 (br s, 1H), 10.70 (br s, 1H), 7.91 (m, 4H), 7.49 (d, *J* = 2.4 Hz, 1H), 7.45 (d, *J* = 8.8 Hz, 1H), 7.04 (dd, *J* = 8.8, 2.5 Hz, 1H), 3.80 (s, 3H). ^{13}C NMR (126 MHz, DMSO-d_6): δ (ppm) 182.47, 167.17, 156.08, 143.81, 132.24, 129.89, 128.53, 125.15, 120.84, 115.32, 114.89, 106.10, 55.70. ESI-MS: *m/z* 360 $[M+H]^+$ (calc. for $C_{16}H_{13}N_3O_3S_2$: 359.04). EA: calc. C, 53.47; H, 3.65; N, 11.69; S, 17.84. Found: C, 53.10; H, 3.73; N, 11.94; S, 17.98.

Compound 62

The crude product was purified using column chromatography.

4-(3-(6-methoxybenzo[*d*]thiazol-2-yl)guanidino)benzoic acid

M.p. 275–277 °C. Yield 17 %. ^{1}H NMR (500 MHz, DMSO-d_6): δ (ppm) 12.61 (br s, 1H), 9.38 (br s, 1H), 8.12 (br s, 2H), 7.91 – 7.87 (m, 2H), 7.63 (d, *J* = 8.5 Hz, 2H), 7.49 (d, *J* = 8.8 Hz, 1H), 7.40 (d, *J* = 2.6 Hz, 1H), 6.93 (dd, *J* = 8.8, 2.6 Hz, 1H), 3.78 (s, 3H). ^{13}C NMR (126 MHz, DMSO-d_6): δ (ppm) 171.03, 167.10, 155.47, 153.07, 145.49, 143.47, 132.04, 130.34, 124.30, 119.86, 118.95, 113.76, 104.94, 55.55. ESI-HRMS: *m/z* 343.08539 $[M+H]^+$ (calc. for $C_{16}H_{14}N_4O_3S$: 343.08594 $[M+H]^+$).

Compound 64

1-(3-chloro-4-hydroxyphenyl)-3-(5-chlorobenzo[*d*]thiazol-2-yl)urea

M.p. 317.5–319 °C. Yield 40 %. ^{1}H NMR (500 MHz, DMSO-d_6): δ (ppm) 10.97 (s, 1H), 9.98 (s, 1H), 9.01 (s, 1H), 7.93 (d, *J* = 8.4 Hz, 1H), 7.70 (s, 1H), 7.59 (d, *J* = 2.5 Hz, 1H), 7.27 (dd, *J* = 8.4, 2.0 Hz, 1H), 7.18 (dd, *J* = 8.7, 2.4 Hz, 1H), 6.93 (d, *J* = 8.7 Hz, 1H). ^{13}C NMR (126 MHz, DMSO-d_6): δ (ppm) 161.45, 151.87, 149.93, 149.15, 130.68, 130.53, 130.17, 123.03, 122.84, 121.03, 119.70, 119.40, 119.09, 116.71. ESI-HRMS: *m/z* 353.98581 $[M+H]^+$ (calc. for $C_{14}H_9Cl_2N_3O_2S$: 353.98653 $[M+H]^+$).

Compound 65

1-(3-chloro-4-hydroxyphenyl)-3-(7-chlorobenzo[*d*]thiazol-2-yl)urea

M.p. 272–274 °C. Yield 52 %. ^{1}H NMR (500 MHz, DMSO-d_6): δ (ppm) 9.54 (s, 1H), 7.69 – 7.53 (m, 2H), 7.41 (t, *J* = 7.9 Hz, 1H), 7.32 (d, *J* = 7.8 Hz, 1H), 7.19 (dd, *J* = 8.7, 2.2 Hz, 1H), 6.95 (d, *J* = 8.7 Hz, 1H). ^{13}C NMR (126 MHz, DMSO-d_6): δ (ppm) 159.38, 152.20, 149.29, 149.05, 130.63, 130.58, 127.39, 125.23, 122.50, 120.65, 119.38, 119.30, 118.20, 116.72. ESI-HRMS: *m/z* 353.98566 $[M+H]^+$ (calc. for $C_{14}H_9Cl_2N_3O_2S$: 353.98653 $[M+H]^+$).

Compound 66

6-chlorobenzo[*d*]thiazole

M.p. 37–39 °C. Yield 82%. ^{1}H NMR (300 MHz, $CDCl_3$): δ (ppm) 8.97 (s, 1H), 8.04 (d, *J* = 8.7 Hz, 1H), 7.93 (d, *J* = 2.1 Hz, 1H), 7.48 (dd, *J* = 8.7, 2.1 Hz, 1H). ^{13}C NMR (75 MHz, $CDCl_3$): δ (ppm) 154.43, 151.96, 135.10, 131.81, 127.21, 124.50, 121.61. ESI-HRMS: *m/z* 169.98276 $[M+H]^+$ (calc. for C_7H_4ClNS: 169.98257 $[M+H]^+$).

Compound 77

1-(6-aminobenzo[*d*]thiazol-2-yl)-3-(3-chloro-4-hydroxyphenyl)urea

M.p. 223–224 °C. Yield 77 %. ^{1}H NMR (500 MHz, DMSO-d_6): δ (ppm) 10.48 (s, 1H), 9.88 (s, 1H), 8.98 (s, 1H), 7.60 (d, *J* = 2.6 Hz, 1H), 7.32 (d, *J* = 8.5 Hz, 1H), 7.16 (dd, *J* = 8.7, 2.6 Hz, 1H), 6.97 (d, *J* = 2.2 Hz, 1H), 6.92 (d, *J* = 8.7 Hz, 1H), 6.66 (dd, *J* = 8.5, 2.2 Hz, 1H), 5.07 (br s, 2H). ^{13}C NMR (126 MHz, DMSO-d_6): δ (ppm) 155.24, 152.15, 148.75, 145.19, 139.03, 132.30, 130.98, 120.62, 119.61, 119.33, 119.28,

116.66, 114.00, 104.50. ESI-HRMS: *m/z* 335.03629 $[M+H]^+$ (calc. for $C_{14}H_{11}ClN_4O_2S$: 335.03640 $[M+H]^+$).

Compound 78

1-(3-chloro-4-hydroxyphenyl)-3-(6-hydroxybenzo[*d*]thiazol-2-yl)urea

M.p. 249–250 °C. Yield 85%. ^{1}H NMR (300 MHz, DMSO-d_6): δ (ppm) 10.57 (s, 1H), 9.91 (s, 1H), 9.44 (s, 1H), 8.98 (s, 1H), 7.59 (d, *J* = 2.5 Hz, 1H), 7.44 (d, *J* = 8.6 Hz, 1H), 7.22 (d, *J* = 2.3 Hz, 1H), 7.17 (dd, *J* = 8.8, 2.5 Hz, 1H), 6.92 (d, *J* = 8.7 Hz, 1H), 6.83 (dd, *J* = 8.7, 2.5 Hz, 1H). ^{13}C NMR (75 MHz, DMSO-d_6): δ (ppm) 156.96, 153.68, 152.29, 148.86, 141.49, 132.31, 130.88, 120.71, 120.02, 119.38, 119.33, 116.67, 114.75, 106.68. ESI-HRMS: *m/z* 336.01987 $[M+H]^+$ (calc. for $C_{14}H_{10}ClN_3O_3S$: 336.02042 $[M+H]^+$).

Compound 80

1-(6-(tert-butyl)benzo[*d*]thiazol-2-yl)-3-(3-chloro-4-hydroxyphenyl)urea

M.p. 238–240 °C. Yield 66 %. ^{1}H NMR (500 MHz, DMSO-d_6): δ (ppm) 9.75 (s, 1H), 7.90 (d, *J* = 1.9 Hz, 1H), 7.60 (d, *J* = 2.6 Hz, 1H), 7.56 (d, *J* = 8.5 Hz, 1H), 7.43 (dd, *J* = 8.5, 2.0 Hz, 1H), 7.18 (dd, *J* = 8.8, 2.6 Hz, 1H), 6.95 (d, *J* = 8.7 Hz, 1H), 1.32 (s, 9H). ^{13}C NMR (126 MHz, DMSO-d_6): δ (ppm) 159.43, 152.17, 148.89, 145.88, 145.02, 130.87, 130.77, 123.74, 120.40, 119.36, 119.08, 118.41, 117.78, 116.74, 34.62, 31.45. ESI-HRMS: *m/z* 376.0882 $[M+H]^+$ (calc. for $C_{18}H_{18}ClN_3O_2S$: 376.0881 $[M+H]^+$).

Compound 81

1-(3-chloro-4-hydroxyphenyl)-3-(6-iodobenzo[*d*]thiazol-2-yl)urea

M.p. 271–273 °C. Yield 58 %. ^{1}H NMR (500 MHz, DMSO-d_6): δ (ppm) 10.86 (br s, 1H), 9.94 (s, 1H), 9.01 (s, 1H), 8.30 (s, 1H), 7.66 (dd, *J* = 8.4, 1.6 Hz, 1H), 7.59 (d, *J* = 2.2 Hz, 1H), 7.44 (d, *J* = 8.2 Hz, 1H), 7.18 (dd, *J* = 8.6, 1.8 Hz, 1H), 6.93 (d, *J* = 8.7 Hz, 1H). ^{13}C NMR (126 MHz, DMSO-d_6): δ (ppm) 160.16, 151.89, 149.04, 134.50, 133.90, 130.59, 129.67, 120.90, 119.56, 119.33, 116.65, 86.22. ESI-HRMS: *m/z* 445.9215 $[M+H]^+$ (calc. for $C_{14}H_9ClIN_3O_2S$: 445.9221 $[M+H]^+$).

Compound 88

1-(5-chloro-1*H*-benzo[*d*]imidazol-2-yl)-3-(3-chloro-4-hydroxyphenyl)urea

M.p. 256–258 °C. Yield 28 %. ^{1}H NMR (300 MHz, DMSO-d_6): δ (ppm) 10.98 (s, 1H), 9.94 (s, 1H), 9.34 (s, 1H), 7.69 (d, *J* = 2.5 Hz, 1H), 7.40 (d, *J* = 1.9 Hz, 1H), 7.37 (d, *J* = 8.4 Hz, 1H), 7.18 (dd, *J* = 8.8, 2.5 Hz, 1H), 7.07 (dd, *J* = 8.4, 2.0 Hz, 1H), 6.93 (d, *J* = 8.7 Hz, 1H). ^{13}C NMR (75 MHz, DMSO-d_6): δ (ppm) 152.91, 149.27, 148.69, 136.85, 134.35, 131.21, 125.03, 120.78, 120.64, 119.32, 119.19, 116.66, 114.15, 113.01. ESI-HRMS: *m/z* 337.02505 $[M+H]^+$ (calc. for $C_{14}H_{10}Cl_2N_4O_2$: 337.02536 $[M+H]^+$).

Compound 89

1-(benzo[*d*]oxazol-2-yl)-3-(3-chloro-4-hydroxyphenyl)urea

M.p. 190.5–191.5 °C. Yield 59 %. ^{1}H NMR (500 MHz, DMSO-d_6): δ (ppm) 11.33 (s, 1H), 10.22 (s, 1H), 9.94 (s, 1H), 7.70 (d, *J* = 1.5 Hz, 1H), 7.60 – 7.47 (m, 2H), 7.33 – 7.18 (m, 3H), 6.95 (d, *J* = 8.7 Hz, 1H). ^{13}C NMR (126 MHz, DMSO-d_6): δ (ppm) 156.78, 149.75, 149.39, 147.01, 140.03, 130.11, 124.62, 123.09, 121.47, 120.07, 119.34, 117.45, 116.63, 109.90. ESI-HRMS: *m/z* 304.04807 $[M+H]^+$ (calc. for $C_{14}H_{10}ClN_3O_3$: 304.04835 $[M+H]^+$).

Compound 90

The crude product was purified using column chromatography.

1-(3-chloro-4-hydroxyphenyl)-3-(6-chlorobenzo[*d*]oxazol-2-yl)urea

M.p. 188.5–190.5 °C. Yield 35 %. ^{1}H NMR (500 MHz, DMSO-d_6): δ (ppm) 11.46 (s, 1H), 10.21 (s, 1H), 10.00 (s, 1H), 7.77 (d, *J* = 1.7 Hz, 1H), 7.67 (d, *J* = 2.4 Hz, 1H), 7.52 (d, *J* = 8.3 Hz, 1H), 7.34 (dd, *J* = 8.4, 2.0 Hz, 1H), 7.26 (dd, *J* = 8.8, 2.6 Hz, 1H), 6.94 (d, *J* = 8.7 Hz, 1H). ^{13}C NMR (126 MHz, DMSO-d_6): δ (ppm) 157.70, 152.28, 149.23, 146.84, 138.05, 130.53, 126.96, 124.83, 121.26, 119.88, 119.34, 116.65, 116.62, 110.61. ESI-HRMS: *m/z* 338.00909 $[M+H]^+$ (calc. for $C_{14}H_9Cl_2N_3O_3$: 338.00937 $[M+H]^+$).

Compound 92

1-(benzo[*d*]thiazol-6-yl)-3-(3-chloro-4-hydroxyphenyl)urea

M.p. 224–226 °C. Yield 24 %. ^{1}H NMR (500 MHz, DMSO-d_6): δ (ppm) 9.77 (s, 1H), 9.20 (s, 1H), 8.89 (s, 1H), 8.60 (s, 1H), 8.35 (d, *J* = 2.1 Hz, 1H), 7.97 (d, *J* = 8.8 Hz, 1H), 7.60 (d, *J* = 2.6 Hz, 1H), 7.47 (dd, *J* = 8.8, 2.2 Hz, 1H), 7.11 (dd, *J* = 8.7, 2.6 Hz, 1H), 6.90 (d, *J* = 8.7 Hz, 1H). ^{13}C NMR (126 MHz, DMSO-d_6): δ (ppm) 153.69, 152.69, 148.26, 148.17, 137.64, 134.46, 131.92, 122.92, 120.22, 119.26, 118.82, 118.11, 116.63, 110.26. ESI-HRMS: *m/z* 320.0264 $[M+H]^+$ (calc. for $C_{14}H_{10}ClN_3O_2S$: 320.0255 $[M+H]^+$).

Compound 93

1-(3-chloro-4-hydroxyphenyl)-3-(thiazol-2-yl)urea

M.p. 220–222 °C. Yield 74 %. ^{1}H NMR (500 MHz, DMSO-d_6): δ (ppm) 9.83 (s, 1H), 9.81 (s, 1H), 7.56 (d, *J* = 2.6 Hz, 1H), 7.47 (dd, *J* = 3.9, 1.6 Hz, 1H), 7.20 (dd, *J* = 3.8, 1.5 Hz, 1H), 7.15 (dd, *J* = 8.8, 2.6 Hz, 1H), 6.95 (d, *J* = 8.7 Hz, 1H). ^{13}C NMR (126 MHz, DMSO-d_6): δ (ppm) 160.49, 151.25, 149.00, 133.59, 130.64, 120.41, 119.39, 119.08, 116.78, 113.06. ESI-HRMS: *m/z* 270.0099 $[M+H]^+$ (calc. for $C_{10}H_8ClN_3O_2S$: 270.0099 $[M+H]^+$).

Compound 94

The crude product was recrystallized from Et_2O.

1-(3-chloro-4-hydroxyphenyl)-3-(4,5,6,7-tetrahydrobenzo[*d*]thiazol-2-yl)urea

M.p. 258–260 °C. Yield 58 %. ^{1}H NMR (500 MHz, DMSO-d_6): δ (ppm) 9.91 (br s, 1H), 7.55 (d, *J* = 2.4 Hz, 1H), 7.14 (dd, *J* = 8.7, 2.4 Hz, 1H), 6.94 (d, *J* = 8.7 Hz, 1H), 2.59 (s, 2H), 2.54 (s, 2H), 1.75 (s, 4H). ^{13}C NMR (126 MHz, DMSO-d_6): δ (ppm) 158.38, 151.01, 149.02, 138.46, 130.54, 120.47, 120.31, 119.38, 119.00, 116.77, 24.13, 22.46, 22.07, 21.82. ESI-HRMS: *m/z* 324.05634 $[M+H]^+$ (calc. for $C_{14}H_{14}ClN_3O_2S$: 324.05680 $[M+H]^+$).

Compound 95

The crude product was recrystallized from Et_2O.

1-(3-Chloro-4-hydroxyphenyl)-3-(4-(4-chlorophenyl)thiazol-2-yl)urea

M.p. 206–208 °C. Yield 71 %. ^{1}H NMR (500 MHz, DMSO-d_6): δ (ppm) 10.69 (s, 1H), 9.91 (s, 1H), 8.76 (s, 1H), 7.92 – 7.87 (m, 2H), 7.60 – 7.57 (m, 2H), 7.50 – 7.45 (m, 2H), 7.14 (dd, *J* = 8.7, 2.6 Hz, 1H), 6.93 (d, *J* = 8.7 Hz, 1H). ^{13}C NMR (126 MHz, DMSO-d_6): δ (ppm) 159.31, 151.59, 148.87, 147.41, 133.16, 132.07, 130.69, 128.67, 127.26, 120.67, 119.34, 116.66, 107.89. ESI-HRMS: *m/z* 380.00168 $[M+H]^+$ (calc. for $C_{16}H_{11}Cl_2N_3O_2S$: 380.00218 $[M+H]^+$).

Compound 96

1-(3-chloro-4-hydroxyphenyl)-3-(2,3-dihydro-1*H*-inden-2-yl)urea

M.p. 203–205 °C. Yield 21%. ^{1}H NMR (500 MHz, DMSO-d_6): δ (ppm) 9.59 (br s, 1H), 8.14 (br s, 1H), 7.52 (d, *J* = 2.6 Hz, 1H), 7.29 – 7.19 (m, 2H), 7.19 – 7.10 (m, 2H), 6.97 (dd, *J* = 8.7, 2.6 Hz, 1H), 6.83 (d, *J* = 8.7 Hz, 1H), 6.36 (d, *J* = 7.3 Hz, 1H), 4.48 – 4.31 (m, 1H), 3.25 – 3.09 (m, 2H), 2.84 – 2.67 (m, 2H). ^{13}C NMR (126 MHz, DMSO-d_6): δ (ppm) 155.00, 147.38, 141.23, 132.93, 126.40, 124.56, 119.34, 119.16, 117.90, 116.55, 50.77, 39.70. ESI-HRMS: *m/z* 303.08908 $[M+H]^+$ (calc. for $C_{16}H_{15}ClN_2O_2$: 303.08948 $[M+H]^+$).

Compound 97

1-(3-chloro-4-hydroxyphenyl)-3-(4-methoxyphenethyl)urea

M.p. 161.5–163.5 °C. Yield 21 %. ^{1}H NMR (500 MHz, DMSO-d_6): δ (ppm) 9.58 (br s, 1H), 8.29 (br s, 1H), 7.52 (d, *J* = 2.5 Hz, 1H), 7.14 (d, *J* = 8.5 Hz, 2H), 6.97 (dd, *J* = 8.7, 2.5 Hz, 1H), 6.89 – 6.84 (m, 2H), 6.82 (d, *J* = 8.7 Hz, 1H), 5.98 (t, *J* = 5.5 Hz, 1H), 3.72 (s, 3H), 3.33 – 3.19 (m, 2H), 2.66 (t, *J* = 7.2 Hz, 2H). ^{13}C NMR (126 MHz, DMSO-d_6): δ (ppm) 157.65, 155.20, 147.32, 133.06, 131.35, 129.58, 119.37, 119.14, 117.90, 116.54, 113.78, 54.97, 40.87, 34.96. ESI-HRMS: *m/z* 321.09967 $[M+H]^+$ (calc. for $C_{16}H_{17}ClN_2O_3$: 321.10005 $[M+H]^+$).

Compound 98

1,3-bis(3-chloro-4-hydroxyphenyl)urea

M.p. 254.5–256.5 °C. Yield 94 %. ^{1}H NMR (500 MHz, DMSO-d_6): δ (ppm) 9.71 (br s, 2H), 8.43 (br s, 2H), 7.54 (d, *J* = 2.6 Hz, 2H), 7.06 (dd, *J* = 8.8, 2.6 Hz, 2H), 6.87 (d, *J* = 8.7 Hz, 2H). ^{13}C NMR (126 MHz, DMSO-d_6): δ (ppm) 152.77, 147.99, 132.14, 120.11, 119.22, 118.71, 116.59. ESI-HRMS: *m/z* 313.01361 $[M+H]^+$ (calc. for $C_{13}H_{10}Cl_2N_2O_3$: 313.01412 $[M+H]^+$).

Compound 99

1-(3-chloro-4-hydroxyphenyl)-3-(6-chlorobenzo[*d*]thiazol-2-yl)thiourea

M.p. 232.5–234 °C. Yield 80 %. ^{1}H NMR (300 MHz, DMSO-d_6): δ (ppm) 12.60 (s, 1H), 10.67 (s, 1H), 10.15 (s, 1H), 8.00 (s, 1H), 7.75 – 7.27 (m, 4H), 6.95 (d, *J* = 8.7 Hz, 1H). ^{13}C NMR (75 MHz, DMSO-d_6): δ (ppm) 150.68, 131.10, 127.32, 126.75, 125.22, 124.04, 121.93, 118.86, 116.10, 114.96. ESI-HRMS: *m/z* 369.96365 $[M+H]^+$ (calc. for $C_{14}H_9Cl_2N_3OS_2$: 369.96368 $[M+H]^+$).

Compound 100

The crude product was recrystallized from water.

1-(3-chloro-4-hydroxyphenyl)-3-(6-chlorobenzo[*d*]thiazol-2-yl)guanidine

M.p. 274–275 °C. Yield 38 %. ^{1}H NMR (300 MHz, DMSO-d_6): δ (ppm) 10.58 (s, 1H), 8.68 (s, 1H), 8.09 (d, *J* = 2.0 Hz, 1H), 7.67 (d, *J* = 8.0 Hz, 1H), 7.52 – 7.40 (m, 2H), 7.18 (dd, *J* = 8.7, 2.5 Hz, 1H), 7.11 (d, *J* = 8.7 Hz, 1H). ^{13}C NMR (75 MHz, DMSO-d_6): δ (ppm) 164.14, 155.06, 152.54, 130.55, 128.14, 127.02, 126.42, 125.50, 121.91, 119.91, 117.09. ESI-HRMS: *m/z* 353.00214 $[M+H]^+$ (calc. for $C_{14}H_{10}Cl_2N_4OS$: 353.00251 $[M+H]^+$).

Compound 101

2-chloro-4-((6-chlorobenzo[*d*]thiazol-2-yl)amino)phenol

M.p. 213–214.5 °C. Yield 30 %. ^{1}H NMR (500 MHz, DMSO-d_6): δ (ppm) 10.49 (br s, 1H), 9.92 (br s, 1H), 7.94 – 7.85 (m, 2H), 7.54 (d, *J* = 8.6 Hz, 1H), 7.40 (dd, *J* = 8.8, 2.6 Hz, 1H), 7.31 (dd, *J* = 8.6, 2.2 Hz, 1H), 6.98 (d, *J* = 8.8 Hz, 1H). ^{13}C NMR (126 MHz, DMSO-d_6): δ (ppm) 162.53, 150.83, 148.56, 132.94, 131.53, 126.01, 125.88, 120.74, 119.86, 119.74, 119.43, 118.46, 116.87. ESI-HRMS: *m/z* 310.98016 $[M+H]^+$ (calc. for $C_{13}H_8Cl_2N_2OS$: 310.98072 $[M+H]^+$).

Compound 102

3-Chloro-4-hydroxy-*N*-(6-methoxybenzo[*d*]thiazol-2-yl)benzamide

M.p. 301.5–302.5 °C. Yield 69 %. ^{1}H NMR (300 MHz, DMSO-d_6): δ (ppm) 12.51 (br s, 1H), 11.25 (br s, 1H), 8.21 (s, 1H), 7.97 (d, *J* = 8.6 Hz, 1H), 7.66 (d, *J* = 8.9 Hz, 1H), 7.59 (s, 1H), 7.17 – 6.96 (m, 2H), 3.82 (s, 3H). ^{13}C NMR (75 MHz, DMSO-d_6): δ (ppm) 164.08, 157.27, 156.85, 156.21, 142.57, 132.85, 130.34, 128.93, 123.50, 120.96, 119.89, 116.34, 115.00, 104.66, 55.64. ESI-HRMS: *m/z* 335.02466 $[M+H]^+$ (calc. for $C_{15}H_{11}ClN_2O_3S$: 335.02517 $[M+H]^+$).

Compound 103

N-(3-chloro-4-hydroxyphenyl)-6-methoxybenzo[*d*]thiazole-2-carboxamide

M.p. 260–261.5 °C. Yield 58 %. ^{1}H NMR (500 MHz, DMSO-d_6): δ (ppm) 10.94 (br s, 1H), 10.09 (br s, 1H), 8.06 (d, *J* = 8.4 Hz, 1H), 7.94 (s, 1H), 7.80 (s, 1H), 7.65 (d, *J* = 7.7 Hz, 1H), 7.23 (d, *J* = 8.1 Hz, 1H), 6.97 (d, *J* = 8.2 Hz, 1H), 3.88 (s, 3H). ^{13}C NMR (126 MHz, DMSO-d_6): δ (ppm) 161.76, 158.62, 157.88, 149.87, 147.05, 138.22, 130.34, 124.71, 122.22, 120.81, 119.09, 117.30, 116.36, 104.79, 55.84. ESI-HRMS: *m/z* 335.02466 $[M+H]^+$ (calc. for $C_{15}H_{11}ClN_2O_3S$: 335.02517 $[M+H]^+$).

Compound 104

The crude product was purified using column chromatography.

1-(3-chloro-4-hydroxybenzyl)-3-(6-methoxybenzo[*d*]thiazol-2-yl)urea

M.p. 249–251 °C. Yield 20 %. ^{1}H NMR (500 MHz, DMSO-d_6): δ (ppm) 10.60 (br s, 1H), 10.08 (br s, 1H), 7.51 (d, *J* = 8.8 Hz, 1H), 7.48 (d, *J* = 2.6 Hz, 1H), 7.29 (d, *J* = 2.1 Hz, 1H), 7.13 (t, *J* = 5.3 Hz, 1H), 7.10 (dd, *J* = 8.3, 2.1 Hz, 1H), 6.98 – 6.90 (m, 2H), 4.25 (d, *J* = 5.9 Hz, 2H), 3.78 (s, 3H). ^{13}C NMR (126 MHz, DMSO-d_6): δ (ppm) 157.80, 155.52, 153.84, 152.01, 143.16, 132.59, 131.25, 128.80, 127.18, 120.19, 119.37, 116.54, 114.15, 104.81, 55.57, 42.01. ESI-HRMS: *m/z* 364.05115 $[M+H]^+$ (calc. for $C_{16}H_{14}ClN_3O_3S$: 364.05172 $[M+H]^+$).

Compound 105

After the reaction was completed (monitored by TLC), 1M aq. HCl was poured to the reaction mixture and the product was extracted to DCM. The organic layer was concentrated and the crude product was recrystallized from MeCN.

1-(3,4-dihydroxybenzyl)-3-(6-methoxybenzo[*d*]thiazol-2-yl)urea

M.p. 141.5–142 °C. Yield 50 %. ^{1}H NMR (500 MHz, DMSO-d_6): δ (ppm) 7.51 (d, *J* = 8.8 Hz, 1H), 7.48 (d, *J* = 2.6 Hz, 1H), 7.15 (br s, 1H), 6.95 (dd, *J* = 8.8, 2.6 Hz, 1H), 6.71 (d, *J* = 2.0 Hz, 1H), 6.68 (d, *J* = 8.0 Hz, 1H), 6.56 (dd, *J* = 8.0, 2.0 Hz, 1H), 4.18 (d, *J* = 5.5 Hz, 2H), 3.78 (s, 3H). ^{13}C NMR (126 MHz, DMSO-d_6): δ (ppm) 158.51, 155.74, 153.64, 145.23, 144.41, 141.36, 131.95, 129.93, 119.61, 118.26, 115.49, 114.93, 114.45, 105.07, 55.65, 42.68. ESI-HRMS: *m/z* 346.08517 $[M+H]^+$ (calc. for $C_{16}H_{15}N_3O_4S$: 346.08560 $[M+H]^+$).

Compound 106

1-(benzo[*d*]thiazol-2-yl)-3-(3-chloro-4-hydroxyphenyl)-1-methylurea

M.p. 171–172 °C. Yield 83 %. ^{1}H NMR (500 MHz, DMSO-d_6): δ (ppm) 10.02 (s, 1H), 9.47 (s, 1H), 7.94 – 7.84 (m, 1H), 7.74 (d, *J* = 7.9 Hz, 1H), 7.57 (d, *J* = 2.6 Hz, 1H), 7.45 – 7.35 (m, 1H), 7.31 (dd, *J* = 8.8, 2.6 Hz, 1H), 7.28 – 7.19 (m, 1H), 6.96 (d, *J* = 8.7 Hz, 1H), 3.75 (s, 3H). ^{13}C NMR (126 MHz, DMSO-d_6): δ (ppm) 161.45, 153.45, 149.66, 148.45, 132.76, 130.50, 125.80, 123.42, 123.09, 121.95, 121.12, 120.29, 119.01, 116.29, 34.55 (d, *J* = 3.0 Hz). ESI-HRMS: *m/z* 334.04080 $[M+H]^+$ (calc. for $C_{15}H_{12}ClN_3O_2S$: 334.04115 $[M+H]^+$).

Compound 107

The crude product was dissolved in Et_2O and filtered. To the filtrate was added PE and the solution was left to crystallize in freezer. Filtration gave the desired pure product.

3-(benzo[*d*]thiazol-2-yl)-1-(3-chloro-4-hydroxyphenyl)-1-methylurea

M.p. 139–141 °C. Yield 53 %. ^{1}H NMR (500 MHz, DMSO-d_6): δ (ppm) 10.28 (br s, 1H), 7.81 (d, *J* = 7.5 Hz, 1H), 7.45 (br s, 1H), 7.38 – 7.30 (m, 2H), 7.19 (t, *J* = 7.9 Hz, 1H), 7.11 (dd, *J* = 8.6, 2.5 Hz, 1H), 6.99 (d, *J* = 8.6 Hz, 1H), 3.26 (s, 3H). ^{13}C NMR (126 MHz, DMSO-d_6): δ (ppm) 151.90, 135.11, 128.70, 126.89, 125.94, 122.65, 121.62, 119.46, 116.66, 37.93. ESI-HRMS: *m/z* 334.0414 $[M+H]^+$ (calc. for $C_{15}H_{12}ClN_3O_2S$: 334.0412 $[M+H]^+$).

Compound 108

The crude product was purified using column chromatography.

1-(3-chloro-4-hydroxyphenyl)-3-(6-methoxybenzo[*d*]thiazol-2-yl)-1-methylurea

M.p. 220 °C decomp. Yield 50 %. ^{1}H NMR (500 MHz, DMSO-d_6): δ (ppm) 10.28 (br s, 1H), 7.45 (d, *J* = 2.2 Hz, 1H), 7.38 (d, *J* = 8.1 Hz, 1H), 7.36 (d, *J* = 2.5 Hz, 1H), 7.11 (dd, *J* = 8.6, 2.5 Hz, 1H), 6.98 (d, *J* = 8.6 Hz, 1H), 6.94 (dd, *J* = 8.8, 2.6 Hz, 1H), 3.77 (s, 3H), 3.25 (s, 3H). ^{13}C NMR (126 MHz, DMSO-d_6): δ (ppm) 155.57, 151.97, 134.94, 131.53, 128.78, 126.95, 119.52, 118.40, 116.70, 114.18, 105.12, 55.60, 37.94. ESI-HRMS: *m/z* 364.0530 $[M+H]^+$ (calc. for $C_{16}H_{14}ClN_3O_3S$: 364.0517 $[M+H]^+$).

Compound 109

1-(benzo[*d*]thiazol-2-yl)-3-(3-chloro-4-hydroxyphenyl)-1,3-dimethylurea

M.p. 227–228.5 °C. Yield 43 %. ^{1}H NMR (500 MHz, DMSO-d_6): δ (ppm) 10.09 (s, 1H), 7.74 (d, *J* = 7.7 Hz, 1H), 7.47 – 7.37 (m, 2H), 7.36 (d, *J* = 2.4 Hz, 1H), 7.23 (t, *J* = 7.9 Hz, 1H), 7.13 (dd, *J* = 8.6, 2.2 Hz, 1H), 6.95 (d, *J* = 8.7 Hz, 1H). ^{13}C NMR (126 MHz, DMSO-d_6): δ (ppm) 165.20, 160.92, 150.53, 137.50,

136.58, 127.60, 126.56, 125.93, 125.38, 123.01, 122.40, 118.67, 115.86, 111.35, 37.16, 31.51. ESI-HRMS: *m/z* 348.05661 $[M+H]^+$ (calc. for $C_{16}H_{14}ClN_3O_2S$: 348.05680 $[M+H]^+$).

Compound 110

2-(allylamino)-5-hydroxy-1*H*-indole-3-carbonitrile

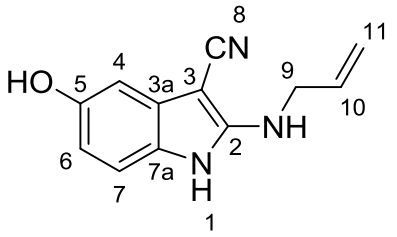

M.p. 165–167 °C. Yield 22 %. ^{1}H NMR (400 MHz, DMSO-d_6): δ (ppm) 10.60 (br s, 1H, N*H* indole), 8.76 (s, 1H, OH), 7.25 (t, *J* = 6.3 Hz, 1H, N*H*-allyl), 6.91 (d, *J* = 8.4 Hz, 1H, H-7), 6.51 (d, *J* = 2.3 Hz, 1H, H-4), 6.36 (dd, *J* = 8.4, 2.3 Hz, 1H, H-6), 6.00 – 5.81 (m, 1H, H-10), 5.26 – 5.19 (m, 1H, trans-H-11), 5.15 – 5.10 (m, 1H, cis-H-11), 3.93 – 3.87 (m, 2H, H-9). ^{13}C NMR (101 MHz, DMSO-d_6): δ (ppm) 153.27 (C-2), 152.23 (C-5), 135.28 (C-10), 129.53 (C-3a), 125.68 (C-7a), 118.27 (C-8), 115.50 (C-11), 110.57 (C-7), 107.92 (C-6), 101.05 (C-4), 61.04 (C-3), 44.89 (C-9). IR (KBr) *v* 3400, 3270, 2190, 1600, 1477, 1328, 1197, 1071, 929 827, 625 cm^{-1}. ESI-HRMS: *m/z* 231.12488 $[M+NH_4]^+$ (calc. for $C_{12}H_{11}N_3O$: 231.12404 $[M+ NH_4]^+$).

Compound 111

5-hydroxy-2-(prop-2-yn-1-ylamino)-1*H*-indole-3-carbonitrile

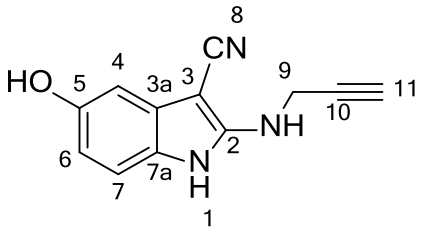

M.p. 198–199 °C. Yield 10 %. ^{1}H NMR (400 MHz, DMSO-d_6): δ (ppm) 10.88 (br s, 1H, N*H* indole), 8.82 (s, 1H, OH), 7.43 (t, *J* = 6.5 Hz, 1H, N*H*-propargyl), 6.97 (d, *J* = 8.4 Hz, 1H, H-7), 6.55 (d, *J* = 2.3 Hz, 1H, H-4), 6.40 (dd, *J* = 8.4, 2.3 Hz, 1H, H-6), 4.06 (dd, *J* = 6.5, 2.3 Hz, 3H, H-9), 3.22 (t, *J* = 2.3 Hz, 1H, H-11). ^{13}C NMR (101 MHz, DMSO-d_6): δ (ppm) 152.55 (C-2), 152.36 (C-5), 129.25 (C-3a), 125.74 (C-7a), 117.83 (C-8), 110.90 (C-7), 108.41 (C-6), 101.17 (C-4), 81.29 (C-10), 73.98 (C-11), 62.29 (C-3), 32.40 (C-9). IR (KBr) *v* 3376, 3294, 2196, 1586, 1476, 1352, 1205, 1097, 793, 685 cm^{-1}. ESI-HRMS: *m/z* 212.0816 $[M+H]^+$ (calc. for $C_{12}H_9N_3O$: 212.0818 $[M+H]^+$).

Compound 112

2-amino-5-hydroxy-1-(prop-2-yn-1-yl)-1*H*-indole-3-carbonitrile

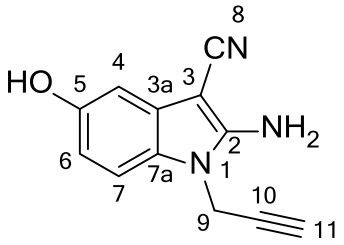

M.p. 155–170 °C. Yield 14 %. ^{1}H NMR (400 MHz, DMSO-d_6): δ (ppm) 9.01 (s, 1H, O*H*), 6.95 (d, *J* = 8.2 Hz, 1H, H-7), 6.85 (br s, 2H, NH_2), 6.69 (d, *J* = 2.1 Hz, 1H, H-4), 6.55 (dd, *J* = 8.2, 2.1 Hz, 1H, H-6), 4.85 (d, *J* = 2.5 Hz, 2H, H-9), 3.31 (t, *J* = 2.4 Hz, 1H, H-11). ^{13}C NMR (101 MHz, DMSO-d_6): δ (ppm) 152.44 (C-2), 152.22 (C-5), 133.22 (C-3a), 119.33 (C-7a), 117.84 (C-8), 115.84 (C-7), 109.93 (C-6), 96.79 (C-4), 78.29 (C-10), 74.99 (C-11), 45.57 (C-3), 31.09 (C-9). IR (KBr) *v* 3435, 3361, 3278, 2200, 1650, 1490, 1377, 1171, 935, 691 cm^{-1}. ESI-HRMS: *m/z* 212.08265 $[M+H]^+$ (calc. for $C_{12}H_9N_3O$: 212.08184 $[M+H]^+$).

Compound 113

2-amino-5-chloro-1*H*-indole-3-carbonitrile

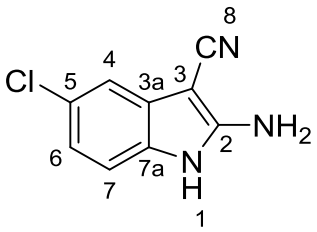

M.p. 252–254°C. Yield 48 %. ^{1}H NMR (500 MHz, DMSO-d_6): δ (ppm) 10.84 (br s, 1H, N*H* indole), 7.11 (d, *J* = 8.3 Hz, 1H, H-7), 7.08 (d, *J* = 1.7 Hz, 1H, H-4), 6.93 (br s, 2H, NH_2), 6.89 (dd, *J* = 8.3, 1.9 Hz, 1H, H-6). ^{13}C NMR (126 MHz, DMSO-d_6): δ (ppm) 154.63 (C-2), 130.82 (C-7a), 129.90 (C-3a), 125.06 (C-5), 119.19 (C-6), 117.06 (C-8), 114.21 (C-4), 111.42 (C-7), 61.67 (C-3). ESI-HRMS: *m/z* 192.03227 $[M+H]^+$ (calc. for $C_9H_6ClN_3$: 192.03230 $[M+H]^+$). Anal. calc. for $C_9H_6ClN_3$: C 56.41, H 3.16, N 21.93, found: C 56.79, H 3.53, N 21.54.

Compound 114

2,3,4,6-tetrahydro-1*H*-indolo[2,3-*b*]quinolin-11-amine

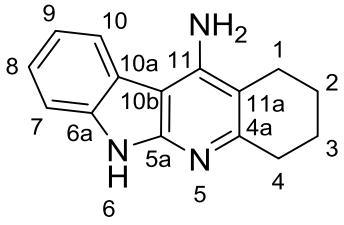

M.p. 335 °C decomp. . Yield 25 %. ^{1}H NMR (400 MHz, DMSO-d_6): δ (ppm) 11.04 (s, 1H, NH), 8.23 (d, *J* = 7.8 Hz, 1H, H-10), 7.31 (d, *J* = 8.0 Hz, 1H, H-7), 7.24 (t, *J* = 7.6 Hz, 1H, H-8), 7.08 (t, *J* = 7.5 Hz, 1H, H-9), 5.96 (br s, 2H, NH_2), 2.78 (t, *J* = 5.9 Hz, 2H, H-4), 2.55 (t, *J* = 5.9 Hz, 2H, H-1), 1.70 – 1.90 (m, 4H, H-2,3). ^{13}C NMR (101 MHz, DMSO-d_6): δ (ppm) 153.18 (C-4a), 151.45 (C-5a), 147.39 (C-11), 137.24 (C-6a), 123.33 (C-8), 121.06 (C-10a), 120.91 (C-10), 118.30 (C-9), 109.87 (C-7), 106.69 (C-11a), 98.50 (C-10b), 33.20 (C-4), 22.97 (C-1), 22.87 (2C, C-2,3). IR (KBr) *v* 3454, 3363, 3053, 2939, 2849, 1627, 1457, 1257, 729, 583 cm^{-1}. ESI-HRMS: *m/z* 238.1333 $[M+H]^+$ (calc. for $C_{15}H_{15}N_3$: 238.1339 $[M+H]^+$).

Compound 115

9-methoxy-2,3,4,6-tetrahydro-1*H*-indolo[2,3-*b*]quinolin-11-amine

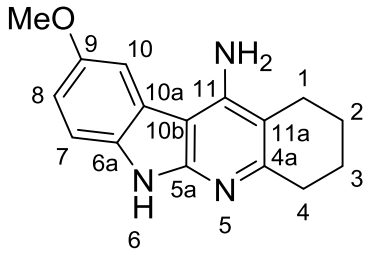

M.p. 305–307 °C. Yield 16 %. ^{1}H NMR (400 MHz, DMSO-d_6): δ (ppm) 10.80 (s, 1H, NH), 7.80 (d, *J* = 2.4 Hz, 1H, H-10), 7.20 (d, *J* = 8.6 Hz, 1H, H-7), 6.87 (dd, *J* = 8.7, 2.4 Hz, 1H, H-8), 5.98 (br s, 2H, NH_2), 2.76 (t, *J* = 6.0 Hz, 2H, H-4), 2.54 (t, *J* = 6.0 Hz, 2H, H-1), 1.90 – 1.70 (m, 4H, H-2,3). ^{13}C NMR (101 MHz, DMSO-d_6): δ (ppm) 153.17 (C-4a), 153.01 (C-9), 152.03 (C-5a), 147.42 (C-11), 131.94 (C-6a), 121.47 (C-10a), 111.60 (C-8), 110.22 (C-7), 106.16 (C-11a), 105.37 (C-10), 98.79 (C-10b), 55.96 (O*C*H$_3$), 33.21 (C-4), 23.02 (C-1), 22.88 (2C, C-2,3). IR (KBr) *v* 3343, 3133, 3044, 2936, 1620, 1471, 1215, 1036, 793, 653 cm^{-1}. ESI-HRMS: *m/z* 268.14533 $[M+H]^+$ (calc. for $C_{16}H_{17}N_3O$: 268.14444 $[M+H]^+$).

Compound 116

6-benzyl-2,3,4,6-tetrahydro-1*H*-indolo[2,3-*b*]quinolin-11-amine

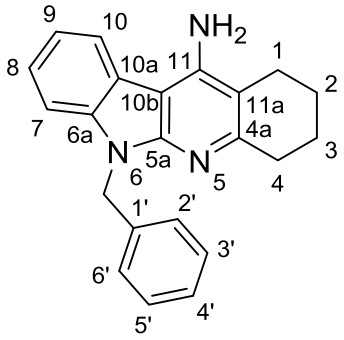

M.p. 199–200 °C. Yield 54 %. ^{1}H NMR (400 MHz, $CDCl_3$): δ (ppm) 7.83 (d, *J* = 7.6 Hz, 1H, H-10), 7.40 – 7.10 (m, 8H, ArH), 5.65 (s, 2H, N-C*H*$_2$-Ph), 4.72 (br s, 2H, NH_2), 3.00 (t, *J* = 6.0 Hz, 2H, H-4), 2.63 (t, *J* = 6.1 Hz, 2H, H-1), 2.03 – 1.84 (m, 4H, H-2,3). ^{13}C NMR (101 MHz, $CDCl_3$): δ (ppm) 154.65 (C-4a), 151.20

(C-5a), 147.02 (C-11), 138.48 (C-6a), 137.98 (C-1‘), 128.60 (2C, C-3‘,5‘), 127.16 (2C, C-2‘,6‘), 124.26 (C-8), 120.95 (C-10a), 120.22 (C-10), 119.56 (C-4‘), 109.71 (C-7), 108.31 (C-11a), 99.63 (C-10b), 44.84 (N-*C*H_2-Ph), 33.83 (C-4), 23.26, 23.18, 23.09. IR (KBr) *v* 3436, 3550, 3031, 2929, 1622, 1461, 1343, 1177, 732, 642 cm^{-1}. ESI-HRMS: *m/z* 328.18224 $[M+H]^+$ (calc. for $C_{22}H_{21}N_3$: 328.18082 $[M+H]^+$).

4.3 Biological evaluation

4.3.1 ABAD enzymatic activity assay

(performed at University of St Andrews, prof. Frank Gunn-Moore group)

4.3.1.1 Enzyme kinetics

Purification of ABAD was performed according the described conditions [118]. The kinetic parameters of the ABAD mediated reduction of acetoacetyl-CoA were measured using recombinant ABAD enzyme (0.02 µg/mL, 740 pM), NADH (250 µM) and a range of acetoacetyl-CoA concentrations (0 – 140 µM). Solutions were prepared in assay buffer (10 mM HEPES buffer, ± 0.5 % (w/v) gelatin (porcine skin), pH 7.4 at 37 °C). Reaction progression was measured via a decrease in NADH absorbance at 340 nm using a SpectraMAX 250 spectrophotometer. A reaction time of 800 s was employed yielding steady state conditions ($R^2 > 0.9$). Non-linear regression analysis was performed using GraphPad Prism, utilising the Michaelis-Menten equation.

The kinetic parameters of the ABAD mediated reduction of acetoacetyl-CoA were assessed with respect to the co-factor, NADH, using recombinant ABAD enzyme (0.02 µg/mL, 740 pM), 120 µM acetoacetyl-CoA and a range of NADH concentrations (0 – 600 µM). Experiments were performed as described for acetoacetyl-CoA above.

A V_{max} value of 10.64 ± 0.42 µmol min^{-1} mg^{-1} and a K_m value of 11.79 ± 1.86 µM were calculated with respect to acetoacetyl-CoA (Fig. 25). A concentration of 120 µM acetoacetyl-CoA was selected for subsequent experiments.

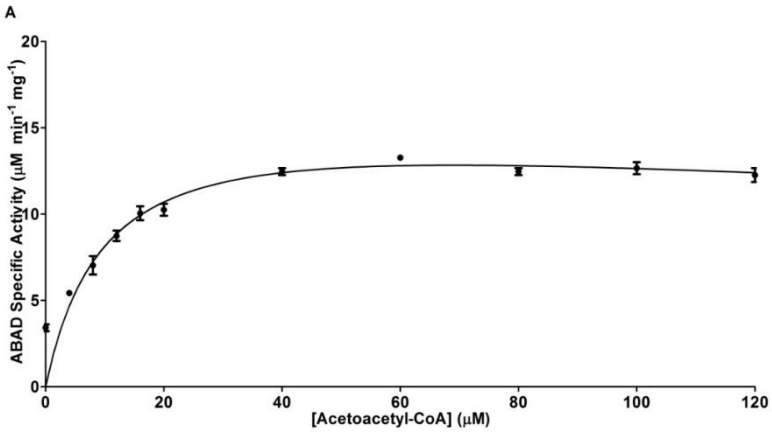

Figure 25. ABAD enzyme activity in the presence of the indicated concentrations of acetoacetyl-CoA. A V_{max} value of 10.64 ± 0.42 µM min^{-1} mg^{-1} and a K_m value of 11.79 ± 1.86 µM were calculated with respect to acetoacetyl-CoA. Values shown are an average of two independent experiments each with two technical repeats ± SEM.

A V_{max} value of 15.54 ± 0.95 µmol min^{-1} mg^{-1} and a K_m value of 99.84 ± 21.34 µM were calculated with respect to NADH (Fig. 26). A cofactor concentration of 250 µM NADH was selected for subsequent experiments.

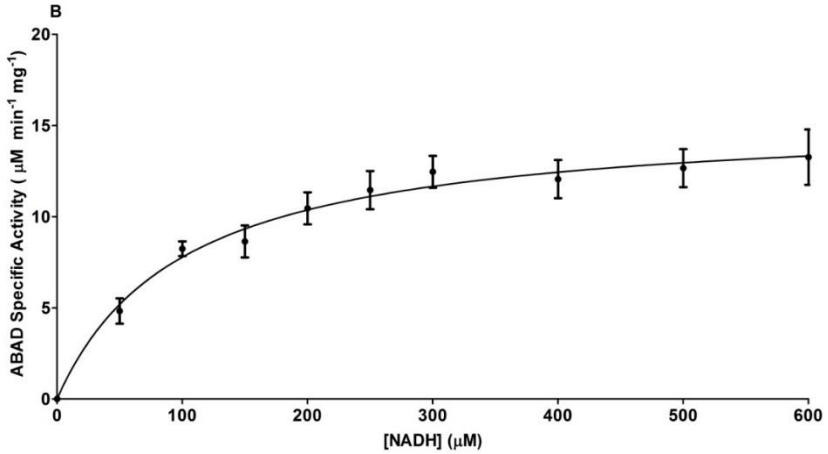

Figure 26. ABAD enzyme activity in the presence of the indicated concentrations of NADH. A V_{max} value of 15.54 ± 0.95 µmol min^{-1} mg^{-1} and a K_m value of 99.84 ± 21.34 µM were calculated with respect to NADH. Values shown are an average of two independent experiments each with two technical repeats ± SEM.

4.3.1.2 Compound screening

Activity assay conditions consisted of ABAD enzyme (0.5 µg/mL), NADH (250 µM), acetoacetyl-CoA (120 µM) and a single compound of interest (25 µM, 1% DMSO (v/v)). Solutions were prepared in assay buffer (10 mM HEPES buffer, 0.5% (w/v)), pH 7.4 at 37°C). Each compound was weighted in milligrams with maximal 0.1 mg deviation to prepare a 10 mM stock solution in DMSO. The DMSO stock solution was further diluted by 10 mM HEPES buffer solution to give a final assay concentration 25 µM 1% DMSO (v/v). Control solutions containing an equivalent concentration of DMSO (1% (v/v)) were also prepared and run concurrently. Reaction progression was measured via a decrease in NADH absorbance at 340 nm using a SpectraMAX M2e spectrophotometer. The reaction period was gated to yield steady state conditions ($R^2 > 0.9$). Calculated IC_{50} values are an average of two independent experiments, each with three technical repeats.

4.3.2 ElogP and ElogD experimental determination

(performed at University of Hradec Kralove, assoc. prof. Kamil Musílek group)

The method of measurement and calculation of ElogP was adapted from Technical guide OECD No. 117 [119]. Based on this method, the ElogD was determined accordingly. All chemicals were purchased from Sigma-Aldrich (St. Louis, MO, USA). Seven standard stock solutions were prepared by dissolving nitrobenzene (ReagentPlus, 99%), chlorobenzene (puriss. p.a., ACS reagent, ≥99.5%), thymol (≥99.0%), biphenyl (ReagentPlus, 99.5%), butylbenzene (≥99%), fluoranthene (98%) and 4,4'-DDT (98%) in HPLC grade methanol and stored in the refrigerator at temperature of 4 °C. Mixed standard solution was prepared prior analysis by adding each of the stock standard solutions (100 µL) to 1.5 ml glass vial and addition of HPLC grade methanol (300 µL). Standard solution for dead time measurement was prepared by dissolving of citric acid (1 mg) in 70% solution of HPLC grade methanol and 30% distilled water (1 mL). The TRIS-HCl buffer for mobile phase was prepared from 0.05 M tris(hydroxymethyl)aminomethane solution by adjusting with 1 M HCl to pH 7.4. The pH measurement was carried out by a multimeter inoLab Multi 9430 IDS (WTW, Weilheim, DEU) with an attached electrode SenTix Mic (WTW, Weilheim, DEU), DuraCal pH buffers (Hamilton, Bonduz, CHE) were used for calibration of pH electrode. All used water was prepared by an Ultrapore Simplicity Water Purification System type 1 (Merck Millipore, Billerica, MA, USA).

The synthesized sample (1 mg) was dissolved in solution of 70% HPLC grade methanol and 30% distilled water (1 mL). Sample solutions were centrifuged by Eppendorf Centrifuge 5418 (Eppendorf, Hamburg, Germany) for 10 minutes at 14000 revolutions per minute and 0.9 mL of centrifuged supernatants was transferred to 1.5 mL glass vials. The analysis was performed by HPLC system Infinity 1260 (Agilent Technologies, Santa Clara, CA, USA) with Infinity 1290 auto sampler (G4226A), Infinity 1260 Quaternary LC pump (G1311B), Infinity 1260 Thermostatted Column Compartment (G1316A), and Infinity 1260 Diode-Array Detector (G4212B). Used LC column was Kinetex® 5 µm C18 100 Å, 100 x 4.6 mm (Phenomenex, Torrance, CA, USA) with an attached SecurityGuard™ system for C18 HPLC column (Phenomenex, Torrance, CA, USA). Duration of the analysis was set to 60 min in a flow rate of mobile phases 1 mL/min and at a temperature of 20°C within the column. Dosage of sample and standard solution from autosampler was set to 10 µL. There was isocratic flow of mobile phases with 70% HPLC grade methanol and 30% distilled water for ElogP measurement and 70% HPLC grade methanol and 30% 0.05 M TRIS-HCl buffer with pH 7.4 for ElogD measurement respectively. Both, analyses of standard solution and sample solutions were performed in triplicate.

The capacity factors (Eq. 2) were calculated from retention times of samples or standards:

$$k = \frac{t_r - t_0}{t_0} \qquad \text{(Eq. 2)}$$

k = capacity factor; t_0 = dead time (retention time of citric acid); t_r = retention time of sample

The ElogP values were calculated (Eq. 3). Linear regression coefficients were obtained from linear regression of ElogP of standard solutions against the log of their capacity factors. The ElogD values were calculated from measurement with 0.05 M Tris-HCl buffer (pH 7.4) as mobile phase B, using the same standard solutions and equations.

$$\text{Elog}\, P = a + b \times \log k \qquad \text{(Eq. 3)}$$

P = octanol/water partition coefficient; a, b = linear regression coefficients; k = capacity factor

4.3.3 Inhibition of monoamine oxidase

(performed at University of St Andrews, prof. Rona R. Ramsay group)

The activity for membrane-bound MAO (Sigma-Aldrich, UK) was determined from the production of hydrogen peroxide, coupled to a dye [Ampliflu Red (Sigma-Aldrich, UK) at a final concentration of 50 µM] *via* horseradish peroxidase (2.5 U/mL) producing the fluorescent resorufin that was measured in a fluorescence plate-reader (Molecular Devices FilterMax F5) at 30°C [120–122]. Under the conditions used, the K_m for tyramine with MAO A was 0.4 mM and for MAO B was 0.16 mM.

The compounds were screened for quenching of the fluorescence of the product, resorufin, by addition of 50 µM compound to 1 and 10 µM resorufin; no quenching was observed. The compounds were also examined for inhibition of HRP used in the assay. Inhibition of horseradish peroxidase (0.025 U/mL) by 50 µM compound was measured in triplicate using H_2O_2 at a concentration of 2×K_m (4 µM since K_m=2.0 ± 0.5 µM) and Ampliflu Red at 200 µM. Inhibition was significant especially for **4b** (Table 18), so the concentration of HRP in the MAO assay was increased to 2.5 U/mL.

Table 18. Inhibition of horseradish peroxidase (0.025 U/mL) by 50 µM compound (displayed as % inhibition).

Compound	% inhibition of HRP
110	33.8
111	47.3
112	25.3
114	6.03
115	27.1
116	17.6

Having adjusted the conditions to minimize artefacts, the IC_{50} values for membrane-bound MAO A and B were determined without and with pre-incubation with the compound (>10 concentrations in duplicate) for 30 min. IC_{50} values were determined from the rates with varied inhibitor concentrations in the presence of $2\times K_m$ substrate concentration with the enzyme added last for time 0, or with the substrate and dye mix added last after pre-incubation of enzyme and inhibitor for 30 min. IC_{50} values after 30 min pre-incubation lower than without pre-incubation would indicate slow binding or inactivation. Data are expressed as a value ± standard deviation, obtained by fitting the data (usually for 10 concentrations in triplicate) to the appropriate three-parameter equation using GraphPad PRISM 4. At least two separate determinations were made for each value reported. Apparent K_i values were derived from a Dixon plot when the enzyme is not pre-incubated with the inhibitor.

4.3.4 Inhibition of cholinesterases

(performed at University of Defence, assoc. prof. Daniel Jun group)

The acetylcholinesterase (AChE; EC 3.1.1.7) and butyrylcholinesterase (BChE; EC 3.1.1.8) inhibitory activity of the tested drugs was determined using modified Ellman´s method [123] and is expressed as IC_{50}, i.e. concentration that reduces the cholinesterase activity by 50%. Human recombinant AChE, human plasma BChE, 5,5´-dithiobis(2-nitrobenzoic acid) (Ellman´s reagent, DTNB), phosphate buffer (PB), acetylthiocholine iodide (ATCI), and butyrylthiocholine iodide (BTCI), were purchased from Sigma-Aldrich. Cholinestrase activity was measured in polystyrene Nunc 96-well microplates with flat bottom shape (ThermoFisher Scientific, USA). All the assays were carried out in PB (0.1 M KH_2PO_4/K_2HPO_4, pH 7.4). Enzyme solutions were prepared in 2 mL aliquots with activity 2.0 U/mL. The assay medium (100 µL) consisted of 40 µL of 0.1 M PB, 20 µL of 0.01 M

DTNB, 10 µL of enzyme, and 20 µL of 0.01 M substrate (ATCI for AChE, BTCI for BChE). Assay solutions with inhibitor (concentration range 10^{-3} – 10^{-9} M) were preincubated for 5 min. The reaction was started by immediate addition of 20 µL of substrate. The activity was determined by measuring the increase in absorbance at 412 nm at 37°C at 2 min intervals using a Multi-mode microplate reader Synergy 2 (Vermont, USA). Each concentration was assayed in triplicate. Software GraphPad Prism 5 (San Diego, USA) was used for the statistical data evaluation.

4.3.5 Antioxidant activity

(performed at University of Defence, assoc. prof. Daniel Jun group)

The DPPH (diphenyl-1-picrylhydrazyl stabile free radical) test is a simple method to determine the antioxidant activity, which is expressed as EC_{50}, i.e. concentration of the substrate causing 50% loss of the DPPH activity. DPPH, methanol, N-acetylcystein and trolox (last two as the refence standards), were purchased from Sigma-Aldrich. For measuring purposes – polystyrene Nunc 96-well microplates with flat bottom shape (ThermoFisher Scientific, USA) were utilized. All the assays were carried out in methanol. DPPH solution was prepared at 0.2 mM concentration. The assay medium (200 µL) consisted of 100 µL DPPH solution, 100 µL of assay solutions with inhibitor (10^{-3} – 10^{-6} M). The reaction time was 30 min. The activity was determined by measuring the increase in absorbance at 517 nm at laboratory temperature using a Multi-mode microplate reader Synergy 2 (Vermont, USA). Each concentration was assayed in triplicate. Software GraphPad Prism 5 (San Diego, USA) was used for the statistical data evaluation [124, 125].

4.3.6 Cell viability

4.3.6.1 Combined MTT and LDH assay

(performed at University Hospital Hradec Králové, dr. Ondřej Soukup group)

The effect of compounds on the cell viability was examined using methodology combining LDH and MTT assay into one experimental setup. Such an assay has been chosen due to the fact, that widely used MTT test is partially dependent on the mitochondrial oxidoreductases [126], whose activity might be influenced by the tested compounds targeted to mitochondria. The protocol for this assay has been described previously [127]. Briefly CHO cell line (Chinese hamster ovary, CHO-K1WT2, CRL-1984 ECACC, Salisbury, UK) were cultured according to ECACC recommended conditions and seeded in a density of 8 000 cells per well as was described earlier [128]. Tested compounds were dissolved in DMSO and subsequently in the growth medium (F-12) supplemented with 1%

PEN/STREP without FBS so that the final concentration of DMSO did not exceed 0.5% (v/v). Cells were exposed to a tested compound in the medium (100 µL) for 24 hours. Then 10 µL of MTT (2.5 mg/mL) was added and 50 µL of the culture supernatant was transferred to a new plate yet containing 50 µL of LDH substrate mixture consisting of lactate (2.5 mg/mL), NAD (2.5 mg/mL), phenazine methansulphate (100 µM) and Triton X-100 (0.1%) in Tris–HCl buffer (pH 8.2). LDH reaction mixture was incubated at 37 °C for 15-30 min until the difference between negative (no treatment) and positive control (0.1% Triton X-100) was obvious. Cellular fraction containing MTT was allowed to produce formazan for another approximately 3 h at 37 °C. Thereafter, medium with MTT was removed and crystals of formazan were dissolved in DMSO (100 µL). Absorbance was measured at 570 nm with 650 nm reference wavelength on Synergy HT reader (BioTek, USA) for both LDH and MTT fraction. IC_{50} was then calculated from the control - subtracted triplicates using non-linear regression (four parameters) of GraphPad Prism 5 software. Final IC_{50} and SEM value was obtained as a mean of at least 3 independent measurements.

4.3.6.2 LDH assay

(performed at University of St Andrews, prof. Frank Gunn-Moore group)

HEK293 and SHSY5Y cells were seeded into clear 96 well plates at a density of 10 000 cells per well and incubated for 24h at 37 °C and 5% CO_2. Following incubation, culture media was gently aspirated and replaced with fresh media containing a titration of selected compounds (10 µM – 100 µM), an appropriate volume of DMSO was added to additional wells as a vehicle control. The plates were incubated for a further 24 h at 37 °C and 5% CO_2. Following incubation 0.1% Triton-X 100 was added to three additional control wells as a positive control and incubated for 15 minutes. A measure of cell death was then made using a Sigma Aldrich lactate dehydrogenase kit (#MAK066) as per manufacturer's instructions. The reported values are an average of three independent experiments each with three technical repeats ± SEM (Figure 8).

4.3.7 Hepatotoxicity

(performed at University of Defence, assoc. prof. Daniel Jun group)

The hepatotoxicity of tested compounds was evaluated using the cell line HepG2 originally from human liver hepatocellular carcinoma (ATCC, Virginia USA). These cells were plated in 96-well plate at density 17×10^3 per well in Dulbecco's Modified Eagle's Medium (DMEM) (Gibco, USA) with 10% FBS (Gibco, USA) and was leaf attached overnight. The incubation was performed under condition 37°C, 5% CO_2 and 80 – 95% air humidity. Stock solutions of tested compounds were prepared in dimethyl sulfoxide (DMSO) (Sigma –Aldrich) and then diluted in DMEM medium. The

stock solutions in medium were serially diluted and added to cells in 96-well culture plates. The final concentration of DMSO was less than 0.25%. The cell viability was detected using 3-(4,5-dimethylthiazol-2-yl)-2,5-diphenyltetrazolium bromide (MTT) assay [114] after 24 h incubation with tested compounds. After 24 h was the medium aspirated and 100 µl MTT solution (0.5 mg/mL) in serum free DMEM medium was added to cells. The cells were then incubated for 1 h. The medium was then aspirated and purple crystals of MTT formazan were dissolved in 100 µL DMSO under shaking. The absorbance was measured with a microplate reader (Beckman Coulter, Inc., California USA) at a test wavelength of 570 nm. The IC_{50} value was calculated using four parametric nonlinear regression with statistic software GraphPad Prism (version 5.04 Prism 5 for Windows, GraphPad Software Inc., USA). The data were obtained from three independent experiments. The IC_{50} value was expressed as mean ± SEM.

4.3.8 PAMPA assay

(performed at University Hospital Hradec Králové, dr. Ondřej Soukup group)

Penetration across the BBB is an essential property for compounds targeting the CNS. In order to predict passive blood-brain penetration of novel compounds modification of the parallel artificial membrane permeation assay (PAMPA) has been used based on reported protocol [116]. The filter membrane of the donor plate was coated with PBL (Polar Brain Lipid, Avanti, USA) in dodecane (4 µL of 20 mg/mL PBL in dodecane) and the acceptor well was filled with 300 µL of PBS pH 7.4 buffer (V_D). Tested compound were dissolved first in DMSO and that diluted with PBS pH 7.4 to reach the final concentration 100 µM in the donor well. Concentration of DMSO did not exceed 0.5% (V/V) in the donor solution. 300 µL of the donor solution was added to the donor wells (V_A) and the donor filter plate was carefully put on the acceptor plate so that coated membrane was "in touch" with both donor solution and acceptor buffer. Test compound diffused from the donor well through the lipid membrane (Area = 0.28 cm^2) to the acceptor well. The concentration of the drug in both donor and the acceptor wells was assessed after 3, 4, 5 and 6 hours of incubation in quadruplicate using the UV plate reader Synergy HT (Biotek, USA) at the maximum absorption wavelength of each compound. Concentration of the compounds was calculated from the standard curve and expressed as the permeability (P_e) according the equation [129, 130]:

$$\log P_e = \log \{C \bullet -\ln(1 - \frac{[drug]_{acceptor}}{[drug]_{equilibrium}})\} \text{ where } C = (\frac{V_D \bullet V_A}{(V_D + V_A)\ Area \bullet time})$$

5 References

[1] WHO | Dementia: a public health priority. *WHO* [online]. [2013-05-15]. http://www.who.int/mental_health/publications/dementia_report_2012/en/

[2] SELKOE, D J. Translating cell biology into therapeutic advances in Alzheimer's disease. *Nature*. 1999, vol. 399, no. 6738 Suppl, p. A23-31. ISSN 0028-0836.

[3] ALZHEIMER'S ASSOCIATION. 2015 Alzheimer's disease facts and figures. *Alzheimer's & Dementia: The Journal of the Alzheimer's Association*. 2015, vol. 11, no. 3, p. 332–384. ISSN 1552-5279.

[4] LAUTENSCHLAGER, N. T., L. A. CUPPLES, V. S. RAO, S. A. AUERBACH, R. BECKER, J. BURKE, H. CHUI, R. DUARA, E. J. FOLEY, S. L. GLATT, R. C. GREEN, R. JONES, H. KARLINSKY, W. A. KUKULL, A. KURZ, E. B. LARSON, K. MARTELLI, A. D. SADOVNICK, L. VOLICER, S. C. WARING, J. H. GROWDON a L. A. FARRER. Risk of dementia among relatives of Alzheimer's disease patients in the MIRAGE study: What is in store for the oldest old? *Neurology*. 1996, vol. 46, no. 3, p. 641–650. ISSN 0028-3878.

[5] BERTRAM, Lars a Rudolph E. TANZI. The genetics of Alzheimer's disease. *Progress in Molecular Biology and Translational Science* [online]. 2012, vol. 107, p. 79–100. ISSN 1878-0814. doi:10.1016/B978-0-12-385883-2.00008-4

[6] CORDER, E. H., A. M. SAUNDERS, W. J. STRITTMATTER, D. E. SCHMECHEL, P. C. GASKELL, G. W. SMALL, A. D. ROSES, J. L. HAINES a M. A. PERICAK-VANCE. Gene dose of apolipoprotein E type 4 allele and the risk of Alzheimer's disease in late onset families. *Science (New York, N.Y.)*. 1993, vol. 261, no. 5123, p. 921–923. ISSN 0036-8075.

[7] GREEN, Robert C., L. Adrienne CUPPLES, Alex KURZ, Sanford AUERBACH, Rodney GO, Dessa SADOVNICK, Ranjan DUARA, Walter A. KUKULL, Helena CHUI, Timi EDEKI, Patrick A. GRIFFITH, Robert P. FRIEDLAND, David BACHMAN a Lindsay FARRER. Depression as a risk factor for Alzheimer disease: the MIRAGE Study. *Archives of Neurology* [online]. 2003, vol. 60, no. 5, p. 753–759. ISSN 0003-9942. doi:10.1001/archneur.60.5.753

[8] LAUNER, L. J., K. ANDERSEN, M. E. DEWEY, L. LETENNEUR, A. OTT, L. A. AMADUCCI, C. BRAYNE, J. R. COPELAND, J. F. DARTIGUES, P. KRAGH-SORENSEN, A. LOBO, J. M. MARTINEZ-LAGE, T. STIJNEN a A. HOFMAN. Rates and risk factors for dementia and Alzheimer's disease: results from EURODEM pooled analyses. EURODEM Incidence Research Group and Work Groups. European Studies of Dementia. *Neurology*. 1999, vol. 52, no. 1, p. 78–84. ISSN 0028-3878.

[9] KIVIPELTO, Miia, Tiia NGANDU, Laura FRATIGLIONI, Matti VIITANEN, Ingemar KÅREHOLT, Bengt WINBLAD, Eeva-Liisa HELKALA, Jaakko TUOMILEHTO, Hilkka SOININEN a Aulikki NISSINEN. Obesity and vascular risk factors at midlife and the risk of dementia and Alzheimer disease. *Archives of Neurology* [online]. 2005, vol. 62, no. 10, p. 1556–1560. ISSN 0003-9942. doi:10.1001/archneur.62.10.1556

[10] YAFFE, Kristine. Metabolic syndrome and cognitive decline. *Current Alzheimer Research*. 2007, vol. 4, no. 2, p. 123–126. ISSN 1567-2050.

[11] TSIVGOULIS, G., A. V. ALEXANDROV, V. G. WADLEY, F. W. UNVERZAGT, R. C. P. GO, C. S. MOY, B. KISSELA a G. HOWARD. Association of higher diastolic blood pressure levels with cognitive impairment. *Neurology* [online]. 2009, vol. 73, no. 8, p. 589–595. ISSN 1526-632X. doi:10.1212/WNL.0b013e3181b38969

[12] SOLOMON, Alina, Miia KIVIPELTO, Benjamin WOLOZIN, Jufen ZHOU a Rachel A. WHITMER. Midlife serum cholesterol and increased risk of Alzheimer's and vascular dementia three

decades later. *Dementia and Geriatric Cognitive Disorders* [online]. 2009, vol. 28, no. 1, p. 75–80. ISSN 1421-9824. doi:10.1159/000231980

[13] RUSANEN, Minna, Miia KIVIPELTO, Charles P. QUESENBERRY, Jufen ZHOU a Rachel A. WHITMER. Heavy smoking in midlife and long-term risk of Alzheimer disease and vascular dementia. *Archives of Internal Medicine* [online]. 2011, vol. 171, no. 4, p. 333–339. ISSN 1538-3679. doi:10.1001/archinternmed.2010.393

[14] PRICE, D L a S S SISODIA. Mutant genes in familial Alzheimer's disease and transgenic models. *Annual review of neuroscience* [online]. 1998, vol. 21, p. 479–505. ISSN 0147-006X. doi:10.1146/annurev.neuro.21.1.479

[15] REDDY, P Hemachandra, Geethalakshmi MANI, Byung S PARK, Joline JACQUES, Geoffrey MURDOCH, William WHETSELL Jr, Jeffrey KAYE a Maria MANCZAK. Differential loss of synaptic proteins in Alzheimer's disease: implications for synaptic dysfunction. *Journal of Alzheimer's disease: JAD*. 2005, vol. 7, no. 2, p. 103-117-180. ISSN 1387-2877.

[16] GOLDE, Todd E. Inflammation takes on Alzheimer disease. *Nature medicine* [online]. 2002, vol. 8, no. 9, p. 936–938. ISSN 1078-8956. doi:10.1038/nm0902-936

[17] REDDY, P Hemachandra a M Flint BEAL. Are mitochondria critical in the pathogenesis of Alzheimer's disease? *Brain research. Brain research reviews* [online]. 2005, vol. 49, no. 3, p. 618–632. doi:10.1016/j.brainresrev.2005.03.004

[18] PERRY, E. K., B. E. TOMLINSON, G. BLESSED, K. BERGMANN, P. H. GIBSON a R. H. PERRY. Correlation of cholinergic abnormalities with senile plaques and mental test scores in senile dementia. *British Medical Journal*. 1978, vol. 2, no. 6150, p. 1457–1459. ISSN 0007-1447.

[19] BARTUS, R. T., R. L. DEAN, B. BEER a A. S. LIPPA. The cholinergic hypothesis of geriatric memory dysfunction. *Science (New York, N.Y.)*. 1982, vol. 217, no. 4558, p. 408–414. ISSN 0036-8075.

[20] TERRY, A. V. a J. J. BUCCAFUSCO. The cholinergic hypothesis of age and Alzheimer's disease-related cognitive deficits: recent challenges and their implications for novel drug development. *The Journal of Pharmacology and Experimental Therapeutics* [online]. 2003, vol. 306, no. 3, p. 821–827. ISSN 0022-3565. doi:10.1124/jpet.102.041616

[21] TAKEDA, A., E. LOVEMAN, A. CLEGG, J. KIRBY, J. PICOT, E. PAYNE a C. GREEN. A systematic review of the clinical effectiveness of donepezil, rivastigmine and galantamine on cognition, quality of life and adverse events in Alzheimer's disease. *International Journal of Geriatric Psychiatry* [online]. 2006, vol. 21, no. 1, p. 17–28. ISSN 0885-6230. doi:10.1002/gps.1402

[22] LAFERLA, Frank M, Kim N GREEN a Salvatore ODDO. Intracellular amyloid-beta in Alzheimer's disease. *Nature reviews. Neuroscience* [online]. 2007, vol. 8, no. 7, p. 499–509. ISSN 1471-003X. doi:10.1038/nrn2168

[23] BAYER, Thomas A a Oliver WIRTHS. Intracellular accumulation of amyloid-Beta - a predictor for synaptic dysfunction and neuron loss in Alzheimer's disease. *Frontiers in aging neuroscience* [online]. 2010, vol. 2, p. 8. ISSN 1663-4365. doi:10.3389/fnagi.2010.00008

[24] HARDY, J A a G A HIGGINS. Alzheimer's disease: the amyloid cascade hypothesis. *Science (New York, N.Y.)*. 1992, vol. 256, no. 5054, p. 184–185. ISSN 0036-8075.

[25] DAHLGREN, Karie N, Arlene M MANELLI, W Blaine STINE Jr, Lorinda K BAKER, Grant A KRAFFT a Mary Jo LADU. Oligomeric and fibrillar species of amyloid-beta peptides differentially affect neuronal viability. *The Journal of biological chemistry* [online]. 2002, vol. 277, no. 35, p. 32046–32053. ISSN 0021-9258. doi:10.1074/jbc.M201750200

[26] GOURAS, G K, J TSAI, J NASLUND, B VINCENT, M EDGAR, F CHECLER, J P GREENFIELD, V HAROUTUNIAN, J D BUXBAUM, H XU, P GREENGARD a N R RELKIN. Intraneuronal Abeta42 accumulation in human brain. *The American journal of pathology*. 2000, vol. 156, no. 1, p. 15–20. ISSN 0002-9440.

[27] WIRTHS, Oliver, Gerd MULTHAUP a Thomas A BAYER. A modified beta-amyloid hypothesis: intraneuronal accumulation of the beta-amyloid peptide--the first step of a fatal cascade. *Journal of neurochemistry* [online]. 2004, vol. 91, no. 3, p. 513–520. ISSN 0022-3042. doi:10.1111/j.1471-4159.2004.02737.x

[28] BARAGE, Sagar H. a Kailas D. SONAWANE. Amyloid cascade hypothesis: Pathogenesis and therapeutic strategies in Alzheimer's disease. *Neuropeptides* [online]. 2015, vol. 52, p. 1–18. ISSN 1532-2785. doi:10.1016/j.npep.2015.06.008

[29] HAASS, Christian a Dennis J. SELKOE. Soluble protein oligomers in neurodegeneration: lessons from the Alzheimer's amyloid beta-peptide. *Nature Reviews. Molecular Cell Biology* [online]. 2007, vol. 8, no. 2, p. 101–112. ISSN 1471-0072. doi:10.1038/nrm2101

[30] TILLEMENT, Laurent, Laurent LECANU a Vassilios PAPADOPOULOS. Alzheimer's disease: effects of β-amyloid on mitochondria. *Mitochondrion* [online]. 2011, vol. 11, no. 1, p. 13–21. ISSN 1872-8278. doi:10.1016/j.mito.2010.08.009

[31] BORGER, Eva, Laura AITKEN, Kirsty E A MUIRHEAD, Zoe E ALLEN, James A AINGE, Stuart J CONWAY a Frank J GUNN-MOORE. Mitochondrial β-amyloid in Alzheimer's disease. *Biochemical Society Transactions* [online]. 2011, vol. 39, no. 4, p. 868–873. ISSN 1470-8752. doi:10.1042/BST0390868

[32] ECKERT, Anne, Karen SCHMITT a Jürgen GÖTZ. Mitochondrial dysfunction - the beginning of the end in Alzheimer's disease? Separate and synergistic modes of tau and amyloid-β toxicity. *Alzheimer's research & therapy* [online]. 2011, vol. 3, no. 2, p. 15. ISSN 1758-9193. doi:10.1186/alzrt74

[33] HANSSON PETERSEN, Camilla A, Nyosha ALIKHANI, Homira BEHBAHANI, Birgitta WIEHAGER, Pavel F PAVLOV, Irina ALAFUZOFF, Ville LEINONEN, Akira ITO, Bengt WINBLAD, Elzbieta GLASER a Maria ANKARCRONA. The amyloid beta-peptide is imported into mitochondria via the TOM import machinery and localized to mitochondrial cristae. *Proceedings of the National Academy of Sciences of the United States of America* [online]. 2008, vol. 105, no. 35, p. 13145–13150. ISSN 1091-6490. doi:10.1073/pnas.0806192105

[34] MUIRHEAD, Kirsty E A, Eva BORGER, Laura AITKEN, Stuart J CONWAY a Frank J GUNN-MOORE. The consequences of mitochondrial amyloid beta-peptide in Alzheimer's disease. *The Biochemical Journal* [online]. 2010, vol. 426, no. 3, p. 255–270. ISSN 1470-8728. doi:10.1042/BJ20091941

[35] PINHO, Catarina Moreira, Pedro Filipe TEIXEIRA a Elzbieta GLASER. Mitochondrial import and degradation of amyloid-β peptide. *Biochimica et biophysica acta* [online]. 2014. ISSN 0006-3002. doi:10.1016/j.bbabio.2014.02.007

[36] BENEK, Ondrej, Laura AITKEN, Lukas HROCH, Kamil KUCA, Frank GUNN-MOORE a Kamil MUSILEK. A Direct interaction between mitochondrial proteins and amyloid-β peptide and its significance for the progression and treatment of Alzheimer`s disease. *Current Medicinal Chemistry*. 2015. ISSN 1875-533X.

[37] YAN, S D, J FU, C SOTO, X CHEN, H ZHU, F AL-MOHANNA, K COLLISON, A ZHU, E STERN, T SAIDO, M TOHYAMA, S OGAWA, A ROHER a D STERN. An intracellular protein that binds amyloid-beta peptide and mediates neurotoxicity in Alzheimer's disease. *Nature* [online]. 1997, vol. 389, no. 6652, p. 689–695. ISSN 0028-0836. doi:10.1038/39522

[38] HE, X Y, H SCHULZ a S Y YANG. A human brain L-3-hydroxyacyl-coenzyme A dehydrogenase is identical to an amyloid beta-peptide-binding protein involved in Alzheimer's disease. *The Journal of biological chemistry*. 1998, vol. 273, no. 17, p. 10741–10746. ISSN 0021-9258.

[39] HE, X Y, G MERZ, Y Z YANG, P MEHTA, H SCHULZ a S Y YANG. Characterization and localization of human type10 17beta-hydroxysteroid dehydrogenase. *European journal of biochemistry / FEBS*. 2001, vol. 268, no. 18, p. 4899–4907. ISSN 0014-2956.

[40] HE, X Y, Y Z YANG, H SCHULZ a S Y YANG. Intrinsic alcohol dehydrogenase and hydroxysteroid dehydrogenase activities of human mitochondrial short-chain L-3-hydroxyacyl-CoA dehydrogenase. *The Biochemical journal*. 2000, vol. 345 Pt 1, p. 139–143. ISSN 0264-6021.

[41] FURUTA, S, A KOBAYASHI, S MIYAZAWA a T HASHIMOTO. Cloning and expression of cDNA for a newly identified isozyme of bovine liver 3-hydroxyacyl-CoA dehydrogenase and its import into mitochondria. *Biochimica et biophysica acta*. 1997, vol. 1350, no. 3, p. 317–324. ISSN 0006-3002.

[42] OFMAN, Rob, Jos P N RUITER, Marike FEENSTRA, Marinus DURAN, Bwee Tien POLL-THE, Johannes ZSCHOCKE, Regina ENSENAUER, Willy LEHNERT, Jörn Oliver SASS, Wolfgang SPERL a Ronald J A WANDERS. 2-Methyl-3-hydroxybutyryl-CoA dehydrogenase deficiency is caused by mutations in the HADH2 gene. *American journal of human genetics*. 2003, vol. 72, no. 5, p. 1300–1307. ISSN 0002-9297.

[43] HE, X Y, G MERZ, P MEHTA, H SCHULZ a S Y YANG. Human brain short chain L-3-hydroxyacyl coenzyme A dehydrogenase is a single-domain multifunctional enzyme. Characterization of a novel 17beta-hydroxysteroid dehydrogenase. *The Journal of biological chemistry*. 1999, vol. 274, no. 21, p. 15014–15019. ISSN 0021-9258.

[44] POWELL, A J, J A READ, M J BANFIELD, F GUNN-MOORE, S D YAN, J LUSTBADER, A R STERN, D M STERN a R L BRADY. Recognition of structurally diverse substrates by type II 3-hydroxyacyl-CoA dehydrogenase (HADH II)/amyloid-beta binding alcohol dehydrogenase (ABAD). *Journal of molecular biology* [online]. 2000, vol. 303, no. 2, p. 311–327. ISSN 0022-2836. doi:10.1006/jmbi.2000.4139

[45] HE, Xue-Ying, Jerzy WEGIEL, Ying-Zi YANG, Raju PULLARKAT, Horst SCHULZ a Song-Yu YANG. Type 10 17beta-hydroxysteroid dehydrogenase catalyzing the oxidation of steroid modulators of gamma-aminobutyric acid type A receptors. *Molecular and cellular endocrinology* [online]. 2005, vol. 229, no. 1–2, p. 111–117. ISSN 0303-7207. doi:10.1016/j.mce.2004.08.011

[46] HOLZMANN, Johann, Peter FRANK, Esther LÖFFLER, Keiryn L BENNETT, Christopher GERNER a Walter ROSSMANITH. RNase P without RNA: identification and functional reconstitution of the human mitochondrial tRNA processing enzyme. *Cell* [online]. 2008, vol. 135, no. 3, p. 462–474. ISSN 1097-4172. doi:10.1016/j.cell.2008.09.013

[47] YANG, Song-Yu, Xue-Ying HE a David MILLER. Hydroxysteroid (17β) dehydrogenase X in human health and disease. *Molecular and cellular endocrinology* [online]. 2011, vol. 343, no. 1–2, p. 1–6. ISSN 1872-8057. doi:10.1016/j.mce.2011.06.011

[48] BOYNTON, Tye O'Hara a Lawrence Joseph SHIMKETS. Myxococcus CsgA, Drosophila Sniffer, and human HSD10 are cardiolipin phospholipases. *Genes & Development* [online]. 2015, vol. 29, no. 18, p. 1903–1914. ISSN 1549-5477. doi:10.1101/gad.268482.115

[49] KISSINGER, Charles R, Paul A REJTO, Laura A PELLETIER, James A THOMSON, Richard E SHOWALTER, Melwyn A ABREO, Charles S AGREE, Stephen MARGOSIAK, Jerry J MENG, Robert M AUST, Darin VANDERPOOL, Bin LI, Anna TEMPCZYK-RUSSELL a J Ernest VILLAFRANCA. Crystal structure of human ABAD/HSD10 with a bound inhibitor: implications

for design of Alzheimer's disease therapeutics. *Journal of molecular biology* [online]. 2004, vol. 342, no. 3, p. 943–952. ISSN 0022-2836. doi:10.1016/j.jmb.2004.07.071

[50] LUSTBADER, Joyce W, Maurizio CIRILLI, Chang LIN, Hong Wei XU, Kazuhiro TAKUMA, Ning WANG, Casper CASPERSEN, Xi CHEN, Susan POLLAK, Michael CHANEY, Fabrizio TRINCHESE, Shumin LIU, Frank GUNN-MOORE, Lih-Fen LUE, Douglas G WALKER, Periannan KUPPUSAMY, Zay L ZEWIER, Ottavio ARANCIO, David STERN, Shirley ShiDu YAN a Hao WU. ABAD directly links Abeta to mitochondrial toxicity in Alzheimer's disease. *Science (New York, N.Y.)* [online]. 2004, vol. 304, no. 5669, p. 448–452. ISSN 1095-9203. doi:10.1126/science.1091230

[51] XIE, Yuli, Shixian DENG, Zhenzhang CHEN, Shidu YAN a Donald W LANDRY. Identification of small-molecule inhibitors of the Abeta-ABAD interaction. *Bioorganic & medicinal chemistry letters* [online]. 2006, vol. 16, no. 17, p. 4657–4660. ISSN 0960-894X. doi:10.1016/j.bmcl.2006.05.099

[52] YAN, Yilin, Yangzhong LIU, Mirco SORCI, Georges BELFORT, Joyce W LUSTBADER, Shirley ShiDu YAN a Chunyu WANG. Surface plasmon resonance and nuclear magnetic resonance studies of ABAD-Abeta interaction. *Biochemistry* [online]. 2007, vol. 46, no. 7, p. 1724–1731. ISSN 0006-2960. doi:10.1021/bi061314n

[53] YAN, S D, Y SHI, A ZHU, J FU, H ZHU, Y ZHU, L GIBSON, E STERN, K COLLISON, F AL-MOHANNA, S OGAWA, A ROHER, S G CLARKE a D M STERN. Role of ERAB/L-3-hydroxyacyl-coenzyme A dehydrogenase type II activity in Abeta-induced cytotoxicity. *The Journal of biological chemistry*. 1999, vol. 274, no. 4, p. 2145–2156. ISSN 0021-9258.

[54] HE, Xue Ying, Guang Yeong WEN, George MERZ, Dawei LIN, Ying Zi YANG, Penkaj MEHTA, Horst SCHULZ a Song Yu YANG. Abundant type 10 17 beta-hydroxysteroid dehydrogenase in the hippocampus of mouse Alzheimer's disease model. *Brain research. Molecular brain research*. 2002, vol. 99, no. 1, p. 46–53. ISSN 0169-328X.

[55] YAO, Jia, Ronald W IRWIN, Liqin ZHAO, Jon NILSEN, Ryan T HAMILTON a Roberta Diaz BRINTON. Mitochondrial bioenergetic deficit precedes Alzheimer's pathology in female mouse model of Alzheimer's disease. *Proceedings of the National Academy of Sciences of the United States of America* [online]. 2009, vol. 106, no. 34, p. 14670–14675. ISSN 1091-6490. doi:10.1073/pnas.0903563106

[56] SAYRE, L M, D A ZELASKO, P L HARRIS, G PERRY, R G SALOMON a M A SMITH. 4-Hydroxynonenal-derived advanced lipid peroxidation end products are increased in Alzheimer's disease. *Journal of neurochemistry*. 1997, vol. 68, no. 5, p. 2092–2097. ISSN 0022-3042.

[57] MURAKAMI, Yayoi, Ikuroh OHSAWA, Tadashi KASAHARA a Shigeo OHTA. Cytoprotective role of mitochondrial amyloid beta peptide-binding alcohol dehydrogenase against a cytotoxic aldehyde. *Neurobiology of aging* [online]. 2009, vol. 30, no. 2, p. 325–329. ISSN 1558-1497. doi:10.1016/j.neurobiolaging.2007.07.002

[58] DYE, Richelin V, Karen J MILLER, Elyse J SINGER a Andrew J LEVINE. Hormone replacement therapy and risk for neurodegenerative diseases. *International journal of Alzheimer's disease* [online]. 2012, vol. 2012, p. 258454. ISSN 2090-0252. doi:10.1155/2012/258454

[59] REN, Yimin, Hong Wei XU, Fleur DAVEY, Margaret TAYLOR, Jim AITON, Peter COOTE, Fang FANG, Jun YAO, Doris CHEN, John Xi CHEN, Shi Du YAN a Frank J GUNN-MOORE. Endophilin I expression is increased in the brains of Alzheimer disease patients. *The Journal of biological chemistry* [online]. 2008, vol. 283, no. 9, p. 5685–5691. ISSN 0021-9258. doi:10.1074/jbc.M707932200

[60] RAMJAUN, A R, A ANGERS, V LEGENDRE-GUILLEMIN, X K TONG a P S MCPHERSON. Endophilin regulates JNK activation through its interaction with the germinal center kinase-

like kinase. *The Journal of biological chemistry* [online]. 2001, vol. 276, no. 31, p. 28913–28919. ISSN 0021-9258. doi:10.1074/jbc.M103198200

[61] YANG, Xin, Yu YANG, Jiang WU a Jie ZHU. Stable expression of a novel fusion peptide of thioredoxin-1 and ABAD-inhibiting peptide protects PC12 cells from intracellular amyloid-beta. *Journal of molecular neuroscience: MN*. 2007, vol. 33, no. 2, p. 180–188. ISSN 0895-8696.

[62] YAO, Jun, Heng DU, Shiqiang YAN, Fang FANG, Chaodong WANG, Lih-Fen LUE, Lan GUO, Doris CHEN, David M. STERN, Frank J. GUNN-MOORE, John Xi CHEN, Ottavio ARANCIO a Shirley ShiDu YAN. Inhibition of Amyloid-beta (A beta) Peptide-Binding Alcohol Dehydrogenase-A beta Interaction Reduces A beta Accumulation and Improves Mitochondrial Function in a Mouse Model of Alzheimer's Disease. *Journal of Neuroscience* [online]. 2011, vol. 31, no. 6, p. 2313–2320. ISSN 0270-6474. doi:10.1523/JNEUROSCI.4717-10.2011

[63] LIM, Yun-An, Amandine GRIMM, Maria GIESE, Ayikoe Guy MENSAH-NYAGAN, J Ernest VILLAFRANCA, Lars M ITTNER, Anne ECKERT a Jürgen GÖTZ. Inhibition of the mitochondrial enzyme ABAD restores the amyloid-β-mediated deregulation of estradiol. *PloS one* [online]. 2011, vol. 6, no. 12, p. e28887. ISSN 1932-6203. doi:10.1371/journal.pone.0028887

[64] AYAN, Diana, René MALTAIS a Donald POIRIER. Identification of a 17β-hydroxysteroid dehydrogenase type 10 steroidal inhibitor: a tool to investigate the role of type 10 in Alzheimer's disease and prostate cancer. *ChemMedChem* [online]. 2012, vol. 7, no. 7, p. 1181–1184. ISSN 1860-7187. doi:10.1002/cmdc.201200129

[65] VALASANI, Koteswara R., Qinru SUN, Gang HU, Jianping LI, Fang DU, Yaopeng GUO, Emily A. CARLSON, Xueqi GAN a Shirley S. YAN. Identification of Human ABAD Inhibitors for Rescuing A beta-Mediated Mitochondrial Dysfunction. *Current Alzheimer Research* [online]. 2014, vol. 11, no. 2, p. 128–136. ISSN 1567-2050. doi:10.2174/1567205011666140130150108

[66] HE, X.-Y. a S.-Y. YANG. Roles of type 10 17beta-hydroxysteroid dehydrogenase in intracrinology and metabolism of isoleucine and fatty acids. *Endocrine, Metabolic & Immune Disorders Drug Targets*. 2006, vol. 6, no. 1, p. 95–102. ISSN 1871-5303.

[67] LEÓN, Rafael, Antonio G. GARCIA a José MARCO-CONTELLES. Recent advances in the multitarget-directed ligands approach for the treatment of Alzheimer's disease. *Medicinal Research Reviews* [online]. 2013, vol. 33, no. 1, p. 139–189. ISSN 1098-1128. doi:10.1002/med.20248

[68] CAVALLI, Andrea, Maria Laura BOLOGNESI, Anna MINARINI, Michela ROSINI, Vincenzo TUMIATTI, Maurizio RECANATINI a Carlo MELCHIORRE. Multi-target-directed ligands to combat neurodegenerative diseases. *Journal of Medicinal Chemistry* [online]. 2008, vol. 51, no. 3, p. 347–372. ISSN 0022-2623. doi:10.1021/jm7009364

[69] BAUTISTA-AGUILERA, Oscar M., Gerard ESTEBAN, Irene BOLEA, Katarina NIKOLIC, Danica AGBABA, Ignacio MORALEDA, Isabel IRIEPA, Abdelouahid SAMADI, Elena SORIANO, Mercedes UNZETA a José MARCO-CONTELLES. Design, synthesis, pharmacological evaluation, QSAR analysis, molecular modeling and ADMET of novel donepezil-indolyl hybrids as multipotent cholinesterase/monoamine oxidase inhibitors for the potential treatment of Alzheimer's disease. *European Journal of Medicinal Chemistry* [online]. 2014, vol. 75, p. 82–95. ISSN 1768-3254. doi:10.1016/j.ejmech.2013.12.028

[70] RAMSAY, Rona R. Monoamine oxidases: the biochemistry of the proteins as targets in medicinal chemistry and drug discovery. *Current topics in medicinal chemistry*. 2012, vol. 12, no. 20, p. 2189–2209. ISSN 1873-4294.

[71] RIEDERER, Peter, Walter DANIELCZYK a Edna GRÜNBLATT. Monoamine oxidase-B inhibition in Alzheimer's disease. *Neurotoxicology* [online]. 2004, vol. 25, no. 1–2, p. 271–277. ISSN 0161-813X. doi:10.1016/S0161-813X(03)00106-2

[72] YOUDIM, Moussa B. H., Dale EDMONDSON a Keith F. TIPTON. The therapeutic potential of monoamine oxidase inhibitors. *Nature Reviews. Neuroscience* [online]. 2006, vol. 7, no. 4, p. 295–309. ISSN 1471-003X. doi:10.1038/nrn1883

[73] PIZZINAT, N., N. COPIN, C. VINDIS, A. PARINI a C. CAMBON. Reactive oxygen species production by monoamine oxidases in intact cells. *Naunyn-Schmiedeberg's Archives of Pharmacology*. 1999, vol. 359, no. 5, p. 428–431. ISSN 0028-1298.

[74] STERLING, Jeffrey, Yaacov HERZIG, Tamar GOREN, Nina FINKELSTEIN, David LERNER, Willy GOLDENBERG, Istvan MISKOLCZI, Sandor MOLNAR, Ferenc RANTAL, Tivadar TAMAS, Gyorgy TOTH, Adela ZAGYVA, Andras ZEKANY, Gila LAVIAN, Aviva GROSS, Rachel FRIEDMAN, Michal RAZIN, Wei HUANG, Boris KRAIS, Michael CHOREV, Moussa B. YOUDIM a Marta WEINSTOCK. Novel Dual Inhibitors of AChE and MAO Derived from Hydroxy Aminoindan and Phenethylamine as Potential Treatment for Alzheimer's Disease. *Journal of Medicinal Chemistry* [online]. 2002, vol. 45, no. 24, p. 5260–5279. ISSN 0022-2623. doi:10.1021/jm020120c

[75] BOLEA, Irene, Jordi JUÁREZ-JIMÉNEZ, Cristóbal DE LOS RÍOS, Mourad CHIOUA, Ramón POUPLANA, F. Javier LUQUE, Mercedes UNZETA, José MARCO-CONTELLES a Abdelouahid SAMADI. Synthesis, biological evaluation, and molecular modeling of donepezil and N-[(5-(benzyloxy)-1-methyl-1H-indol-2-yl)methyl]-N-methylprop-2-yn-1-amine hybrids as new multipotent cholinesterase/monoamine oxidase inhibitors for the treatment of Alzheimer's disease. *Journal of Medicinal Chemistry* [online]. 2011, vol. 54, no. 24, p. 8251–8270. ISSN 1520-4804. doi:10.1021/jm200853t

[76] BOLEA, Irene, Alejandro GELLA, Leticia MONJAS, Concepción PÉREZ, María Isabel RODRÍGUEZ-FRANCO, José MARCO-CONTELLES, Abdelouahid SAMADI a Mercedes UNZETA. Multipotent, permeable drug ASS234 inhibits Aβ aggregation, possesses antioxidant properties and protects from Aβ-induced apoptosis in vitro. *Current Alzheimer Research*. 2013, vol. 10, no. 8, p. 797–808. ISSN 1875-5828.

[77] WANG, Li, Gerard ESTEBAN, Masaki OJIMA, Oscar M. BAUTISTA-AGUILERA, Tsutomu INOKUCHI, Ignacio MORALEDA, Isabel IRIEPA, Abdelouahid SAMADI, Moussa B. H. YOUDIM, Alejandro ROMERO, Elena SORIANO, Raquel HERRERO, Ana Patricia FERNÁNDEZ FERNÁNDEZ, null RICARDO-MARTÍNEZ-MURILLO, José MARCO-CONTELLES a Mercedes UNZETA. Donepezil + propargylamine + 8-hydroxyquinoline hybrids as new multifunctional metal-chelators, ChE and MAO inhibitors for the potential treatment of Alzheimer's disease. *European Journal of Medicinal Chemistry* [online]. 2014, vol. 80, p. 543–561. ISSN 1768-3254. doi:10.1016/j.ejmech.2014.04.078

[78] VALASANI, K R, Q SUN, G HU, J LI, F DU, Y GUO, E A CARLSON, X GAN a S S YAN. Identification of Human ABAD Inhibitors for Rescuing Aβ-Mediated Mitochondrial Dysfunction. *Current Alzheimer research*. 2014. ISSN 1875-5828.

[79] PAJOUHESH, Hassan a George R. LENZ. Medicinal chemical properties of successful central nervous system drugs. *NeuroRx: The Journal of the American Society for Experimental NeuroTherapeutics* [online]. 2005, vol. 2, no. 4, p. 541–553. ISSN 1545-5343. doi:10.1602/neurorx.2.4.541

[80] WENLOCK, Mark C., Rupert P. AUSTIN, Patrick BARTON, Andrew M. DAVIS a Paul D. LEESON. A comparison of physiochemical property profiles of development and marketed oral drugs. *Journal of Medicinal Chemistry* [online]. 2003, vol. 46, no. 7, p. 1250–1256. ISSN 0022-2623. doi:10.1021/jm021053p

[81] ALELYUNAS, Yun W., James R. EMPFIELD, Dennis MCCARTHY, Russell C. SPREEN, Khanh BUI, Luciana PELOSI-KILBY a Cindy SHEN. Experimental solubility profiling of marketed CNS drugs, exploring solubility limit of CNS discovery candidate. *Bioorganic & Medicinal Chemistry Letters* [online]. 2010, vol. 20, no. 24, p. 7312–7316. ISSN 1464-3405. doi:10.1016/j.bmcl.2010.10.068

[82] SONG, Eun Young, Navneet KAUR, Mi-Young PARK, Yinglan JIN, Kyeong LEE, Guncheol KIM, Ki Youn LEE, Jee Sun YANG, Jae Hong SHIN, Ky-Youb NAM, Kyoung Tai NO a Gyoonhee HAN. Synthesis of amide and urea derivatives of benzothiazole as Raf-1 inhibitor. *European Journal of Medicinal Chemistry* [online]. 2008, vol. 43, no. 7, p. 1519–1524. ISSN 0223-5234. doi:10.1016/j.ejmech.2007.10.008

[83] SIDDIQUI, Nadeem a Waquar AHSAN. Benzothiazole incorporated barbituric acid derivatives: synthesis and anticonvulsant screening. *Archiv Der Pharmazie* [online]. 2009, vol. 342, no. 8, p. 462–468. ISSN 1521-4184. doi:10.1002/ardp.200900002

[84] LI, Zheng, Shuxiu XIAO, Guoqiang TIAN, Anguo ZHU, Xu FENG a Jing LIU. Microwave Promoted Environmentally Benign Synthesis of 2-Aminobenzothiazoles and Their Urea Derivatives. *Phosphorus, Sulfur, and Silicon and the Related Elements* [online]. 2008, vol. 183, no. 5, p. 1124–1133. doi:10.1080/10426500701578506

[85] WO2006/18662.

[86] SATOH, Motohide, Hisateru ARAMAKI, Masaki YAMASHITA, Masafumi INOUE, Hiroshi KAWAKAMI, Hisashi SHINKAI, Hiroshi NAKAMURA, Yuji MATSUZAKI a Shuichi WAMAKI. 6-(Heterocyclyl-substituted Benzyl) -4-Oxoquinoline Compound and Use Thereof as HIV Integrase Inhibitor [online]. US2008207618 (A1). 28. srpen 2008. [vid. 2015-01-13]. http://worldwide.espacenet.com/publicationDetails/biblio;jsessionid=24A9CD15A7C6B851E3242770FA8962EE.espacenet_levelx_prod_3?FT=D&date=20080828&DB=&locale=en_EP&CC=US&NR=2008207618A1&KC=A1&ND=1

[87] MANGRAVITE, John A. Palladium catalyzed reduction of nitrobenzene. *Journal of Chemical Education* [online]. 1983, vol. 60, no. 5, p. 439. ISSN 0021-9584. doi:10.1021/ed060p439

[88] DU, Zhen-Ting, Jing LU, Hong-Rui YU, Yan XU a An-Pai LI. A facile demethylation of ortho substituted aryl methyl ethers promoted by AlCl3. *Journal of Chemical Research* [online]. 2010, no. 4, p. 222–227. ISSN 1747-5198. doi:10.3184/030823410X12708998015900

[89] HROCH, Lukas, Ondrej BENEK, Patrick GUEST, Laura AITKEN, Ondrej SOUKUP, Jana JANOCKOVA, Karel MUSIL, Vlastimil DOHNAL, Rafael DOLEZAL, Kamil KUCA, Terry K SMITH, Frank GUNN-MOORE a Kamil MUSILEK. Design, synthesis and in vitro evaluation of benzothiazole-based ureas as potential ABAD/17β-HSD10 modulators for Alzheimer's disease treatment. *Bioorganic & Medicinal Chemistry Letters* [online]. nedatováno [vid. 2016-06-02]. ISSN 0960-894X. doi:10.1016/j.bmcl.2016.05.087

[90] VALASANI, Koteswara R, Gang HU, Michael O CHANEY a Shirley S YAN. Structure-based design and synthesis of benzothiazole phosphonate analogues with inhibitors of human ABAD-Aβ for treatment of Alzheimer's disease. *Chemical biology & drug design* [online]. 2013, vol. 81, no. 2, p. 238–249. ISSN 1747-0285. doi:10.1111/cbdd.12068

[91] HROCH, Lukas, Laura AITKEN, Ondrej BENEK, Martin DOLEZAL, Kamil KUCA, Frank GUNN-MOORE a Kamil MUSILEK. Benzothiazoles - scaffold of interest for CNS targeted drugs. *Current Medicinal Chemistry*. 2015, vol. 22, no. 6, p. 730–747. ISSN 1875-533X.

[92] FURLAN, Alessandro, Francesco COLOMBO, Andrea KOVER, Nathalie ISSALY, Cristina TINTORI, Lucilla ANGELI, Vincent LEROUX, Sébastien LETARD, Mercedes AMAT, Yasmine ASSES, Bernard MAIGRET, Patrice DUBREUIL, Maurizio BOTTA, Rosanna DONO, Joan BOSCH, Oreste PICCOLO, Daniele PASSARELLA a Flavio MAINA. Identification of new aminoacid

amides containing the imidazo[2,1-b]benzothiazol-2-ylphenyl moiety as inhibitors of tumorigenesis by oncogenic Met signaling. *European Journal of Medicinal Chemistry* [online]. 2012, vol. 47, p. 239–254. ISSN 0223-5234. doi:10.1016/j.ejmech.2011.10.051

[93] *ACD/Labs PhysChemSuite 12.0, Advanced Chemistry Development, Inc., Toronto, On, Canada, www.acdlabs.com, 2012.* nedatováno.

[94] OECD. *Test No. 117: Partition Coefficient (n-octanol/water), HPLC Method* [online]. B.m.: OECD Publishing, 2004 [vid. 2015-11-09]. OECD Guidelines for the Testing of Chemicals, Section 1. ISBN 978-92-64-06982-4. http://www.oecd-ilibrary.org/environment/test-no-117-partition-coefficient-n-octanol-water-hplc-method_9789264069824-en

[95] WU, Yong-Qian, David C. LIMBURG, Douglas E. WILKINSON a Gregory S. HAMILTON. Formation of nitrogen-containing heterocycles using di(imidazole-1-yl)methanimine. *Journal of Heterocyclic Chemistry* [online]. 2003, vol. 40, no. 1, p. 191–193. ISSN 1943-5193. doi:10.1002/jhet.5570400129

[96] WU, Yong-Qian, Sean K. HAMILTON, Douglas E. WILKINSON a Gregory S. HAMILTON. Direct synthesis of guanidines using di(imidazole-1-yl)methanimine. *The Journal of Organic Chemistry*. 2002, vol. 67, no. 21, p. 7553–7556. ISSN 0022-3263.

[97] TSURUOKA, A., Y. KAKU, H. KAKINUMA, I. TSUKADA, M. YANAGISAWA, K. NARA a T. NAITO. Synthesis and antifungal activity of novel thiazole-containing triazole antifungals. II. Optically active ER-30346 and its derivatives. *Chemical & Pharmaceutical Bulletin*. 1998, vol. 46, no. 4, p. 623–630. ISSN 0009-2363.

[98] GUO, Yan-Jin, Ri-Yuan TANG, Ping ZHONG a Jin-Heng LI. Copper-catalyzed tandem reactions of 2-halobenzenamines with isothiocyanates under ligand- and base-free conditions. *Tetrahedron Letters* [online]. 2010, vol. 51, no. 4, p. 649–652. ISSN 0040-4039. doi:10.1016/j.tetlet.2009.11.086

[99] PRAT, G, V PÉREZ, A RUBI, M CASAS a M UNZETA. The novel type B MAO inhibitor PF9601N enhances the duration of L-DOPA-induced contralateral turning in 6-hydroxydopamine lesioned rats. *Journal Of Neural Transmission (Vienna, Austria: 1996)*. 2000, vol. 107, no. 4, p. 409–417. ISSN 0300-9564.

[100] BAUTISTA-AGUILERA, Oscar M., Abdelouahid SAMADI, Mourad CHIOUA, Katarina NIKOLIC, Slavica FILIPIC, Danica AGBABA, Elena SORIANO, Lucía DE ANDRÉS, María Isabel RODRÍGUEZ-FRANCO, Stefano ALCARO, Rona R. RAMSAY, Francesco ORTUSO, Matilde YAÑEZ a José MARCO-CONTELLES. N-Methyl-N-((1-methyl-5-(3-(1-(2-methylbenzyl)piperidin-4-yl)propoxy)-1H-indol-2-yl)methyl)prop-2-yn-1-amine, a new cholinesterase and monoamine oxidase dual inhibitor. *Journal of Medicinal Chemistry* [online]. 2014, vol. 57, no. 24, p. 10455–10463. ISSN 1520-4804. doi:10.1021/jm501501a

[101] JUÁREZ-JIMÉNEZ, Jordi, Eduarda MENDES, Carles GALDEANO, Carla MARTINS, Daniel B. SILVA, José MARCO-CONTELLES, Maria DO CARMO CARREIRAS, F. Javier LUQUE a Rona R. RAMSAY. Exploring the structural basis of the selective inhibition of monoamine oxidase A by dicarbonitrile aminoheterocycles: role of Asn181 and Ile335 validated by spectroscopic and computational studies. *Biochimica Et Biophysica Acta* [online]. 2014, vol. 1844, no. 2, p. 389–397. ISSN 0006-3002. doi:10.1016/j.bbapap.2013.11.003

[102] SONG, Mee-Sook, Dmitriy MATVEYCHUK, Erin M. MACKENZIE, Maryana DUCHCHERER, Darrell D. MOUSSEAU a Glen B. BAKER. An update on amine oxidase inhibitors: Multifaceted drugs. *Progress in Neuro-Psychopharmacology and Biological Psychiatry* [online]. 2013, vol. 44, p. 118–124. ISSN 0278-5846. doi:10.1016/j.pnpbp.2013.02.001

[103] KIM, H., S. O. SABLIN a R. R. RAMSAY. Inhibition of monoamine oxidase A by beta-carboline derivatives. *Archives of Biochemistry and Biophysics* [online]. 1997, vol. 337, no. 1, p. 137–142. ISSN 0003-9861. doi:10.1006/abbi.1996.9771

[104] CAO, Rihui, Wenlie PENG, Zihou WANG a Anlong XU. beta-Carboline alkaloids: biochemical and pharmacological functions. *Current Medicinal Chemistry*. 2007, vol. 14, no. 4, p. 479–500. ISSN 0929-8673.

[105] LANDWEHR, Jens a Reinhard TROSCHÜTZ. Synthesis of 3-EWG-Substituted 2-Amino-5-hydroxyindoles via Nenitzescu Reaction. *Synthesis* [online]. 2005, no. 14, p. 2414–2420. ISSN 0039-7881, 1437-210X. doi:10.1055/s-2005-872074

[106] YANG, Xiaobo, Hua FU, Renzhong QIAO, Yuyang JIANG a Yufen ZHAO. A Simple Copper-Catalyzed Cascade Synthesis of 2-Amino-1H-indole-3-carboxylate Derivatives. *Advanced Synthesis & Catalysis* [online]. 2010, vol. 352, no. 6, p. 1033–1038. ISSN 1615-4169. doi:10.1002/adsc.200900887

[107] MARCO-CONTELLES, José, Elena PÉREZ-MAYORAL, Abdelouahid SAMADI, María do Carmo CARREIRAS a Elena SORIANO. Recent Advances in the Friedländer Reaction. *Chemical Reviews* [online]. 2009, vol. 109, no. 6, p. 2652–2671. ISSN 0009-2665. doi:10.1021/cr800482c

[108] JIANG, Min, Jian LI, Feng WANG, Yichao ZHAO, Feng ZHAO, Xiaochun DONG a Weili ZHAO. A facile copper-catalyzed one-pot domino synthesis of 5,12-dihydroindolo[2,1-b]quinazolines. *Organic Letters* [online]. 2012, vol. 14, no. 6, p. 1420–1423. ISSN 1523-7052. doi:10.1021/ol3001624

[109] MEDVEDEV, A. E., R. R. RAMSAY, A. S. IVANOV, A. V. VESELOVSKY, V. I. SHVEDOV, O. V. TIKHONOVA, A. P. BARRADAS, C. K. DAVIDSON, T. A. MOSKVITINA, O. A. FEDOTOVA a L. N. AXENOVA. Inhibition of monoamine oxidase by pirlindole analogues: 3D-QSAR analysis. *Neurobiology (Budapest, Hungary)*. 1999, vol. 7, no. 2, p. 151–158. ISSN 1216-8068.

[110] KORABECNY, Jan, Rafael DOLEZAL, Pavla CABELOVA, Anna HOROVA, Eva HRUBA, Jan RICNY, Lukas SEDLACEK, Eugenie NEPOVIMOVA, Katarina SPILOVSKA, Martin ANDRS, Kamil MUSILEK, Veronika OPLETALOVA, Vendula SEPSOVA, Daniela RIPOVA a Kamil KUCA. 7-MEOTA–donepezil like compounds as cholinesterase inhibitors: Synthesis, pharmacological evaluation, molecular modeling and QSAR studies. *European Journal of Medicinal Chemistry* [online]. 2014, vol. 82, p. 426–438. ISSN 0223-5234. doi:10.1016/j.ejmech.2014.05.066

[111] WANG, Xinglong, Wenzhang WANG, Li LI, George PERRY, Hyoung-gon LEE a Xiongwei ZHU. Oxidative stress and mitochondrial dysfunction in Alzheimer's disease. *Biochimica et Biophysica Acta (BBA) - Molecular Basis of Disease* [online]. 2014, vol. 1842, no. 8, Misfolded Proteins, Mitochondrial Dysfunction, and Neurodegenerative Diseases, p. 1240–1247. ISSN 0925-4439. doi:10.1016/j.bbadis.2013.10.015

[112] PISOSCHI, Aurelia Magdalena a Aneta POP. The role of antioxidants in the chemistry of oxidative stress: A review. *European Journal of Medicinal Chemistry* [online]. 2015, vol. 97, p. 55–74. ISSN 0223-5234. doi:10.1016/j.ejmech.2015.04.040

[113] SOUKUP, Ondrej, Daniel JUN, Jana ZDAROVA-KARASOVA, Jiri PATOCKA, Kamil MUSILEK, Jan KORABECNY, Jan KRUSEK, Martina KANIAKOVA, Vendula SEPSOVA, Jana MANDIKOVA, Frantisek TREJTNAR, Miroslav POHANKA, Lucie DRTINOVA, Michal PAVLIK, Gunnar TOBIN a Kamil KUCA. A resurrection of 7-MEOTA: a comparison with tacrine. *Current Alzheimer Research*. 2013, vol. 10, no. 8, p. 893–906. ISSN 1875-5828.

[114] MOSMANN, T. Rapid colorimetric assay for cellular growth and survival: application to proliferation and cytotoxicity assays. *Journal of Immunological Methods*. 1983, vol. 65, no. 1–2, p. 55–63. ISSN 0022-1759.

[115] PATOCKA, Jiri, Daniel JUN a Kamil KUCA. Possible role of hydroxylated metabolites of tacrine in drug toxicity and therapy of Alzheimer's disease. *Current Drug Metabolism*. 2008, vol. 9, no. 4, p. 332–335. ISSN 1389-2002.

[116] DI, Li, Edward H. KERNS, Kristi FAN, Oliver J. MCCONNELL a Guy T. CARTER. High throughput artificial membrane permeability assay for blood-brain barrier. *European Journal of Medicinal Chemistry*. 2003, vol. 38, no. 3, p. 223–232. ISSN 0223-5234.

[117] PRATI, F., E. ULIASSI a M. L. BOLOGNESI. Two diseases, one approach: multitarget drug discovery in Alzheimer's and neglected tropical diseases. *MedChemComm* [online]. 2014, vol. 5, no. 7, p. 853–861. ISSN 2040-2511. doi:10.1039/C4MD00069B

[118] AITKEN, Laura, Steven D QUINN, Cibran PEREZ-GONZALEZ, Ifor D W SAMUEL, Jcarlos PENEDO a Frank J GUNN-MOORE. Morphology-specific inhibition of β-amyloid aggregates by 17β-hydroxysteroid dehydrogenase type 10. *ChemBioChem* [online]. 2016, p. n/a-n/a. ISSN 1439-7633. doi:10.1002/cbic.201600081

[119] OECD. *Test No. 117: Partition Coefficient (n-octanol/water), HPLC Method*. B.m.: OECD Publishing, nedatováno.

[120] ZHOU, M. a N. PANCHUK-VOLOSHINA. A one-step fluorometric method for the continuous measurement of monoamine oxidase activity. *Analytical Biochemistry* [online]. 1997, vol. 253, no. 2, p. 169–174. ISSN 0003-2697. doi:10.1006/abio.1997.2392

[121] HOLT, Andrew a Monica M. PALCIC. A peroxidase-coupled continuous absorbance plate-reader assay for flavin monoamine oxidases, copper-containing amine oxidases and related enzymes. *Nature Protocols* [online]. 2006, vol. 1, no. 5, p. 2498–2505. ISSN 1750-2799. doi:10.1038/nprot.2006.402

[122] ESTEBAN, Gerard, Jennifer ALLAN, Abdelouahid SAMADI, Andrea MATTEVI, Mercedes UNZETA, José MARCO-CONTELLES, Claudia BINDA a Rona R. RAMSAY. Kinetic and structural analysis of the irreversible inhibition of human monoamine oxidases by ASS234, a multi-target compound designed for use in Alzheimer's disease. *Biochimica Et Biophysica Acta* [online]. 2014, vol. 1844, no. 6, p. 1104–1110. ISSN 0006-3002. doi:10.1016/j.bbapap.2014.03.006

[123] ELLMAN, G. L., K. D. COURTNEY, V. ANDRES a R. M. FEATHER-STONE. A new and rapid colorimetric determination of acetylcholinesterase activity. *Biochemical Pharmacology*. 1961, vol. 7, p. 88–95. ISSN 0006-2952.

[124] MOLYNEUX, Philip. The use of the stable free radical diphenylpicrylhydrazyl (DPPH) for estimating antioxidant. *Songklanakarin Journal of Science and Technology*. 2004, vol. 26, no. 2, p. 211–219. ISSN 0125-3395.

[125] PAN, Ying, Yicun CHEN, Qingnan LI, Xiaoyu YU, Jinzhi WANG a Jinhong ZHENG. The synthesis and evaluation of novel hydroxyl substituted chalcone analogs with in vitro anti-free radicals pharmacological activity and in vivo anti-oxidation activity in a free radical-injury Alzheimer's model. *Molecules (Basel, Switzerland)* [online]. 2013, vol. 18, no. 2, p. 1693–1703. ISSN 1420-3049. doi:10.3390/molecules18021693

[126] BERNAS, Tytus a Jurek DOBRUCKI. Mitochondrial and nonmitochondrial reduction of MTT: interaction of MTT with TMRE, JC-1, and NAO mitochondrial fluorescent probes. *Cytometry*. 2002, vol. 47, no. 4, p. 236–242. ISSN 0196-4763.

[127] ABE, K. a N. MATSUKI. Measurement of cellular 3-(4,5-dimethylthiazol-2-yl)-2,5-diphenyltetrazolium bromide (MTT) reduction activity and lactate dehydrogenase release using MTT. *Neuroscience Research*. 2000, vol. 38, no. 4, p. 325–329. ISSN 0168-0102.

[128] MALINAK, David, Rafael DOLEZAL, Jan MAREK, Sarka SALAJKOVA, Ondrej SOUKUP, Marcela VEJSOVA, Jan KORABECNY, Jan HONEGR, Marek PENHAKER, Kamil MUSILEK a Kamil KUCA. 6-Hydroxyquinolinium salts differing in the length of alkyl side-chain: synthesis and antimicrobial activity. *Bioorganic & Medicinal Chemistry Letters* [online]. 2014, vol. 24, no. 22, p. 5238–5241. ISSN 1464-3405. doi:10.1016/j.bmcl.2014.09.060

[129] SUGANO, K., H. HAMADA, M. MACHIDA a H. USHIO. High throughput prediction of oral absorption: improvement of the composition of the lipid solution used in parallel artificial membrane permeation assay. *Journal of Biomolecular Screening* [online]. 2001, vol. 6, no. 3, p. 189–196. ISSN 1087-0571. doi:10.1089/108705701300362728

[130] WOHNSLAND, F. a B. FALLER. High-throughput permeability pH profile and high-throughput alkane/water log P with artificial membranes. *Journal of Medicinal Chemistry*. 2001, vol. 44, no. 6, p. 923–930. ISSN 0022-2623.

6 Summary in English

Alzheimer's disease (AD) is the most common cause of senile dementia worldwide. Despite being subject to intensive research, the pathogenic mechanisms of AD are still not fully understood and consequently an effective treatment is yet to be developed. Although the aetiology of AD is still unknown, a build-up of amyloid-beta peptide (A*β*) is considered to play an important role in disease progression. The original amyloid cascade hypothesis proposed that insoluble extracellular plaques were responsible for the majority of A*β* toxicity. This hypothesis has since been refined, as recent data indicates that soluble intracellular oligomers are now responsible for the majority of A*β* induced toxic effects. The mitochondrial dysfunction also plays an important role in the pathophysiology of AD. A*β* was detected inside mitochondria and several mitochondrial proteins were found to interact directly with A*β*. Such interactions can affect a protein's function and cause damage to the mitochondria, which finally results in progression of AD.

The background for the experimental part of this dissertation thesis was literature review summarizing current knowledge on mitochondrial proteins directly interacting with A*β* in order to identify potential drug targets for AD treatment. A deeper look was taken on mitochondrial enzyme A*β* binding alcohol dehydrogenase (ABAD), which appeared to be the most promising drug target.

The aim of the experimental work was design, synthesis and evaluation of novel compounds targeting the mitochondrial enzymes connected to AD pathophysiology (e.g. ABAD or monoamine oxidase). For this purpose were employed two different paradigms: the classical ''one-target one-compound'' and the innovative ''multitarget-directed ligand'' (MTDL) strategy. Compounds designed according to MTDL approach should be able to intervene simultaneously in the different pathological events underlying the aetiology of AD.

Together, more than one hundred potential ABAD inhibitors and seven MTDLs targeting monoamine oxidase and cholinesterases were designed and synthesized. Several of these compounds showed promising *in vitro* activity and as such present structural leads for further anti-AD drug research and development.

7 Shrnutí v českém jazyce

Alzheimerova nemoc (AD) je celosvětově nejběžnější příčinou stařecké demence. Přes intenzivní výzkum se zatím nepodařilo odhalit mechanismus vzniku tohoto onemocnění, a proto pro něj neexistuje kauzální léčba. Přestože je etiologie AD neznámá, víme, že peptid beta-amyloid (A*β*) hraje důležitou role v jejím rozvoji. Původní teorie amyloidní kaskády předpokládala, že extracelulární amyloidní plaky jsou zodpovědné za toxické působní A*β*. Tato teorie byla později upravena na základě nových poznatků, která naznačují, že za toxicitu jsou zodpovědné zejména rozpustné oligomerní formy A*β* a jejich působení uvnitř buněk. Důležitou roli v patofyziologie AD má také poškození mitochondrií. A*β* byl detekován uvnitř mitochondrií, kde přímo interaguje s několika mitochondriálními proteiny. Interakce s A*β* ovlivňuje funkci těchto enzymů, což poškozuje mitochondrie a v konečném důsledku může vést k rozvoji AD.

Základem pro experimentální část této práce bylo sepsání literární rešerše, shrnující současné poznatky o mitochondriálních enzymech interagujících s A*β*, za účelem nalézt potenciální cíle pro terapii AD. Následně byla věnována pozornost zejména mitochondriálnímu enzymu ABAD, který se jevil jako velmi vhodný cíl pro farmakoterapii.

Cílem experimentální práce byl design, syntéza a testování nových sloučenin ovlivňujících mitochondriální enzymy, které se účastní rozvoje AD (např. ABAD nebo monoaminooxidasa). Za tímto účelem byly využity dva různé přístupy k designu nových sloučenin: klasický ‘‘jedna molekula – jeden cíl’’ a novější ‘‘multitarget-directed ligand’’ (MTDL) strategie. Sloučeniny navržené systémem MTDL by měly současně ovlivňovat více patologických procesů podílejících se na rozvoji AD.

Celkem bylo v rámci této práce připraveno více jak sto nových potenciálních inhibitorů ABAD a sedm MTDL sloučenin inhibujících současně cholinesterasy a monoaminooxidasu. Několik sloučenin vykázalo při *in vitro* testování slibnou aktivitu a mohou tak posloužit jako strukturní základ pro další výzkum a vývoj léčiv v oblasti AD.

8 Outputs

8.1 Publications

1) BENEK, Ondrej, Kamil MUSILEK a Kamil KUCA. [Mitochondrial enzyme ABAD and its role in the development and treatment of Alzheimer's disease]. *Ceska a Slovenská farmacie: casopis Ceské farmaceuticke spolecnosti a Slovenske farmaceuticke spolecnosti*. 2012, vol. 61, no. 4, p. 144–149. ISSN 1210-7816.

2) KORABECNY, Jan, Katarina SPILOVSKA, Ondrej BENEK, Kamil MUSILEK, Ondrej SOUKUP a Kamil KUCA. [Tacrine and its derivatives in the therapy of Alzheimers disease]. *Ceska a Slovenska Farmacie: Casopis Ceske Farmaceuticke Spolecnosti a Slovenske Farmaceuticke Spolecnosti*. 2012, vol. 61, no. 5, p. 210–221. ISSN 1210-7816.

3) BENEK, Ondrej, Kamil MUSILEK, Anna HOROVA, Vlastimil DOHNAL, Rafael DOLEZAL a Kamil KUCA. Preparation, In Vitro Screening and Molecular Modelling of Monoquaternary Compounds Related to the Selective Acetylcholinesterase Inhibitor BW284c51. *Medicinal Chemistry (Shāriqah (United Arab Emirates))*. 2014, vol. 11, no. 1, p. 21–29. ISSN 1875-6638. DOI: 10.2174/15734064106661404281531l0. IF = 1.387

4) HROCH, Lukas, Laura AITKEN, Ondrej BENEK, Martin DOLEZAL, Kamil KUCA, Frank GUNN-MOORE a Kamil MUSILEK. Benzothiazoles - scaffold of interest for CNS targeted drugs. *Current Medicinal Chemistry*. 2015, vol. 22, no. 6, p. 730–747. ISSN 1875-533X. DOI: 10.2174/092986732266614121212063l. IF = 3. 853

5) BENEK, Ondrej, Laura AITKEN, Lukas HROCH, Kamil KUCA, Frank GUNN-MOORE a Kamil MUSILEK. A Direct interaction between mitochondrial proteins and amyloid-β peptide and its significance for the progression and treatment of Alzheimer`s disease. *Current Medicinal Chemistry*. 2015. ISSN 1875-533X. DOI: 10.2174/092986732266615011416305l. IF = 3. 853

6) BENEK, Ondrej, Ondrej SOUKUP, Marketa PASDIOROVA, Lukas HROCH, Vendula SEPSOVA, Petr JOST, Martina HRABINOVA, Daniel JUN, Kamil KUCA, Dominykas ZALA, Rona R. RAMSAY, José MARCO-CONTELLES a Kamil MUSILEK. Design, Synthesis and in vitro Evaluation of Indolotacrine Analogues as Multitarget-Directed Ligands for the Treatment of Alzheimer's Disease. *ChemMedChem* [online]. 2015, in press. ISSN 1860-7187. DOI: 10.1002/cmdc.201500383. IF = 2.968

7) ANDRS, Martin, Darina MUTHNA, Martina REZACOVA, Martina SEIFRTOVA, Pavel SIMAN, Jan KORABECNY, Ondrej BENEK, Rafael DOLEZAL, Ondrej SOUKUP, Daniel JUN a Kamil KUCA. Novel caffeine derivatives with antiproliferative activity. *RSC Advances* [online]. 2016, vol. 6, no. 39, p. 32534–32539. ISSN 2046-2069. DOI: 10.1039/C5RA22889A. IF = 3.840

8) HROCH, Lukas, Ondrej BENEK, Patrick GUEST, Laura AITKEN, Ondrej SOUKUP, Jana JANOCKOVA, Karel MUSIL, Vlastimil DOHNAL, Rafael DOLEZAL, Kamil KUCA, Terry K SMITH, Frank GUNN-MOORE a Kamil MUSILEK. Design, synthesis and in vitro evaluation of benzothiazole-based ureas as potential ABAD/17β-HSD10 modulators for Alzheimer's disease treatment. *Bioorganic & Medicinal Chemistry Letters* [online]. 2016, in press. ISSN 0960-894X. DOI: 10.1016/j.bmcl.2016.05.087. IF= 2.420

8.2 Conference proceedings

Lectures

1) Benek, O. Inhibitory interakce ABAD-Aβ jako potenciální léčiva Alzheimerovy nemoci. **2. Květinův den**, Brno (ČR), 23. 5. 2013.

2) Benek, O. Mitochondrial enzyme ABAD: A potential target for treatment of Alzheimer's disease. **COST CM1103 Training School**, Istanbul (Turkey), 9. – 13. 9. 2013.

3) Musilek, K.; Benek, O.; Hroch, L.; Guest, P.; Aitken, L.; Soukup, O.; Kuca, K.; Ramsay, R.; Gunn-Moore, F. Benzothiazoles - Scaffold of interest for CNS targeted drugs. **Neuropathology and Neuropharmacology of monoaminergic systems** Bordeaux (France) 8. – 10. 10. 2014, Abstract book.

4) Benek, O.; Hroch, L.; Guest, P.; Aitken, L.; Pasdiorova, M.; Soukup, O.; Kuca, K.; Gunn-Moore, F.; Musilek, K. ABAD Modulators for AD Modifying Treatment – Design, Synthesis and In vitro Screening. **49th Advances in Organic, Bioorganic and Pharmaceutical Chemistry – „Liblice 2014"** Lazne Belohrad (Czech Republic) 7. – 9. 11. 2014, Abstract book.

5) Benek, O. Benzothiazolyl ureas as ABAD modulators for treatment of Alzheimer's disease. **COST CM1103 Training School**, Belgrade (Serbia), 6. – 8. 5. 2015.

Posters

1) Musilek, K.; Benek, O.; Korabecny, J.; Kuca, K.; Gunn-Moore, F. Analogues of benzthiazole ureas as potential inhibitors of mitochondrial enzymes with implications for AD. **Alzheimer's Research UK Conference 2012** Birmingham (UK), 27. – 28. 3. 2012, *Book of abstracts*.

2) Benek, O., Musilek, K., Kuca, K., Korabecny, J., Spilovska, K., Gunn-Moore, F. Benzothiazoleurea analogues as inhibitors of ABAD-Aβ interaction in Alzheimer's disease. **62. Česko-Slovenské Farmakologické dni** Košice (SK) 25. – 27. 6. 2012.

3) Benek, O.; Musilek, K.; Kuca, K.; Korabecny, J.; Spilovska, K.; Gunn-Moore, F.; Benzothiazolyl urea analogues as inhibitors of ABAD-Aβ interaction in Alzheimer's disease. **55. Česko-slovenská psychofarmakologická konference** Lázně Jeseník (ČR) 4. – 8. 1. 2013.

4) Benek, O.; Spilovska, K.; Korabecny, J.; Kuca, K.; Gunn-Moore, F.; Musilek, K. Inhibitors of ABAD-Aβ interaction as potential AD treatment. **11th International Conference Alzheimer's and Parkinson's Diseases** Florence (Italy) 6. – 10. 3. 2013, *Neurodegenerative Diseases 2013*, *11 (S1), ISBN 978-3-318-02391-6*.

5) Hroch, L.; Benek, O.; Korábečný, J.; Gunn-Moore, F.; Musílek, K. Modulátory ABAD jako potenciální léčiva Alzheimerovy nemoci. **42. konference Syntéza a analýza léčiv**, 2. – 5. 9. 2013, Abstract Book.

6) Hroch, L.; Benek, O.; Guest, P.; Aitken, L.; Gunn-Moore, F.; Musilek K. Novel indole-based modulators of Aβ-ABAD interaction for treatment of Alzheimer's disease. **COST CM1103 Training School** Istanbul (Turkey) 9. – 13. 9. 2013, Abstract book.

7) Benek, O.; Hroch, L.; Kuca, K.; Guest, P.; Aitken, L.; Gunn-Moore, F.; Musilek, K. Synthesis and evaluation of benzothiazolylurea analogues as inhibitors of ABAD-Aβ interaction for treatment of Alzheimer's disease. **COST CM1103 Training School** Istanbul (Turkey) 9. – 13. 9. 2013, Abstract book.

8) Benek, O.; Hroch, L.; Guest, P.; Aitken, L.; Smith, T.; Soukup, O.; Kuca, K.; Ramsay, R.; Gunn-Moore, F.; Musilek, K. Design, synthesis and evaluation of ABAD modulators. **WG1-2 COST meeting** Smolenice (Slovakia) 22. – 24. 4. 2014, Abstract book.

9) Hroch, L.; Benek, O.; Guest, P.; Aitken, L.; Gunn-Moore, F.; Musilek K. Novel ABAD and Aβ-ABAD Interaction Modulators for Treatment of Alzheimer's Disease. **4th Meeting of the Paul**

Ehrlich MedChem Euro-PhD Network Hradec Králové (ČR) 20. – 22. 6. 2014, Abstract Book, P-28.

10) Musilek, K.; Benek, O.; Hroch, L.; Guest, P.; Kucera, T.; Aitken, L.; Kuca, K.; Gunn-Moore, F. ABAD modulators for AD modifying treatment – synthesis, in vitro screening and molecular modelling. **23th International Symposium on Medicinal Chemistry** Lisbon (Portugal) 7. – 11. 9. 2014, ChemMedChem, M019, p. 209.

11) Hroch L.; Benek O.; Kuca K., Guest P.; Aitken L.; Gunn-Moore F.; Musilek K. Design, synthesis and evaluation of novel ABAD modulators for treatment of Alzheimer's disease. **23th International Symposium on Medicinal Chemistry** Lisbon (Portugal) 7. – 11. 9. 2014, ChemMedChem, M008, p. 201.

12) Benek, O.; Hroch, L.; Guest, P.; Aitken, L.; Pasdiorova, M.; Soukup, O.; Kuca, K.; Gunn-Moore, F.; Musilek, K. ABAD Modulators for AD Modifying Treatment – Design, Synthesis and In vitro Screening. **5th Targeting Mitochondria** Berlin (Germany) 29. – 31. 10. 2014, Abstract book.

9 Attachments

Attachment I

BENEK, Ondrej, Laura AITKEN, Lukas HROCH, Kamil KUCA, Frank GUNN-MOORE a Kamil MUSILEK. A Direct interaction between mitochondrial proteins and amyloid-β peptide and its significance for the progression and treatment of Alzheimer`s disease. *Current Medicinal Chemistry*. 2015. ISSN 1875-533X. DOI: 10.2174/0929867322666150114163051.

Attachment II

BENEK, Ondrej, Kamil MUSILEK a Kamil KUCA. [Mitochondrial enzyme ABAD and its role in the development and treatment of Alzheimer's disease]. *Ceska a Slovenská farmacie: casopis Ceské farmaceuticke spolecnosti a Slovenske farmaceuticke spolecnosti*. 2012, vol. 61, no. 4, p. 144–149. ISSN 1210-7816.

Attachment III

HROCH, Lukas, Ondrej BENEK, Patrick GUEST, Laura AITKEN, Ondrej SOUKUP, Jana JANOCKOVA, Karel MUSIL, Vlastimil DOHNAL, Rafael DOLEZAL, Kamil KUCA, Terry K SMITH, Frank GUNN-MOORE a Kamil MUSILEK. Design, synthesis and in vitro evaluation of benzothiazole-based ureas as potential ABAD/17β-HSD10 modulators for Alzheimer's disease treatment. *Bioorganic & Medicinal Chemistry Letters* [online]. 2016, in press. ISSN 0960-894X. DOI: 10.1016/j.bmcl.2016.05.087.

Attachment IV

BENEK, Ondrej, Ondrej SOUKUP, Marketa PASDIOROVA, Lukas HROCH, Vendula SEPSOVA, Petr JOST, Martina HRABINOVA, Daniel JUN, Kamil KUCA, Dominykas ZALA, Rona R. RAMSAY, José MARCO-CONTELLES a Kamil MUSILEK. Design, Synthesis and in vitro Evaluation of Indolotacrine Analogues as Multitarget-Directed Ligands for the Treatment of Alzheimer's Disease. *ChemMedChem* [online]. 2015, in press. ISSN 1860-7187. DOI: 10.1002/cmdc.201500383.